

DIGITAL ACCESS TO SCHOLARSHIP AT HARVARD
DASH.HARVARD.EDU

HARVARD LIBRARY


Regulation of Hepatic Fuel Utilization and Storage Through BAD-Dependent Glucose Signaling

Citation

Lane, Elizabeth. 2018. Regulation of Hepatic Fuel Utilization and Storage Through BAD-Dependent Glucose Signaling. Doctoral dissertation, Harvard University, Graduate School of Arts & Sciences.

Link

http://nrs.harvard.edu/urn-3:HUL.InstRepos:41121254

Terms of use

This article was downloaded from Harvard University's DASH repository, and is made available under the terms and conditions applicable to Other Posted Material (LAA), as set forth at https://harvardwiki.atlassian.net/wiki/external/NGY5NDE4ZjgzNTc5NDQzMGIzZWZhMGFlOWI2M2EwYTg

Accessibility

https://accessibility.huit.harvard.edu/digital-accessibility-policy

Share Your Story

The Harvard community has made this article openly available.
Please share how this access benefits you. Submit a story

Regulation of Hepatic Fuel Utilization and Storage Through BAD-dependent Glucose Signaling

A dissertation presented

by

Elizabeth Lane

to

The Division of Medical Sciences

in partial fulfillment of the requirements

for the degree of

Doctor of Philosophy

in the subject of

Biological and Biomedical Sciences

Harvard University

Cambridge, Massachusetts

June 2018

© 2018 Elizabeth Lane

All rights reserved.

Regulation of Hepatic Fuel Utilization and Storage Through BAD-dependent Glucose Signaling

Abstract

Metabolic adaptation to fed and fasted states is intricately controlled by nutrient and hormonal signals. In the fed state, the liver stores glucose first as glycogen and then converts excess glucose to fat through *de novo* lipogenesis (DNL). During fasting, the liver produces glucose first though glycogen breakdown and then through *de novo* synthesis, a process known as gluconeogenesis, which is coupled to fatty acid oxidation. When dysregulated, these processes can lead to metabolic disorders such as diabetes and fatty liver disease.

In the liver, the glucose-phosphorylating enzyme glucokinase (GK) is a key regulator of the balance between glycolysis and gluconeogenesis, and the attendant changes in fat metabolism. Hepatic GK is modulated by hormonal and nutrient signals, including multiple regulatory proteins. Here we investigated the relevance of the BCL2-associated agonist of cell death (BAD), a protein that activates GK when phosphorylated at serine 155 residue in response to glucose and insulin. We demonstrate that loss of BAD reprograms hepatic metabolism towards diminished glycolysis and DNL, increased fatty acid oxidation, and exaggerated gluconeogenesis that escapes suppression by insulin. These metabolic alterations are rescued by reconstitution with a GK-activating phosphomimic variant of BAD. Conversely, loss of GK ablates the capacity of phospho-BAD to regulate hepatic substrate metabolism, indicating that GK mediates BAD's function in the liver. We further show that BAD's effects on DNL are mediated by the Carbohydrate Response Element Binding Protein (ChREBP), a key transcription factor regulating hepatic DNL in response to glucose stimulation. We identified a novel ChREBP-interacting protein that recruits GlcNAc transferase (OGT) to ChREBP, promoting ChREBP O-GlcNAcylation and activity. Deletion of GK or BAD leads to diminished hexosamine biosynthesis, OGT recruitment to ChREBP,

ChREBP O-GlcNAcylation, and lipogenic gene expression in response to glucose. Remarkably, these changes can be rescued by GlcNAc supplementation. The physiologic relevance of BAD's effect on hepatic metabolism is evident from the ability of a BAD phosphomimic variant to counteract unrestrained gluconeogenesis and improve glycemia in leptin-resistant and high fat diet models of diabetes and insulin resistance, and by altered BAD phosphorylation in liver biopsies of patients with fatty liver disease.

Table of Contents

Abstract iii
Table of Contents v
List of Figures and Tables vi
Acknowledgments viii
CHAPTER 1: Introduction 1
1.1 Brief overview of hepatic adaptive metabolism 2
1.2 Glucokinase and hepatic glucose sensing 4
1.3 ChREBP: A glucose sensing transcription factor 6
1.4 Hormonal regulation of hepatic metabolism 8
1.5 Regulation of hepatic metabolism by the BCL-2 family protein BAD 11
1.6 Objectives and overview of this thesis dissertation 15
References 18
CHAPTER 2: HCF-1 Links BAD-Mediated Glucose Signaling to *de Novo* Lipogenesis through ChREBP Regulation 25
SUMMARY 26
INTRODUCTION 27
RESULTS 30
DISCUSSION 61
METHODS 66
CONTRIBUTIONS 80
REFERENCES 81
CHAPTER 3: Regulation of Hepatic Energy Metabolism and Gluconeogenesis by BAD 87
SUMMARY 88
INTRODUCTION 89
RESULTS 91
DISSCUSSION 128
METHODS 132
CONTRIBUTIONS 139
REFERENCES 140
CHAPTER 4: Discussion and Future Directions 145
4.1 The physiological relevance of the HCF-1:ChREBP axis in hepatic metabolism and insulin sensitivity 146
4.2 Therapeutic potential of phospho-BAD mimicry 150
References 154

List of Figures and Tables

CHAPTER 1

Figures:

Figure 1.1. Overview of hepatic metabolism 3
Figure 1.2. Diagram of hepatic insulin signaling 9
Figure 1.3. Mechanisms of insulin resistance 12
Figure 1.4. Dual role of BAD in metabolism and apoptosis 14
Figure 1.5. Thesis at a glance 17

CHAPTER 2

Figures:

Figure 2.1. BAD-dependent changes in glucose-induced lipogenic program 31
Figure 2.2. BAD's hepatic function is modulated by its phosphorylation status 33
Figure 2.3. The effect of BAD modifications on lipogenic gene expression 34
Figure 2.4. ChREBP is required for BAD's effect on lipogenesis 39
Figure 2.5. Identification of HCF-1 as a novel ChREBP interacting protein 42
Figure 2.6. HCF-1 interacts with ChREBP and is required for its O-GlcNAcylation 45
Figure 2.7. HCF-1 regulates ChREBP function and lipogenesis downstream of BAD 48
Figure 2.8. Regulation of ChREBP protein levels by BAD phosphorylation 50
Figure 2.9. Hexosamine biosynthesis is an intermediate between BAD and ChREBP regulation via HCF-1 53
Figure 2.10. Rescue of the HCF-1-ChREBP regulatory module in *Bad* -/- hepatocytes following supplementation with glucosamine 55
Figure 2.11. Increased BAD phosphorylation and HCF-1 levels in livers of human NASH patients 59
Figure 2.12. Proposed model of biochemical modulation of *de novo* lipogenesis by BAD and HCF-1 62

Tables:

Table 2.1. qPCR Primers 37
Table 2.2. Retention times and MRM transitions for hexosamines 57
Table 2.3. List of Human Liver Specimens 60

CHAPTER 3

Figures:

Figure 3.1. Hepatic glucose metabolism in the absence of BAD 92
Figure 3.2. BAD-modulation of hepatic glucose metabolism. 94
Figure 3.3. The effect of BAD phosphorylation on gluconeogenesis 98
Figure 3.4. BAD's hepatic function is modulated by its phosphorylation status. 101
Figure 3.5. BAD-dependent modulation of hepatic energy metabolism 103
Figure 3.6. Changes in the expression of genes involved in fatty acid metabolism following hepatic manipulation of BAD and GK. 106
Figure 3.7. Hepatic function of BAD is GK-dependent 110
Figure 3.8. Hepatic insulin resistance in the absence of BAD 111
Figure 3.9. Peripheral insulin action and additional metabolic parameters in *Bad* +/+ and -/- mice. 114
Figure 3.10. Altered insulin signaling upon hepatic manipulation of BAD and GK 117
Figure 3.11. Insulin signaling in the absence of BAD. 119
Figure 3.12. Metabolic effects of BAD in ob/ob liver. 123
Figure 3.13. Metabolic effects of BAD in ob/ob and HFD-treated mice 125

Tables:

Table 3.1. Summary of oligomycin-inhibitable portion of OCR in the absence and presence of ADP. 104

CHAPTER 4

Figures:

Figure 4.1. Potential mechanism for epigenetic regulation of lipogenic genes by HCF-1 149
Figure 4.2. Comparison of phospho-BAD SAHB and the allosteric GKA RO0281675 152

Acknowledgments

I would like to thank everyone who supported me throughout my PhD work, which was both very challenging and rewarding at times. First, I would like to thank my advisor Dr. Nika Danial. Under her mentorship, I have grown as an independent researcher, gaining experience not only in research at the bench but also writing and scientific presentation skills. The skills I gained under her tutorship were not only invaluable for completing my PhD but I believe will also be valuable for my future career.

I would also thank my dissertation advisory committee members; Drs. Loren Walensky, Suzanne Gaudet and Pere Puigserver for their thoughtful and insightful feedback during the course of my dissertation work. Additionally, I would like to thank my dissertation examiners; Drs. Loren Walensky, Nada Kaalany, Alexander Banks, and Valentina Perissi for taking the time to critically evaluate my work. I would also like to thank Drs. Richard Lee, William Anderson, and Susanne Jakobs with whom I taught during my PhD.

My gratitude also extends to Drs. Mark Herman, Donald Scott and Howard Towle for providing reagents that were necessary to complete my PhD work. I'd further like to thank Mark Herman for meeting with me when I first started working on ChREBP and providing scientific feedback. I would like to acknowledge Dr, Daina Avizonis and Gaëlle Bridon for metabolite measurements at the Rosalind and Morris Goodman Cancer Research Centre and the Taplin Taplin Mass Spectrometry Facility at Harvard Medical School under the direction of Drs. Ross Tomaino and Steven Gygi for proteomic analysis of FLAG-ChREBP IPs. I was also fortunate to have access to human liver tissue in my thesis work through The Liver Tissue Cell Distribution System, Minneapolis, Minnesota.

My colleagues in the Danial lab have been an invaluable resource throughout my PhD. I would especially like to thank Dong Wook Choi who worked closely with me during the last year my PhD studies to help complete the project. I would specifically like to thank past lab members;

Alfredo Gimenez-Cassina and Luisa Garcia-Haro who were instrumental at the start of my PhD. My thanks also go out to the amazing laboratory technicians, Elaura Patton, Meghan Tedoldi, and Lindsay Evans, who managed the mouse colony and helped with *in vivo* experiments throughout my PhD. I also thank current and past members, Acalia Fu, MCarmen Fernandez-Aguera, Pei Hsuan, Ana Lako, Sofia Riberio, Erik Norberg, Sanda Ljubicic, and Illana Stanley for their support, friendship, and scientific advice. I also appreciate all the members of the Division of Metabolism and Chronic Diseases here at DFCI for creating a great work environment on our lab floor where there was productive scientific exchange and reagent sharing across lab boundaries.

I could not have done this without the support of my friends and family who provided emotional, career and scientific support throughout my PhD. Thank you to trapeze, dance, and the friends I made at those activities for providing an outlet that helped keep me sane. Thank you also to all the friends I have made in the program who made the PhD experience much more rewarding. I am very grateful for the support and love from my family. My Aunt Cathy and Uncle Julio for their support and coffee dates over the years. My Grandma, Jan, for her love and many visits to Boston. My brothers/brother in-law, Paul, Ben and Dave, and sisters/sister in-law, Jess, Em and Sarah for their love and encouragement and their visits to Boston, and my Dad, Ted, and my Mom, Norma, for always willing to pick up the phone and provide love and support or send random gifts in the mail to cheer me up. Lastly, I would like to thank my husband, Ryoji Amamoto, who fed me when I was busy and provided me much needed emotional support and encouragement during pivotal parts of my PhD.

CHAPTER 1
Introduction

1.1 Brief overview of hepatic adaptive metabolism

The liver plays an important role in the homeostatic regulation of glucose and lipid utilization, storage, and production in response to nutrient and hormonal signals such as glucose and insulin (Lin and Accili, 2011; Oosterveer and Schoonjans, 2013). In the fed state, when nutrient availability is high, the liver favors glucose utilization and storage. Glucose is first stored as glycogen, but once glycogen stores are replete, glucose carbons are converted to fat through a process known as *de novo* lipogenesis (Figure 1.1). *De novo* lipogenesis is regulated at the transcriptional level by both insulin and glucose (Dentin et al., 2004; Horton et al., 2002; Uyeda and Repa, 2006), and requires the glucose-derived lipogenic precursor malonyl-CoA and the lipogenic cofactor NADPH, a product of the pentose phosphate pathway and the malic enzyme (Alves-Bezerra and Cohen, 2017; Sanders and Griffin, 2016) (Figure 1.1B).

In the fasted state, the liver produces glucose through glycogen breakdown and then through *de novo* synthesis from glucose in a process known as gluconeogenesis (Petersen et al., 2017). Hepatic glucose production is intertwined with fatty acid oxidation (FAO), the TCA cycle and mitochondrial electron transport chain activity, which supply the gluconeogenic pathway with carbon substrates, reducing equivalents and ATP (Satapati et al., 2012) (Figure 1.1B). These metabolic pathways are also regulated at both transcriptional and post-transcriptional levels. Key transcriptional regulators of the gluconeogenic programs include FOXO1, HNF4 and PGC1α (Anyamaneeratch et al., 2015; Banks et al., 2011; Petersen et al., 2017). At post-transcriptional level, acetyl-CoA derived from FAO is an important regulator of gluconeogenesis through its allosteric activation of pyruvate carboxylase (PC), which generate oxaloacetate for the phosphoenolpyruvate carboxykinase (PEPCK) reaction (Han et al., 2016) (Figure 1.1B).

While *de novo* lipogenesis and gluconeogenesis are important components of adaptive metabolism under normal physiologic conditions, their dysregulation can lead to a variety of metabolic diseases. For example, excessive *de novo* lipogenesis is associated with diabetes

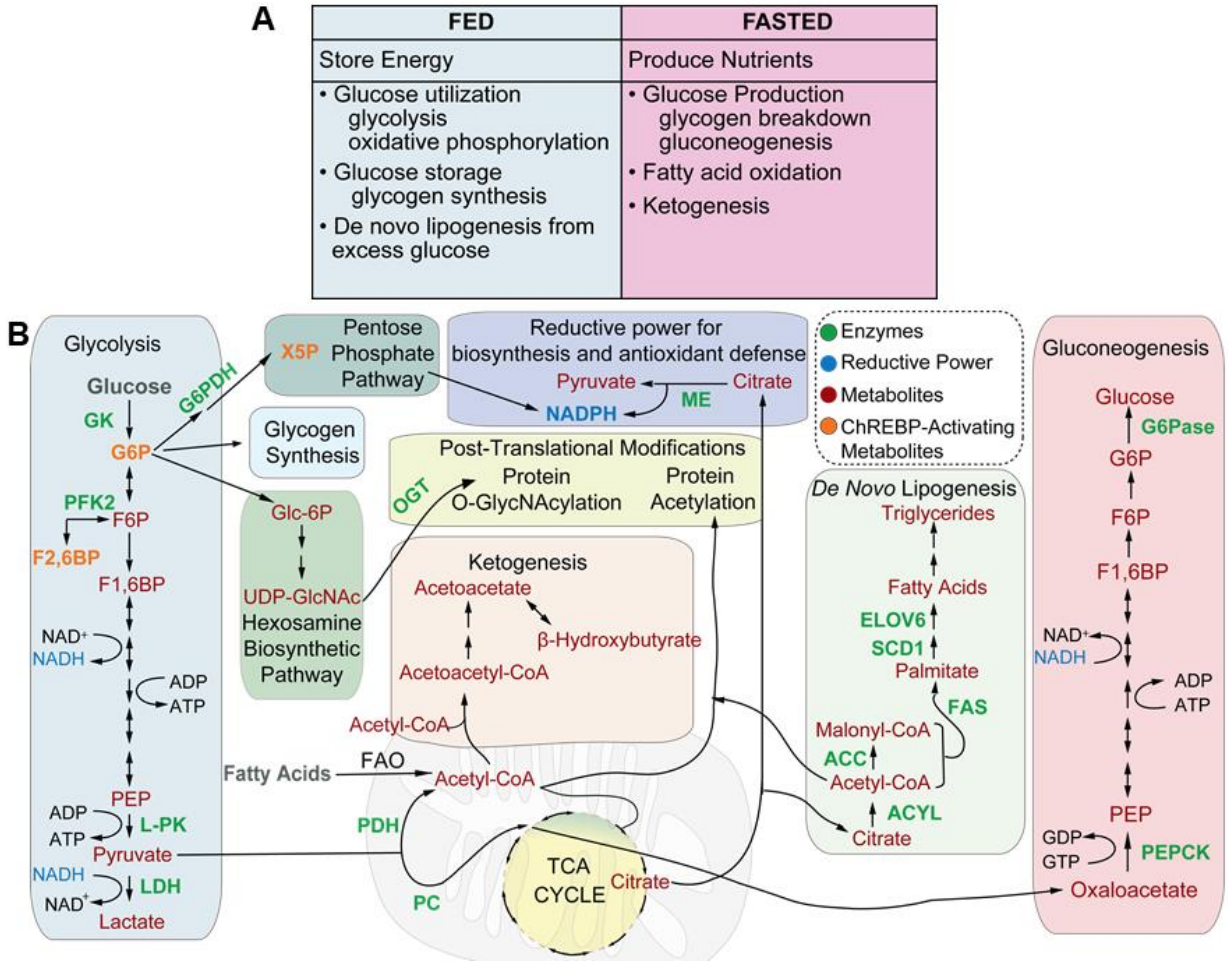


Figure 1.1. Overview of hepatic metabolism

(A) Overview of hepatic glucose and fat metabolism summarizing their utilization and storage in fed and fasted states. **(B)** Schematics of hepatic substrate metabolism.

Abbreviations: Metabolites: G6P- Glucose-6-phosphate, F6P, Fructose-6-phosphate, F26,BP- Fructose-2,6-Bisphosphate, GAP- Glyceraldehyde phosphate, 3PG- 3-phosphoglycerate, 2PG- 2-phosphoglycerate, X5P- xyulose-5-phosphate, Glc-6P- Glucosamine-6-phosphate, UDP-GlcNAc-Uridine diphosphate N-acetylglucosamine.

Enzymes: G6PDH- Glucose-6-phosphate dehydrogenase, GK- Glucokinase, PFK2- Phosphofructokinase 2, PK- Pyruvate kinase, LDH- Lactate dehydrogenase, PDH- Pyruvate dehydrogenase, PC- Pyruvate carboxylase, OGT- O-linked N-actetylglucosamine transferase, ME- Malic enzyme, ACC- Acetyl-CoA carboxylase, ACLY- ATP citrate lyase, FAS- Fatty acid synthase, SCD1- Stearoyl-CoA desaturase-1, ELOV6- Elongation of very long chain fatty acids protein 6, PEPCK- Phosphoenolpyruvate carboxykinase, and G6Pase- Glucose 6-phosphatase.

and nonalcoholic fatty liver disease (NAFLD) (Birkenfeld and Shulman, 2014; Samuel and Shulman, 2018), and unrestrained gluconeogenesis leads to hyperglycemia and its attendant health complications over time (DeFronzo et al., 2015). As such, how the liver senses glucose availability to promote its storage or production is an active area of research.

1.2 Glucokinase and hepatic glucose sensing

The glucose phosphorylating enzyme glucokinase (GK, Hexokinase IV), is an important modulator of hepatic substrate metabolism (Matschinsky, 2009; Nissim et al., 2012). Compared to other hexokinase isoforms, GK has unique kinetic properties such as a low affinity for glucose (~ 8 mM), positive substrate cooperativity, and lack of end product inhibition (Agius, 2016b). These features make GK well suited for sensing physiologic blood glucose fluctuations. GK expression is restricted to liver, pancreatic β-cells and certain hypothalamic neurons, and its cardinal role in physiologic control of blood glucose levels is further evident from a number of human pathologies caused by naturally-occurring *GK* mutations. Specifically, GK loss-of-function mutations are linked to maturity onset diabetes of the young type 2 (MODY2) and permanent neonatal diabetes mellitus (PNDM), while gain-of-function mutations in the enzyme are associated with persistent hyperinsulinemic hypoglycemia of infancy (PHHI), which presents with abnormally low blood glucose concentrations (Matschinsky, 2009). For these reasons, drug discovery efforts for therapeutic modulation of GK has gained considerable attention over the past years (Grimsby et al., 2008; Matschinsky, 2013; Meininger et al., 2011; Pfefferkorn et al., 2012; Sarabu et al., 2012).

GK regulates hepatic glucose utilization and storage by stimulating glycogen and lipid synthesis while suppressing gluconeogenesis (Dentin et al., 2004; Oosterveer and Schoonjans, 2013; Postic et al., 1999; Velho et al., 1996). GK-catalyzed production of glucose-6-phosphate (G6P) functions as either a substrate or an allosteric activator/inhibitor of many metabolic pathways. For example, G6P activates glycogen synthase while allosterically inhibiting glycogen phosphorylase, thereby promoting glucose storage as glycogen (Oosterveer and Schoonjans,

2013) (Figure 1.1B). Furthermore, metabolism of G6P through the glycolytic pathway generates pyruvate, which can enter the TCA cycle for oxidative metabolism, generating energy as well as biosynthetic precursors for other metabolic pathways (Oosterveer and Schoonjans, 2013) (Figure 1.1B). This includes generation of citrate, which is metabolized to acetyl-CoA and then malonyl-CoA for *de novo* lipogenesis (Oosterveer and Schoonjans, 2013)(Figure 1.1B). Concomitant allosteric inhibition of FAO by malonyl-CoA ensures that fatty acids are not synthesized and oxidized in a futile cycle (Foster, 2012). With FAO inhibited, gluconeogenic flux is also reduced (Lee et al., 2017; Petersen et al., 2017). Other G6P-utilizing reactions through the pentose phosphate pathway generate nucleotides as well as reducing equivalents in the form of NADPH to support *de novo* lipogenesis (Alves-Bezerra and Cohen, 2017; Oosterveer and Schoonjans, 2013) (Figure 1.1B).

Consistent with its central role in hepatic substrate metabolism, GK activity is regulated at multiple levels, including transcriptional regulation downstream of the insulin signaling pathway (Agius, 2016b) (Figure 1.2). In addition, GK activity is modulated by several binding partners such as glucokinase regulatory protein (GKRP), the bi-functional enzyme 6-phosphofructo-2-kinase/fructose 2,6-bisphosphatase (PFK2/FBP2) and BCL-2-associated Agonist of Cell Death (BAD) [reviewed in (Agius, 2016b)]. GKRP inhibits GK by binding to its allosteric site predominately at low glucose concentrations and sequestering the enzyme in the nucleus (Agius, 2016b; Baltrusch et al., 2001; Detheux et al., 1991; Farrelly et al., 1999). This interaction is strengthened by fructose-6-phosphate (F6P) and inhibited by fructose-1-phosphate (F1P) (Detheux et al., 1991). In humans, a common variant of GKRP (GKRP-446L), which has lower nuclear accumulation and less inhibitory effect on GK, results in high plasma and hepatic triglycerides and low fasting blood glucose levels, a phenotype consistent with increased lipogenesis and diminished gluconeogenesis (Beer et al., 2009; Orho-Melander et al., 2008; Rees et al., 2012). While GKRP inhibits GK activity, PFK2/FBP2 and BAD activate the enzyme (Agius, 2016b; Baltrusch et al., 2001; Danial et al., 2003). Both PFK2/FBP2 and BAD increase the Vmax

of the enzyme without affecting its affinity for glucose (Baltrusch et al., 2012; Szlyk et al., 2014). Beyond activating GK, PFK2/FBP2 enhances glycolysis by generating fructose 1,6 bisphosphate, which in turn leads to allosteric activation of the glycolytic enzyme PFK1 (Okar et al., 2004). The interaction between GK and PFK2/FBP2 or BAD is increased at high glucose concentrations or in the fed state (Baltrusch et al., 2012; Cullen et al., 2014) (data not shown). Collectively, these data point to PFK2/FBP2 and BAD as physiological activators of GK in response to high glucose.

1.3 ChREBP: A glucose sensing transcription factor

In addition to providing biosynthetic precursors for metabolic pathways such as *de novo* lipogenesis, glucose metabolism can provide signals to activate the transcription of glycolytic and lipogenic genes. Carbohydrate Response Element Binding Protein (ChREBP) has emerged as the primary transcription factor that activates the expression of glucose responsive genes (Abdul-Wahed et al., 2017; Agius, 2016a; Ma et al., 2005). ChREBP is a basic-helix-loop-helix transcription factor that binds to carbohydrate response elements (ChOREs) in the promoters of target genes as a tetrameric complex with its obligate binding partner MLX (Stoeckman et al., 2004). Genetic studies in rodents have demonstrated the physiologic relevance of ChREBP in regulating *de novo* lipogenesis and the development of hepatic steatosis (Dentin et al., 2006; Iizuka et al., 2004; Iizuka et al., 2006). Moreover, polymorphisms in the *ChREBP* gene are linked to increased plasma triglycerides in humans (Kooner et al., 2008). Beyond *de novo* lipogenesis, ChREBP-dependent transcriptional programs may also modulate hepatic ATP homeostasis in response to excess carbohydrate and in NAFLD. This is consistent with the observation that hepatic ChREBP targets include genes that down regulate phosphate ester pools to preserve hepatic Pi and ATP (Agius, 2016a).

As a glucose-responsive transcription factor, ChREBP activation requires GK and is believed to be dependent on glucose metabolites rather than glucose per se (Abdul-Wahed et al., 2017; Agius, 2016a; Dentin et al., 2004). In particular, three phospho-metabolites of G6P, xyulose-5-phosphate (X5P), or fructose 2,6 bisphosphate (F2,6BP) have been shown to activate

ChREBP (Arden et al., 2012; Dentin et al., 2012; Kabashima et al., 2003) (Figure 1.1B). The molecular mechanisms whereby ChREBP is activated by these metabolites await further studies. Increased glucose metabolism can also elevate flux through the hexosamine biosynthesis pathway, increasing UDP-GlcNAc, the substrate for protein O-GlcNAcylation (Figure 1.1B). O-GlcNAcylation of ChREBP increases its DNA binding affinity, transcriptional activity, and protein stability (Guinez et al., 2011; Sakiyama et al., 2010; Yang and Qian, 2017). However, the mechanisms controlling ChREBP O-GlcNAcylation are not fully understood. DNA-binding and transcriptional activity of ChREBP can also be modulated by acetylation in response to glucose stimulation (Bricambert et al., 2010). This may depend on glucose-dependent enrichment of acetyl-CoA pools (Figure 1.1B), which may alter protein acetylation (Wellen et al., 2009).

Other glucose-dependent ChREBP post translational modifications include phosphorylation. Specifically, ChREBP is phosphorylated by PKA/AMPK and sequesterd by 14-3-3 proteins in the cytosol under low glucose conditions or during fasting (Kawaguchi et al., 2001). This interaction may be further stabilized by AMP, an indicator of low energy status, and by ketone bodies, which are metabolites produced from fatty acids under starvation conditions (Nakagawa et al., 2013; Sato et al., 2016) (Figure 1.1B). ChREBP can be dephosphorylated by a PP2A-like phosphatase activated by X5P, which promotes its nuclear translocation (Kabashima et al., 2003). However, ChREBP phospho-mutants remain glucose responsive (Tsatsos and Towle, 2006), and a pool of ChREBP resides in the nucleus even in the absence of glucose stimulation (Davies et al., 2008; Kim et al., 2016), indicating the existence of additional glucose-dependent regulatory mechanisms apart from ChREBP phosphorylation status and nuclear translocation.

Structure-function analyses, together with theoretical modeling of ChREBP structure based on conserved sequences across Mondo glucose-responsive transcription factor family members, revealed a potential mechanism whereby G6P may activate ChREBP (Li et al., 2006; McFerrin and Atchley, 2012). These studies uncovered an N-terminal glucose sensing module (GSM) in ChREBP composed of two domains; a low-glucose inhibitory domain (LID) and a

transactivation domain known as glucose-response activation conserved element (GRACE), which can potentially bind G6P (Li et al., 2006; McFerrin and Atchley, 2012). In the LID/GRACE model of ChREBP activation, ChREBP is repressed by intermolecular contacts within the GSM under low glucose conditions, which are relieved upon G6P binding.

1.4 Hormonal regulation of hepatic metabolism

Under physiologic conditions, nutrient cues work together with hormonal signals to promote metabolic adaptation to fed and fasted states. Glucagon, which is secreted from the pancreatic α-cells in response to low blood glucose levels, is a major regulator of the fasting response and stimulates hepatic glucose production (Jiang and Zhang, 2003). Insulin, on the other hand is secreted from the pancreatic β-cells in response to high blood glucose concentrations (Tokarz et al., 2018). Insulin acts both on the liver and peripheral tissues to promote glucose storage in the form of glycogen and fat, lowering blood glucose levels.

Insulin binding to the insulin receptor (IR) triggers receptor autophosphorylation and activation (Avruch, 1998; Titchenell et al., 2017) (Figure 1.2). The insulin signaling pathway controls a myriad of cellular pathways, including hepatic glycolysis, gluconeogenesis, glycogen synthesis, and lipogenesis, in addition to other canonical insulin-regulated pathways such as protein synthesis, cell growth and survival (Titchenell et al., 2017) (Figure 1.2). In particular, the insulin receptor substrate (IRS) proteins exert metabolic effects through activation of PI3K and 3-phosphoinositide-dependent protein kinase 1 (PDK1) (Guo et al., 2009; Titchenell et al., 2017). PDK1 then phosphorylates and activates AKT, which in turn modulates the activity of key metabolic enzymes and transcription factors in the liver (Hatting et al., 2018; Titchenell et al., 2017; Yecies et al., 2011) (Figure 1.2). Insulin promotes glucose utilization and storage to glycogen and fat in multiple ways including, transcriptional induction of *Gk* via the sterol

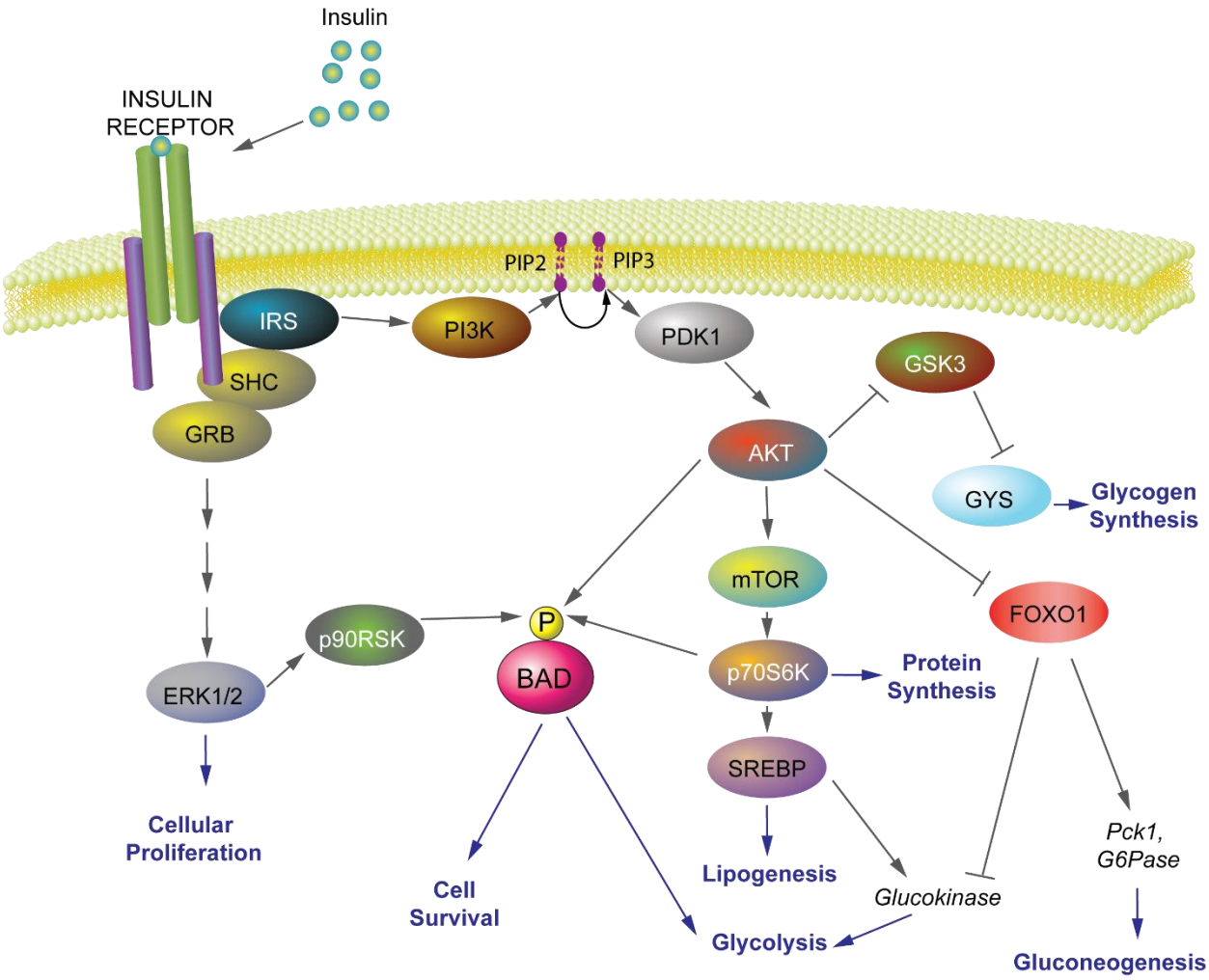


Figure 1.2. Diagram of hepatic insulin signaling

Simplified schematic of the insulin signaling pathway and its effects on multiple metabolic processes in the liver.

Abbreviations: AKT- Protein kinase B, BAD- BCL-2-associated Agonist of Cell Death, ERK- Extracellular signal-regulated kinase, FOXO1- Forkhead box O1, GSK3- Glycogen synthase kinase, GYS- Glycogen synthase, G6Pase- Glucose-6 phosphatase, GRB- growth factor receptor-bound protein, IRS- Insulin receptor substrate, mTOR- mammalian target of rapamycin, p90RSK-, p90 ribosomal S6 kinase, p70S6K- Ribosomal protein S6 kinase, Pck1- Phosphoenolpyruvate carboxykinase, PI3K- Phosphatidylinositol-4,5-bisphosphate 3-kinase, PIP2- Phosphatidylinositol-4,5-bisphosphate, PIP3- Phosphatidylinositol-3,4,5-triphosphate, PDK1- 3-phosphoinositide-dependent protein kinase 1, SHC- SHC-transforming protein 1, SREBP- Sterol regulatory element binding protein.

regulatory element binding protein (SREBP) (Agius, 2016b; Lin and Accili, 2011). SREBP shares lipogenic target genes with ChREBP and mediates insulin's effects on *de novo* lipogenesis (DeBose-Boyd and Ye, 2018; Titchenell et al., 2017). Insulin activates SREBP by both stimulating its transcription and enhancing its proteolytic processing to an active form (DeBose-Boyd and Ye, 2018; Owen et al., 2012; Titchenell et al., 2017).

In addition to promoting hepatic glycolysis and lipogenesis, insulin represses gluconeogenesis (Hatting et al., 2018). Insulin inhibition of FOXO1, which normally promotes the transcription of two key gluconeogenic genes, glucose 6-phosphatase (G6Pase) and PEPCK (*Pck*) (Figure 1.2), is an important mechanism whereby gluconeogenesis is suppressed in the fed state (Liao et al., 1998; Lu et al., 2012; Postic et al., 2004). This occurs through AKT-mediated phosphorylation of FOXO1, its subsequent binding to 14-3-3 proteins and nuclear export (Tikhanovich et al., 2013). Deletion of AKT results in hyperglycemia that can be rescued by hepatic deletion of *Foxo1*, demonstrating the importance of the AKT:FOXO1 axis in regulating hepatic glucose production (Lu et al., 2012). Beyond suppression of gluconeogenesis, systemic inhibition of hepatic glucose production by insulin is also mediated by inhibition of adipocyte lipolysis, which diminishes FAO, reducing equivalents, and energy required for gluconeogenesis (Hatting et al., 2018). Thus, insulin regulates hepatic glucose production by both direct and indirect mechanisms.

Hepatic insulin resistance, defined broadly as resistance to insulin action, results in increased hepatic glucose production and hyperglycemia that can develop into type 2 diabetes (T2D) (Hatting et al., 2018; Michael et al., 2000). At the molecular level, insulin resistance is often associated with inhibition of IRS phosphorylation in response to insulin (Copps and White, 2012). The pathophysiology of insulin resistance continues to be an active area of investigation, and many mechanisms have been proposed including hyper activation of negative feedback loops that normally dampen insulin signaling such as inflammation, elevated diacylglycerols and/or ceramides, ER stress as well as high ROS levels (Copps and White, 2012; Samuel and Shulman,

2016) (Figure 1.3). Most of these mechanisms inhibit insulin signaling at the level of IRS through activation of IRS inhibitory kinases (Copps and White, 2012) (Figure 1.3). A number of IRS inhibitory kinases are regulated by insulin signaling such as mTOR, p70S6K, and ERK and are elements of negative feedback loops (Copps and White, 2012) (Figure 1.3). IRS proteins can additionally be inhibited by heterologous kinases, whose activity is regulated independently of insulin such as c-Jun N-terminal kinase (JNK) and protein kinase C (PKC) (Copps and White, 2012) (Figure 1.3). JNK can be activated in response to increased ROS levels while PKC isoforms are activated by diacylglycerols (Copps and White, 2012) (Figure 1.3). Both of these IRS inhibitory pathways can be activated by dysregulated lipid metabolism (Copps and White, 2012; Samuel and Shulman, 2016; Vial et al., 2010). As such, hepatic nutrient and energy sensing pathways and insulin signaling are tightly integrated with dysregulated insulin signaling impacting hepatic substrate metabolism, and altered hepatic metabolism affecting hepatic insulin sensitivity (Copps and White, 2012; Newgard, 2012; Samuel and Shulman, 2016)

1.5 Regulation of hepatic metabolism by the BCL-2 family protein BAD

BCL-2 proteins, which are best known for their cell death/survival function, are active components of select physiologic pathways carrying "day jobs" in other homeostatic pathways beyond regulation of apoptosis (Bonneau et al., 2013; Giménez-Cassina and Danial, 2015; Hardwick et al., 2012). The first evidence of a non-apoptotic role for a BCL-2 protein in regulation of glucose metabolism and systemic glucose homeostasis emerged from studies showing that BAD, a BCL-2 family protein best known for its apoptotic function, binds and activates GK when phosphorylated in response to insulin and other nutrient signals (Danial et al., 2003; Danial et al., 2008; Giménez-Cassina et al., 2014; Szlyk et al., 2014). This post translational modification occurs on a conserved serine residue within an amphipathic α-helical region known as the BCL-2 Homology (BH)-3 domain; serine 155 (S155, amino acid

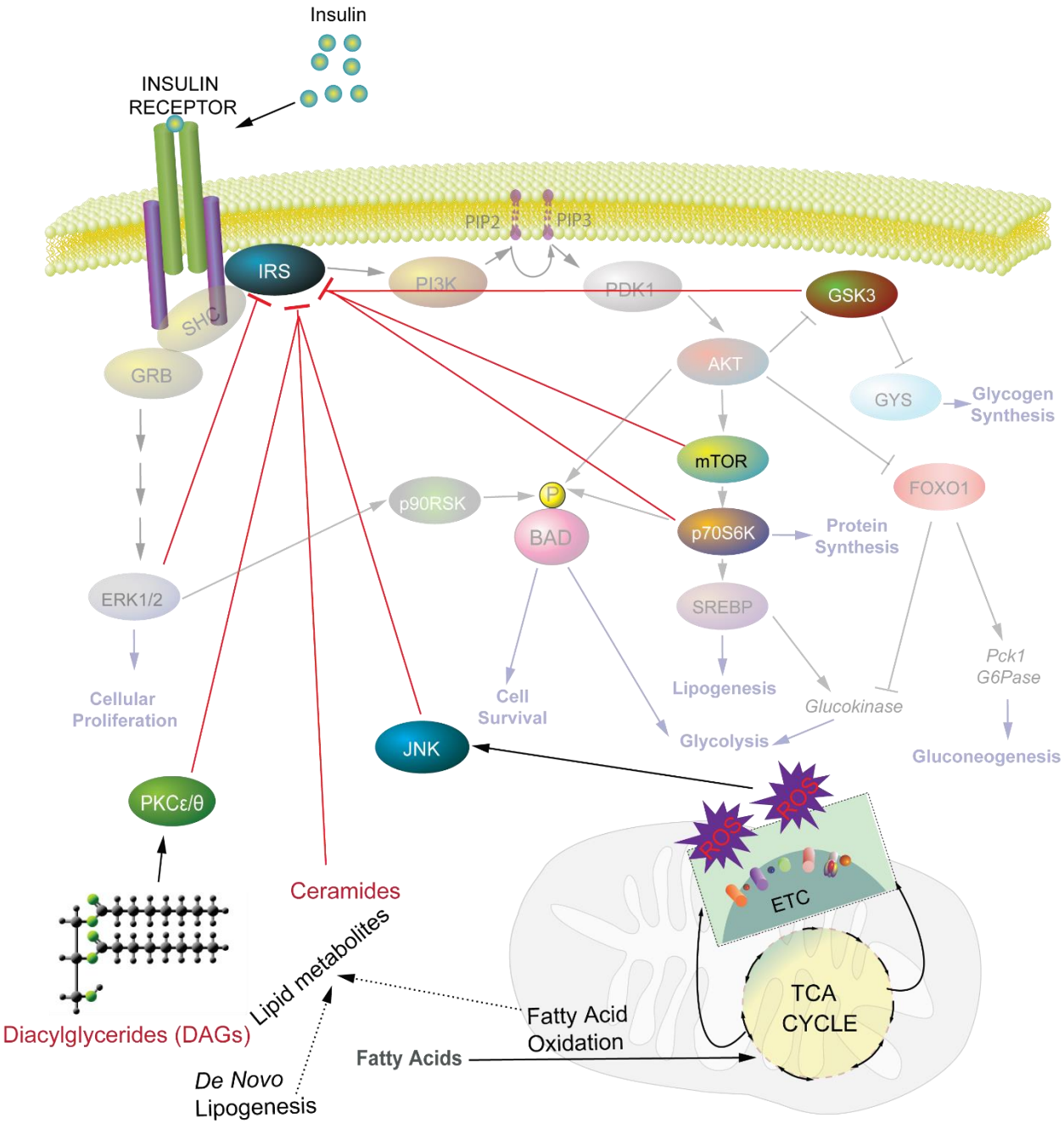


Figure 1.3. Simplified schematic of mechanisms underlying insulin resistance

Abbreviations: JNK- c-Jun N-terminal kinase, PKC- Protein kinase C, ROS- Reactive oxygen species, AKT- Protein kinase B, BAD- BCL-2-associated Agonist of Cell Death, ERK-Extracellular signal-regulated kinase, FOXO1- Forkhead box O1, GSK3- Glycogen synthase kinase, GYS- Glycogen synthase, G6Pase- Glucose-6 phosphatase, GRB- growth factor receptor-bound protein, IRS- Insulin receptor substrate, mTOR- mammalian target of rapamycin, p90RSK-, p90 ribosomal S6 kinase, p70S6K- Ribosomal protein S6 kinase, Pck1- Phosphoenolpyruvate carboxykinase, PI3K- Phosphatidylinositol-4,5-bisphosphate 3-kinase, PIP2- Phosphatidylinositol-4,5-bisphosphate, PIP3- Phosphatidylinositol-3,4,5-triphosphate, PDK1- 3-phosphoinositide-dependent protein kinase 1, SHC- SHC-transforming protein 1, SREBP- Sterol regulatory element binding protein.

enumeration based on the mouse sequence of BAD equivalent to S118 in human BAD) (Figure 1.4). The BH3 domain of BAD, which normally binds and inactivates pro-survival BCL-2, BCL-X_L, BCL-w is also required to engage GK (Nat Med 2008). However, S155 phosphorylation blocks the capacity of this domain to engage BCL-2 family partners while enabling its activation of GK (Giménez-Cassina and Danial, 2015) (Figure 1.4).

BAD S155 is the target of multiple kinases downstream of nutrient and insulin signaling including AKT, p70S6K and p90RSK that either phosphorylate S155 directly or modify upstream priming phosphorylation sites (S112 and S136), facilitating S155 phosphorylation (Danial et al., 2003; Danial, 2008; Danial et al., 2008; Giménez-Cassina et al., 2014) (Figure 1.2). When dephosphorylated, BAD can engage the mitochondrial apoptosis machinery through BH3 domain-dependent binding and neutralization of the pro-survival BCL-2, BCL-XL and BCL-w proteins. However, dephosphorylated BAD per se is not sufficient to trigger apoptosis, rather it plays a permissive role and sensitizes cells to apoptosis when sufficient cellular damage has accumulated (Giménez-Cassina and Danial, 2015). Other studies showed that, in the absence of cellular damage, dephosphorylated BAD is permissive to FAO (Giménez-Cassina and Danial, 2015). The BAD BH3 domain is not only required but sufficient to activate GK, as evident from the capacity of hydrocarbon-stapled peptides modeled after the phospho-BAD BH3 helix to activate GK (Danial et al., 2008; Ljubicic et al., 2015; Szlyk et al., 2014). Biochemical and structural dissection of the BAD-GK complex has also revealed that this helix directly engages GK near its active site and increases the Vmax of the enzyme without drastic effects on its affinity for glucose (Szlyk et al., 2014).

The physiological relevance of BAD in glucose metabolism is evident from impaired glucose tolerance, fasting hyperglycemia, and reduced glucose stimulation of insulin secretion when BAD is deleted or prevented from being phosphorylated (Danial et al., 2003; Danial et al., 2008; Giménez-Cassina et al., 2014). These alterations phenocopy loss-of-GK function in

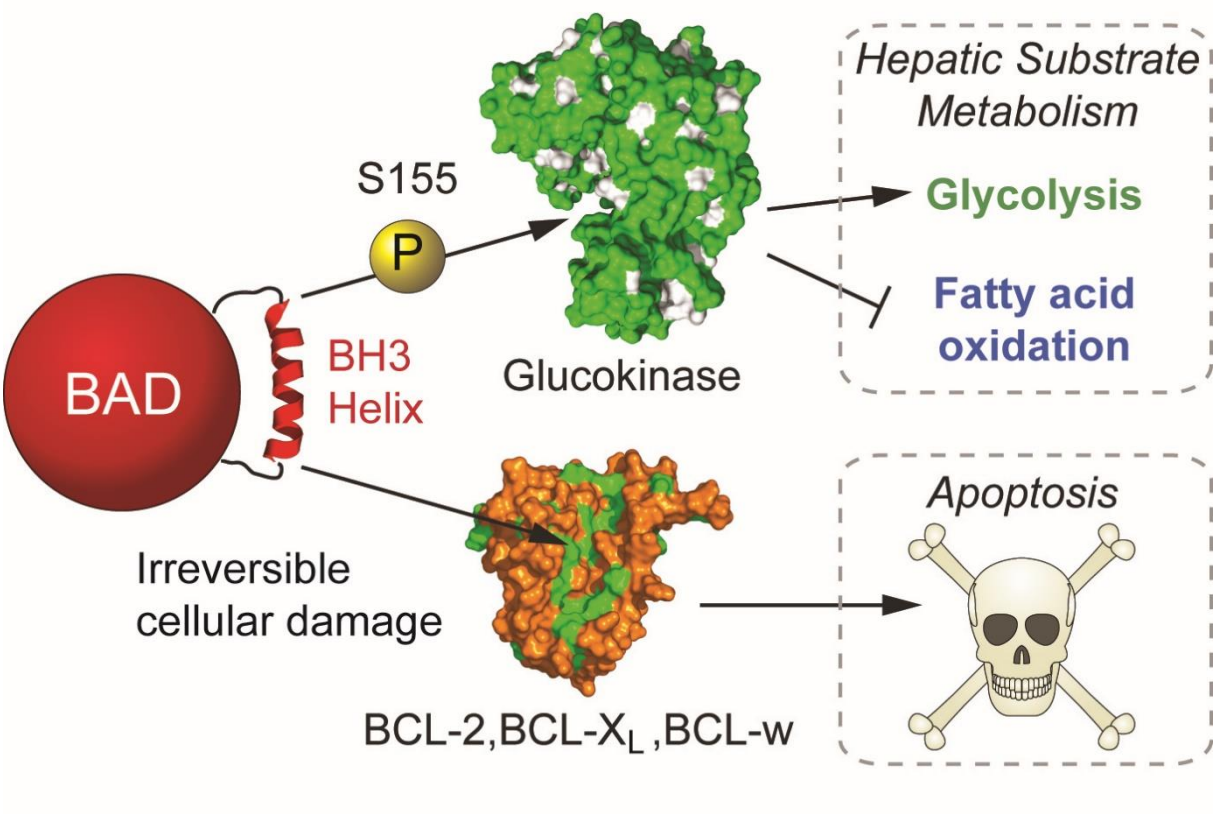


Figure 1.4. Dual role of BAD in metabolism and apoptosis
BAD BH3 domain interactions and their outcomes.

liver and in pancreatic β-cells, where GK activity normally regulates the glucose dose responsiveness of insulin secretion.

1.6 Objectives and overview of this dissertation

The studies described in this dissertation interrogate the physiologic relevance of BAD in hepatic adaptation to fed and fasted states. In **Chapter 2**, we provide a combination of biochemical and genetic evidence showing that BAD phosphorylation is required for hepatic *de novo* lipogenesis via ChREBP. We also take advantage of the wild type and BAD-deficient hepatocytes as a discovery platform to gain new molecular insights into how ChREBP is normally activated in response to glucose. Specifically, unbiased ChREBP-interaction proteomics under the setting where glucose stimulation of ChREBP is intact (wild type) versus impaired (BAD-deficiency) led to the identification of host cell factor 1 (HCF-1) as a novel ChREBP binding protein. We then separately characterize the biochemical mechanisms and functional relevance of HCF-1 in glucose activation of ChREBP and *de novo* lipogenesis. These studies revealed that HCF-1 resides at the promoters of lipogenic genes, and functions as an adaptor protein required for the recruitment of O-GlcNAc transferase (OGT) to ChREBP, its O-GlcNAcylation and transcriptional activity downstream of the hexosamine biosynthesis pathway in response to glucose stimulation (Figure 1.5). We also show that BAD phosphorylation and HCF-1 levels are increased in human liver samples obtained from patients with non-alcoholic steatohepatitis (NASH), a pathophysiologic setting where *de novo* lipogenesis is augmented.

In **Chapter 3**, we investigate the physiologic outcomes of BAD modifications in hepatic substrate metabolism and fasting responses. We show that, in the fasted state, loss of BAD or its phosphorylation reprograms hepatic metabolism towards diminished glycolysis, increased fatty acid oxidation, and exaggerated gluconeogenesis that escapes suppression by insulin (Figure 1.5). We provide evidence that these metabolic alterations are related to BAD's capacity to activate GK. Importantly, hepatic expression of the BAD phosphomimic variant in leptin-resistant and high fat diet models of diabetes and insulin resistance resets the balance between hepatic

glycolysis and gluconeogenesis, counteracts unrestrained gluconeogenesis, and improves glycemia. Collectively, the studies described in Chapters 2 and 3 provide insights into both mechanistic underpinnings and functional relevance of the BAD:GK axis in hepatic substrate metabolism in both normal physiology and pathophysiology.

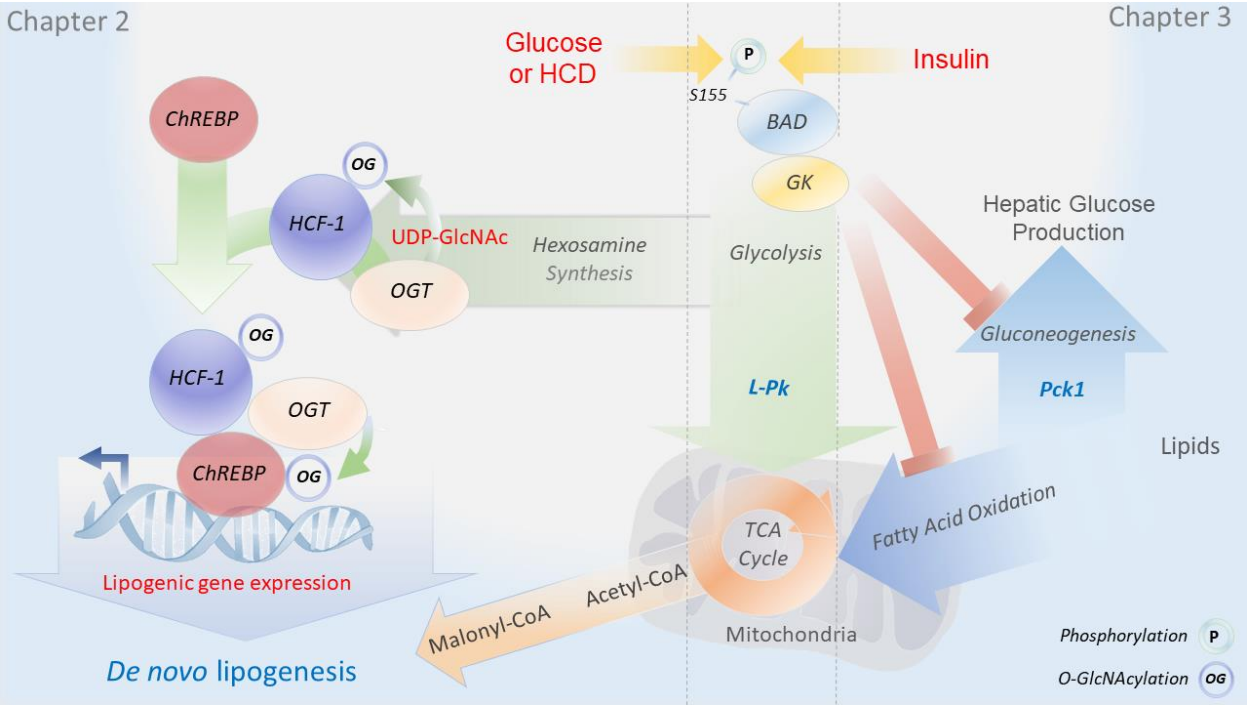


Figure 1.5. Thesis at a glance

Chapter 2: Activation of the BAD:GK pathway promotes *de novo* lipogenesis both by providing biosynthetic precursors in form of malonyl Co-A and by stimulating lipogenic gene expression through ChREBP. Full induction of the ChREBP transcriptional program by glucose requires hexosamine biosynthesis and HCF-1-dependent recruitment of OGT to ChREBP, which increases ChREBP O-GlcNAcylation, stability and activity.

Chapter 3: BAD phosphorylation stimulates a metabolic program in hepatocytes that is characterized by GK activation, increased glycolysis, reduced FAO and gluconeogenesis that is relevant for the homeostatic control of hepatic glucose production.

Abbreviations: HCF-1- Host cell factor 1, OGT- O-GlcNAc transferase, ChREBP- Carbohydrate response element binding protein, BAD- BCL-2-associated Agonist of Cell Death, GK- glucokinase, L-Pk- Liver pyruvate kinase, Pck1- Phosphoenolpyruvate carboxykinase.

References

Abdul-Wahed, A., Guilmeau, S., and Postic, C. (2017). Sweet Sixteenth for ChREBP: Established Roles and Future Goals. Cell Metab *26*, 324-341.

Agius, L. (2016a). Dietary carbohydrate and control of hepatic gene expression: mechanistic links from ATP and phosphate ester homeostasis to the carbohydrate-response element-binding protein. Proc Nutr Soc *75*, 10-18.

Agius, L. (2016b). Hormonal and Metabolite Regulation of Hepatic Glucokinase. Annu Rev Nutr *36*, 389-415.

Alves-Bezerra, M., and Cohen, D.E. (2017). Triglyceride Metabolism in the Liver. Comprehensive Physiology *8*, 1-8.

Anyamaneeratch, K., Rojvirat, P., Sukjoi, W., and Jitrapakdee, S. (2015). Insights into Transcriptional Regulation of Hepatic Glucose Production. International review of cell and molecular biology *318*, 203-253.

Arden, C., Tudhope, S., Petrie, J., Al-Oanzi, Z., Cullen, K., Lange, A., Towle, H., and Agius, L. (2012). Fructose 2,6-bisphosphate is essential for glucose-regulated gene transcription of glucose-6-phosphatase and other ChREBP target genes in hepatocytes. The Biochemical journal *443*, 111-123.

Avruch, J. (1998). Insulin signal transduction through protein kinase cascades. Molecular and cellular biochemistry *182*, 31-48.

Baltrusch, S., Lenzen, S., Okar, D.A., Lange, A.J., and Tiedge, M. (2001). Characterization of glucokinase-binding protein epitopes by a phage-displayed peptide library. Identification of 6-phosphofructo-2-kinase/fructose-2,6-bisphosphatase as a novel interaction partner. J Biol Chem *276*, 43915-43923.

Baltrusch, S., Schmitt, H., Brix, A., Langer, S., and Lenzen, S. (2012). Additive activation of glucokinase by the bifunctional enzyme 6-phosphofructo-2-kinase/fructose-2,6-bisphosphatase and the chemical activator LY2121260. Biochemical pharmacology *83*, 1300-1306.

Banks, A.S., Kim-Muller, J.Y., Mastracci, T.L., Kofler, N.M., Qiang, L., Haeusler, R.A., Jurczak, M.J., Laznik, D., Heinrich, G., Samuel, V.T., et al. (2011). Dissociation of the glucose and lipid regulatory functions of FoxO1 by targeted knockin of acetylation-defective alleles in mice. Cell Metab *14*, 587-597.

Beer, N.L., Tribble, N.D., McCulloch, L.J., Roos, C., Johnson, P.R., Orho-Melander, M., and Gloyn, A.L. (2009). The P446L variant in GCKR associated with fasting plasma glucose and triglyceride levels exerts its effect through increased glucokinase activity in liver. Human molecular genetics *18*, 4081-4088.

Birkenfeld, A.L., and Shulman, G.I. (2014). Nonalcoholic fatty liver disease, hepatic insulin resistance, and type 2 Diabetes. Hepatology (Baltimore, Md.) *59*, 713-723.

Bonneau, B., Prudent, J., Popgeorgiev, N., and Gillet, G. (2013). Non-apoptotic roles of Bcl-2 family: the calcium connection. Biochimica et biophysica acta *1833*, 1755-1765.

Bricambert, J., Miranda, J., Benhamed, F., Girard, J., Postic, C., and Dentin, R. (2010). Salt-inducible kinase 2 links transcriptional coactivator p300 phosphorylation to the prevention of ChREBP-dependent hepatic steatosis in mice. The Journal of clinical investigation *120*, 4316-4331.

Copps, K.D., and White, M.F. (2012). Regulation of insulin sensitivity by serine/threonine phosphorylation of insulin receptor substrate proteins IRS1 and IRS2. Diabetologia *55*, 2565-2582.

Cullen, K.S., Al-Oanzi, Z.H., O'Harte, F.P., Agius, L., and Arden, C. (2014). Glucagon induces translocation of glucokinase from the cytoplasm to the nucleus of hepatocytes by transfer between 6-phosphofructo 2-kinase/fructose 2,6-bisphosphatase-2 and the glucokinase regulatory protein. Biochimica et biophysica acta *1843*, 1123-1134.

Danial, N., Gramm, C., Scorrano, L., Zhang, C.-Y., Krauss, S., Ranger, A., Datta, S., Greenberg, M., Licklider, L., Lowell, B., et al. (2003a). BAD and glucokinase reside in a mitochondrial complex that integrates glycolysis and apoptosis. Nature *424*, 952-956.
Danial, N.N. (2008). BAD: undertaker by night, candyman by day. Oncogene *27 Suppl 1*, S53-70.

Danial, N.N., Walensky, L.D., Zhang, C.Y., Choi, C.S., Fisher, J.K., Molina, A.J., Datta, S.R., Pitter, K.L., Bird, G.H., Wikstrom, J.D., et al. (2008). Dual role of proapoptotic BAD in insulin secretion and beta cell survival. Nature medicine *14*, 144-153.

Davies, M.N., O'Callaghan, B.L., and Towle, H.C. (2008). Glucose activates ChREBP by increasing its rate of nuclear entry and relieving repression of its transcriptional activity. J Biol Chem *283*, 24029-24038.

DeBose-Boyd, R.A., and Ye, J. (2018). SREBPs in Lipid Metabolism, Insulin Signaling, and Beyond. Trends in biochemical sciences *43*, 358-368.

DeFronzo, R.A., Ferrannini, E., Groop, L., Henry, R.R., Herman, W.H., Holst, J.J., Hu, F.B., Kahn, C.R., Raz, I., Shulman, G.I., et al. (2015). Type 2 diabetes mellitus. Nature reviews. Disease primers *1*, 15019.

Dentin, R., Benhamed, F., Hainault, I., Fauveau, V., Foufelle, F., Dyck, J.R., Girard, J., and Postic, C. (2006). Liver-specific inhibition of ChREBP improves hepatic steatosis and insulin resistance in ob/ob mice. Diabetes *55*, 2159-2170.

Dentin, R., Pégorier, J.-P., Benhamed, F., Foufelle, F., Ferré, P., Fauveau, V., Magnuson, M., Girard, J., and Postic, C. (2004). Hepatic glucokinase is required for the synergistic action of ChREBP and SREBP-1c on glycolytic and lipogenic gene expression. The Journal of biological chemistry *279*, 20314-20326.

Dentin, R., Tomas-Cobos, L., Foufelle, F., Leopold, J., Girard, J., Postic, C., and Ferré, P. (2012). Glucose 6-phosphate, rather than xylulose 5-phosphate, is required for the activation of ChREBP in response to glucose in the liver. Journal of hepatology *56*, 199-209.

Detheux, M., Vandercammen, A., and Van Schaftingen, E. (1991). Effectors of the regulatory protein acting on liver glucokinase: a kinetic investigation. European journal of biochemistry *200*, 553-561.

Farrelly, D., Brown, K.S., Tieman, A., Ren, J., Lira, S.A., Hagan, D., Gregg, R., Mookhtiar, K.A., and Hariharan, N. (1999). Mice mutant for glucokinase regulatory protein exhibit decreased liver glucokinase: a sequestration mechanism in metabolic regulation. Proceedings of the National Academy of Sciences of the United States of America *96*, 14511-14516.

Foster, D.W. (2012). Malonyl-CoA: the regulator of fatty acid synthesis and oxidation. The Journal of clinical investigation *122*, 1958-1959.

Giménez-Cassina, A., and Danial, N.N. (2015). Regulation of mitochondrial nutrient and energy metabolism by BCL-2 family proteins. Trends in endocrinology and metabolism: TEM *26*, 165-175.

Giménez-Cassina, A., Garcia-Haro, L., Choi, C.S., Osundiji, M.A., Lane, E.A., Huang, H., Yildirim, M.A., Szlyk, B., Fisher, J.K., Polak, K., et al. (2014). Regulation of hepatic energy metabolism and gluconeogenesis by BAD. Cell metabolism *19*, 272-284.

Grimsby, J., Berthel, S.J., and Sarabu, R. (2008). Glucokinase activators for the potential treatment of type 2 diabetes. Current topics in medicinal chemistry *8*, 1524-1532.

Guinez, C., Filhoulaud, G., Rayah-Benhamed, F., Marmier, S., Dubuquoy, C., Dentin, R., Moldes, M., Burnol, A.F., Yang, X., Lefebvre, T., et al. (2011). O-GlcNAcylation increases ChREBP protein content and transcriptional activity in the liver. Diabetes *60*, 1399-1413.

Guo, S., Copps, K.D., Dong, X., Park, S., Cheng, Z., Pocai, A., Rossetti, L., Sajan, M., Farese, R.V., and White, M.F. (2009). The Irs1 branch of the insulin signaling cascade plays a dominant role in hepatic nutrient homeostasis. Molecular and cellular biology *29*, 5070-5083.

Han, H.S., Kang, G., Kim, J.S., Choi, B.H., and Koo, S.H. (2016). Regulation of glucose metabolism from a liver-centric perspective. Experimental & molecular medicine *48*, e218.

Hardwick, J.M., Chen, Y.B., and Jonas, E.A. (2012). Multipolar functions of BCL-2 proteins link energetics to apoptosis. Trends in cell biology *22*, 318-328.

Hatting, M., Tavares, C.D.J.D.J., Sharabi, K., Rines, A.K., and Puigserver, P. (2018). Insulin regulation of gluconeogenesis. Annals of the New York Academy of Sciences *1411*, 21-35.

Horton, J.D., Goldstein, J.L., and Brown, M.S. (2002). SREBPs: activators of the complete program of cholesterol and fatty acid synthesis in the liver. The Journal of clinical investigation *109*, 1125-1131.

Iizuka, K., Bruick, R.K., Liang, G., Horton, J.D., and Uyeda, K. (2004). Deficiency of carbohydrate response element-binding protein (ChREBP) reduces lipogenesis as well as glycolysis. Proceedings of the National Academy of Sciences of the United States of America *101*, 7281-7286.

Iizuka, K., Miller, B., and Uyeda, K. (2006). Deficiency of carbohydrate-activated transcription factor ChREBP prevents obesity and improves plasma glucose control in leptin-deficient (ob/ob) mice. American journal of physiology. Endocrinology and metabolism *291*, E358-364.

Jiang, G., and Zhang, B.B. (2003). Glucagon and regulation of glucose metabolism. American journal of physiology. Endocrinology and metabolism *284*, E671-678.

Kabashima, T., Kawaguchi, T., Wadzinski, B.E., and Uyeda, K. (2003). Xylulose 5-phosphate mediates glucose-induced lipogenesis by xylulose 5-phosphate-activated protein phosphatase in rat liver. Proceedings of the National Academy of Sciences of the United States of America *100*, 5107-5112.

Kawaguchi, T., Takenoshita, M., Kabashima, T., and Uyeda, K. (2001). Glucose and cAMP regulate the L-type pyruvate kinase gene by phosphorylation/dephosphorylation of the carbohydrate response element binding protein. Proceedings of the National Academy of Sciences of the United States of America *98*, 13710-13715.

Kim, M.S., Krawczyk, S.A., Doridot, L., Fowler, A.J., Wang, J.X., Trauger, S.A., Noh, H.L., Kang, H.J., Meissen, J.K., Blatnik, M., et al. (2016). ChREBP regulates fructose-induced glucose production independently of insulin signaling. The Journal of clinical investigation *126*, 4372-4386.

Kooner, J.S., Chambers, J.C., Aguilar-Salinas, C.A., Hinds, D.A., Hyde, C.L., Warnes, G.R., Gomez Perez, F.J., Frazer, K.A., Elliott, P., Scott, J., et al. (2008). Genome-wide scan identifies variation in MLXIPL associated with plasma triglycerides. Nature genetics *40*, 149-151.

Lee, J., Choi, J., Selen Alpergin, E.S., Zhao, L., Hartung, T., Scafidi, S., Riddle, R.C., and Wolfgang, M.J. (2017). Loss of Hepatic Mitochondrial Long-Chain Fatty Acid Oxidation Confers Resistance to Diet-Induced Obesity and Glucose Intolerance. Cell Rep *20*, 655-667.

Li, M.V., Chang, B., Imamura, M., Poungvarin, N., and Chan, L. (2006). Glucose-dependent transcriptional regulation by an evolutionarily conserved glucose-sensing module. Diabetes *55*, 1179-1189.

Liao, J., Barthel, A., Nakatani, K., and Roth, R.A. (1998). Activation of protein kinase B/Akt is sufficient to repress the glucocorticoid and cAMP induction of phosphoenolpyruvate carboxykinase gene. J Biol Chem *273*, 27320-27324.

Lin, H., and Accili, D. (2011). Hormonal regulation of hepatic glucose production in health and disease. Cell metabolism *14*, 9-19.

Ljubicic, S., Polak, K., Fu, A., Wiwczar, J., Szlyk, B., Chang, Y., Alvarez-Perez, J.C., Bird, G.H., Walensky, L.D., Garcia-Ocaña, A., et al. (2015). Phospho-BAD BH3 mimicry protects β cells and restores functional β cell mass in diabetes. Cell reports *10*, 497-504.

Lu, M., Wan, M., Leavens, K.F., Chu, Q., Monks, B.R., Fernandez, S., Ahima, R.S., Ueki, K., Kahn, C.R., and Birnbaum, M.J. (2012). Insulin regulates liver metabolism in vivo in the absence of hepatic Akt and Foxo1. Nature medicine *18*, 388-395.

Ma, L., Tsatsos, N.G., and Towle, H.C. (2005). Direct role of ChREBP.Mlx in regulating hepatic glucose-responsive genes. The Journal of biological chemistry *280*, 12019-12027.
Matschinsky, F.M. (2009). Assessing the potential of glucokinase activators in diabetes therapy. Nat Rev Drug Discov *8*, 399-416.

Matschinsky, F.M. (2013). GKAs for diabetes therapy: why no clinically useful drug after two decades of trying? Trends in pharmacological sciences *34*, 90-99.

McFerrin, L.G., and Atchley, W.R. (2012). A novel N-terminal domain may dictate the glucose response of Mondo proteins. PloS one *7*, e34803.

Meininger, G.E., Scott, R., Alba, M., Shentu, Y., Luo, E., Amin, H., Davies, M.J., Kaufman, K.D., and Goldstein, B.J. (2011). Effects of MK-0941, a novel glucokinase activator, on glycemic control in insulin-treated patients with type 2 diabetes. Diabetes care *34*, 2560-2566.

Michael, M.D., Kulkarni, R.N., Postic, C., Previs, S.F., Shulman, G.I., Magnuson, M.A., and Kahn, C.R. (2000). Loss of insulin signaling in hepatocytes leads to severe insulin resistance and progressive hepatic dysfunction. Molecular cell *6*, 87-97.

Nakagawa, T., Ge, Q., Pawlosky, R., Wynn, R.M., Veech, R.L., and Uyeda, K. (2013). Metabolite regulation of nucleo-cytosolic trafficking of carbohydrate response element-binding protein (ChREBP): role of ketone bodies. The Journal of biological chemistry *288*, 28358-28367.
Newgard, C.B. (2012). Interplay between lipids and branched-chain amino acids in development of insulin resistance. Cell Metab *15*, 606-614.

Nissim, I., Horyn, O., Nissim, I., Daikhin, Y., Wehrli, S.L., Yudkoff, M., and Matschinsky, F.M. (2012). Effects of a glucokinase activator on hepatic intermediary metabolism: study with 13C-isotopomer-based metabolomics. Biochem J *444*, 537-551.

Okar, D.A., Wu, C., and Lange, A.J. (2004). Regulation of the regulatory enzyme, 6-phosphofructo-2-kinase/fructose-2,6-bisphosphatase. Advances in enzyme regulation *44*, 123-154.

Oosterveer, M.H., and Schoonjans, K. (2013). Hepatic glucose sensing and integrative pathways in the liver. Cellular and molecular life sciences : CMLS.

Orho-Melander, M., Melander, O., Guiducci, C., Perez-Martinez, P., Corella, D., Roos, C., Tewhey, R., Rieder, M.J., Hall, J., Abecasis, G., et al. (2008). Common missense variant in the glucokinase regulatory protein gene is associated with increased plasma triglyceride and C-reactive protein but lower fasting glucose concentrations. Diabetes *57*, 3112-3121.

Owen, J.L., Zhang, Y., Bae, S.-H., Farooqi, M.S., Liang, G., Hammer, R.E., Goldstein, J.L., and Brown, M.S. (2012). Insulin stimulation of SREBP-1c processing in transgenic rat hepatocytes requires p70 S6-kinase. Proceedings of the National Academy of Sciences *109*, 16184-16189.

Petersen, M.C., Vatner, D.F., and Shulman, G.I. (2017). Regulation of hepatic glucose metabolism in health and disease. Nature reviews. Endocrinology *13*, 572-587.

Pfefferkorn, J.A., Guzman-Perez, A., Litchfield, J., Aiello, R., Treadway, J.L., Pettersen, J., Minich, M.L., Filipski, K.J., Jones, C.S., Tu, M., et al. (2012). Discovery of (S)-6-(3-cyclopentyl-2-(4-(trifluoromethyl)-1H-imidazol-1-yl)propanamido)nicotini c acid as a hepatoselective glucokinase activator clinical candidate for treating type 2 diabetes mellitus. Journal of medicinal chemistry *55*, 1318-1333.

Postic, C., Dentin, R., and Girard, J. (2004). Role of the liver in the control of carbohydrate and lipid homeostasis. Diabetes & metabolism *30*, 398-408.

Postic, C., Shiota, M., Niswender, K.D., Jetton, T.L., Chen, Y., Moates, J.M., Shelton, K.D., Lindner, J., Cherrington, A.D., and Magnuson, M.A. (1999). Dual roles for glucokinase in glucose

homeostasis as determined by liver and pancreatic beta cell-specific gene knock-outs using Cre recombinase. J Biol Chem *274*, 305-315.

Rees, M.G., Wincovitch, S., Schultz, J., Waterstradt, R., Beer, N.L., Baltrusch, S., Collins, F.S., and Gloyn, A.L. (2012). Cellular characterisation of the GCKR P446L variant associated with type 2 diabetes risk. Diabetologia *55*, 114-122.

Sakiyama, H., Fujiwara, N., Noguchi, T., Eguchi, H., Yoshihara, D., Uyeda, K., and Suzuki, K. (2010). The role of O-linked GlcNAc modification on the glucose response of ChREBP. Biochem Biophys Res Commun *402*, 784-789.

Samuel, V.T., and Shulman, G.I. (2016). The pathogenesis of insulin resistance: integrating signaling pathways and substrate flux. The Journal of clinical investigation *126*, 12.

Samuel, V.T., and Shulman, G.I. (2018). Nonalcoholic Fatty Liver Disease as a Nexus of Metabolic and Hepatic Diseases. Cell metabolism *27*, 22-41.

Sanders, F.W., and Griffin, J.L. (2016). De novo lipogenesis in the liver in health and disease: more than just a shunting yard for glucose. Biol Rev Camb Philos Soc *91*, 452-468.

Sarabu, R., Bizzarro, F.T., Corbett, W.L., Dvorozniak, M.T., Geng, W., Grippo, J.F., Haynes, N.E., Hutchings, S., Garofalo, L., Guertin, K.R., et al. (2012). Discovery of piragliatin--first glucokinase activator studied in type 2 diabetic patients. Journal of medicinal chemistry *55*, 7021-7036.

Satapati, S., Sunny, N.E., Kucejova, B., Fu, X., He, T.T., Méndez-Lucas, A., Shelton, J.M., Perales, J.C., Browning, J.D., and Burgess, S.C. (2012). Elevated TCA cycle function in the pathology of diet-induced hepatic insulin resistance and fatty liver. Journal of lipid research *53*, 1080-1092.

Sato, S., Jung, H., Nakagawa, T., Pawlosky, R., Takeshima, T., Lee, W.-R.R., Sakiyama, H., Laxman, S., Wynn, R.M., Tu, B.P., et al. (2016). Metabolite Regulation of Nuclear Localization of Carbohydrate-response Element-binding Protein (ChREBP): ROLE OF AMP AS AN ALLOSTERIC INHIBITOR. The Journal of biological chemistry *291*, 10515-10527.

Stoeckman, A.K., Ma, L., and Towle, H.C. (2004). Mlx is the functional heteromeric partner of the carbohydrate response element-binding protein in glucose regulation of lipogenic enzyme genes. J Biol Chem *279*, 15662-15669.

Szlyk, B., Braun, C.R., Ljubicic, S., Patton, E., Bird, G.H., Osundiji, M.A., Matschinsky, F.M., Walensky, L.D., and Danial, N.N. (2014). A phospho-BAD BH3 helix activates glucokinase by a mechanism distinct from that of allosteric activators. Nature structural & molecular biology *21*, 36-42.

Tikhanovich, I., Cox, J., and Weinman, S.A. (2013). Forkhead box class O transcription factors in liver function and disease. Journal of gastroenterology and hepatology *28 Suppl 1*, 125-131.
Titchenell, P.M., Lazar, M.A., and Birnbaum, M.J. (2017). Unraveling the Regulation of Hepatic Metabolism by Insulin. Trends in endocrinology and metabolism: TEM *28*, 497-505.

Tokarz, V.L., MacDonald, P.E., and Klip, A. (2018). The cell biology of systemic insulin function. The Journal of cell biology.

Tsatsos, N., and Towle, H. (2006). Glucose activation of ChREBP in hepatocytes occurs via a two-step mechanism. Biochemical and biophysical research communications *340*, 449-456.
Uyeda, K., and Repa, J. (2006). Carbohydrate response element binding protein, ChREBP, a transcription factor coupling hepatic glucose utilization and lipid synthesis. Cell metabolism *4*, 107-110.

Velho, G., Petersen, K.F., Perseghin, G., Hwang, J.H., Rothman, D.L., Pueyo, M.E., Cline, G.W., Froguel, P., and Shulman, G.I. (1996). Impaired hepatic glycogen synthesis in glucokinase-deficient (MODY-2) subjects. The Journal of clinical investigation *98*, 1755-1761.
Vial, G., Dubouchaud, H., and Leverve, X.M. (2010). Liver mitochondria and insulin resistance. Acta biochimica Polonica *57*, 389-392.

Wellen, K.E., Hatzivassiliou, G., Sachdeva, U.M., Bui, T.V., Cross, J.R., and Thompson, C.B. (2009). ATP-citrate lyase links cellular metabolism to histone acetylation. Science (New York, N.Y.) *324*, 1076-1080.

Yang, X., and Qian, K. (2017). Protein O-GlcNAcylation: emerging mechanisms and functions. Nat Rev Mol Cell Biol *18*, 452-465.

Yecies, J.L., Zhang, H.H., Menon, S., Liu, S., Yecies, D., Lipovsky, A.I., Gorgun, C., Kwiatkowski, D.J., Hotamisligil, G.S.S., Lee, C.-H.H., et al. (2011). Akt stimulates hepatic SREBP1c and lipogenesis through parallel mTORC1-dependent and independent pathways. Cell metabolism *14*, 21-32.

CHAPTER 2

HCF-1 Links BAD-mediated Glucose Signaling to *de Novo* Lipogenesis through ChREBP Regulation

SUMMARY

Carbohydrate response element binding protein (ChREBP) has emerged as a key transcription factor regulating *de novo* lipogenesis (DNL) in response to carbohydrates and in hepatic steatosis. As such, mechanisms underlying nutrient modulation of ChREBP function are under active investigation. We provide genetic and biochemical evidence that phosphorylation of the BCL2 agonist of cell death (BAD), a glucokinase (GK) activating protein, is physiologically relevant for ChREBP activation and hepatic DNL. Further, we identify HCF-1 as a new ChREBP-interacting partner that regulates ChREBP O-GlcNAcylation by recruiting OGT to ChREBP in response to glucose stimulation. Blocking BAD phosphorylation leads to diminished hexosamine biosynthesis, HCF-1 O-GlcNAcylation and its association with OGT and ChREBP, ChREBP O-GlcNAcylation, and lipogenic gene expression. However, GlcNAc supplementation is sufficient to reactivate the HCF-1:ChREBP module in the absence of BAD. Importantly, phospho-BAD and HCF-1 levels are elevated in liver biopsies of NASH patients consistent with increased DNL in this setting.

INTRODUCTION

Metabolic adaptation to fed and fasted states is intricately controlled by nutrient and hormonal signals. In the fed state, the liver stores glucose as glycogen, and once glycogen stores are replete, it converts excess glucose to fat through *de novo* lipogenesis (DNL), a process regulated by insulin and glucose-derived metabolic signals (Abdul-Wahed et al., 2017; Sanders and Griffin, 2016; Uyeda and Repa, 2006; Yecies et al., 2011). While storage of excess glucose as lipids is an important component of metabolic adaptation, excessive DNL is associated with pathologies such as nonalcoholic fatty liver disease (NAFLD), where up to 30% of hepatic fat accumulation can be linked to increased hepatic DNL (Donnelly et al., 2005; Softic et al., 2016). NAFLD often co-segregates with obesity, diabetes, metabolic syndrome and cardiovascular disease (Perumpail et al., 2017; Samuel and Shulman, 2018).

Glucose metabolism provides both biosynthetic precursors and regulatory signals for DNL, and evidence indicates that the Carbohydrate Response Element Binding Protein (ChREBP) is an important transcription factor and effector of glucose-derived signals in this process (Abdul-Wahed et al., 2017; Agius, 2016a; Alves-Bezerra and Cohen, 2017; Uyeda and Repa, 2006). Notably, polymorphisms in *ChREBP* are linked to increased plasma triglycerides (Kooner et al., 2008), and increased ChREBP protein levels are associated with human NAFLD (Benhamed et al., 2012). Beyond DNL, ChREBP-dependent transcriptional programs may also constitute a mechanism for modulating hepatic ATP homeostasis in response to excess carbohydrate and in NAFLD. This is consistent with the observation that hepatic ChREBP targets include genes that down regulate phosphate ester pools to preserve hepatic Pi and ATP (Agius, 2016a). Several glucose-derived metabolites can activate ChREBP, including G6P (glucose-6-phosphate), F2-6BP (fructose-2,6-bisphosphate) and X5P (xyulose-5-phosphate) (Arden et al., 2012; Dentin et al., 2012; Iizuka et al., 2013). There is some evidence that X5P can trigger dephosphorylation and nuclear translocation of ChREBP through activation of protein phosphatase 2A (PP2A) (Kabashima et al., 2003). However, ChREBP phospho-mutants remain glucose responsive

(Tsatsos and Towle, 2006), and a pool of ChREBP resides in the nucleus even in the absence of glucose stimulation (Davies et al., 2008; Kim et al., 2016), indicating the existence of additional glucose-dependent regulatory mechanisms apart from ChREBP phosphorylation status and nuclear translocation. Additional glucose-derived metabolic signals in the form of acetyl-CoA and UDP-N-acetylglucosamine (UDP-GlcNAc) can activate ChREBP through acetylation and O-GlcNAcylation, respectively (Bricambert et al., 2010; Guinez et al., 2011; Sakiyama et al., 2010; Yang and Qian, 2017). Specifically, increased glucose metabolism can augment UDP-GlcNAc pools through the hexosamine biosynthesis pathway, and O-GlcNAcylation of ChREBP increases its DNA binding affinity, transcriptional activity, and protein stability (Guinez et al., 2011; Sakiyama et al., 2010; Yang et al., 2017). However, the mechanisms controlling ChREBP O-GlcNAcylation are not fully understood.

The myriad of glucose-dependent signals that converge on ChREBP reflect a complex network of mechanisms controlling gene expression in response to glucose and carbohydrate surplus. In the liver, these signals are controlled by the glucose phosphorylating enzyme glucokinase (GK), the product of the maturity onset diabetes of the young type 2 (MODY2) gene (Matschinsky, 2009; Nissim et al., 2012). In the fed state, hepatic GK regulates glucose utilization and storage by stimulating glycogen and lipid synthesis while suppressing hepatic glucose production (Dentin et al., 2004; Postic et al., 1999; Velho et al., 1996). Genetic evidence also indicates that GK is required for activation of ChREBP by glucose and carbohydrate feeding (Dentin et al., 2004). Hepatic GK activity is regulated by a number of binding partners including GKRP (glucokinase regulatory protein), PFK2/FBP2 (6-phosphofructo-2-kinase/fructose 2,6-bisphosphatase) and BAD (BCL-2-associated Agonist of Cell Death) [reviewed in (Agius, 2016b)]. These endogenous modulators of GK could be components of additional signaling pathways that exert physiologic control over ChREBP activation in response to lipogenic signals. However, given multiple mechanisms that control hepatic GK activity (Agius, 2016a), it is unclear whether any given GK modulatory protein would be singularly relevant in this process. BAD activates GK when

phosphorylated at serine 155 within its BH3 (BCL2 homology 3) domain downstream of the insulin signaling pathway, independent of its capacity to bind other BCL-2 family proteins (Agius, 2016b; Danial et al., 2003; Gimenez-Cassina and Danial, 2015; Giménez-Cassina et al., 2014). This involves direct binding of the BAD BH3 helix near the active site of the enzyme (Szlyk et al., 2014). Activation of GK by phosphorylated BAD stimulates hepatic glucose utilization while suppressing gluconeogenesis and fatty acid oxidation (Giménez-Cassina et al., 2014). However, whether BAD phosphorylation is relevant to DNL analogous to GK activation as part of broader effects on hepatic substrate metabolism is not known and could not be predicted given the multitude of hormonal and nutrient signals that can regulate hepatic GK activity and lipid synthesis. Here, we investigate the necessity and sufficiency of BAD phosphorylation for DNL following glucose stimulation of primary hepatocytes or carbohydrate overload in the liver. Having found that BAD is required for ChREBP activation by glucose, we also utilize the wild type (WT) and BAD-deficient hepatocyte system as a discovery platform to gain new insights into how ChREBP is normally activated in response to glucose. Specifically, unbiased ChREBP-interaction proteomics under the setting where glucose stimulation of ChREBP is intact (WT) versus impaired (BAD-deficiency) led to the identification of Host Cell Factor 1 (HCF-1) as a previously unknown ChREBP binding protein. We show that HCF-1 resides at the promoters of lipogenic genes, and regulates ChREBP O-GlcNAcylation and transcriptional activity downstream of the hexosamine biosynthesis pathway in response to glucose stimulation.

RESULTS

Glucose stimulation of ChREBP activity and *de novo* lipogenesis are altered upon BAD modification

To initially assess BAD's relevance in glucose modulation of hepatic lipogenesis, we undertook ^{14}C glucose tracer studies and quantified incorporation of glucose carbons in lipid fractions in *Bad* +/+ and *Bad* -/- primary hepatocytes following incubation with low and high glucose concentrations (5 and 25 mM, respectively). Compared to *Bad* +/+ (WT) hepatocytes in which glucose stimulation elicited a robust increase in DNL, the contribution of glucose to lipid synthesis was significantly lower in *Bad* -/- hepatocytes (Figure 2.1A). This defect was fully reversed by genetic reconstitution with the adenovirally expressed phosphomimic BAD S155D variant capable of activating GK but not the phospho-deficient BAD AAA variant, harboring triple Ala mutations within the BAD BH3 domain (L151A, S155A, and D156A) that blunt its GK-activating capacity (Danial et al., 2008; Giménez-Cassina et al., 2014) (Figures 2.1A, 2.2 and 2.3A). Notably, expression of the BAD S155D variant did not lead to additional augmentation of lipogenesis in WT hepatocytes beyond the level seen in GFP-expressing control hepatocytes (Figure 2.1A, *Bad* +/+: BAD S155D vs *Bad* +/+: GFP). These observations suggest that, at least in this acute setting, phospho-BAD does not lead to hyper-stimulation of the lipogenic program by glucose.

Hepatic lipogenesis is substantially regulated at the transcriptional level (Wang et al., 2015), prompting examination of whether BAD-dependent alterations in this pathway are associated with altered lipogenic gene transcription. In the liver, the sterol regulatory element-binding protein-1_C (SREBP-1_C) and ChREBP transcription factors, which have overlapping target genes, mediate the input from insulin and glucose to the lipogenic gene program, respectively (Abdul-Wahed et al., 2017; Agius, 2016b; Herman et al., 2012; Uyeda and Repa, 2006; Yecies et al., 2011). Because our primary focus was on regulation of lipogenesis by glucose, we performed all subsequent measurements in hepatocytes in response to glucose

Figure 2.1. BAD-dependent changes in glucose-induced lipogenic program

(A) Incorporation of glucose carbons into lipids in *Bad* +/+ and -/- hepatocytes reconstituted with the indicated adenoviruses and treated with 1μCi of $U^{14}C$-glucose tracer for 4 hrs. Data are presented as percent increase in label incorporation from 5 to 25 mM glucose (glc) treatment (n=3-4 independent hepatocyte isolations). **(B)** Relative expression of lipogenic genes in *Bad* +/+ and -/- primary hepatocytes reconstituted with the indicated adenoviruses and treated with 5 or 25 mM glucose for 20 hrs (n=5 independent hepatocyte isolations). **(C)** ChoRE luciferase reporter activity in *Bad* +/+ *and* -/- primary hepatocytes treated as in (B). Data are represented as percent increase in reporter activity upon glucose stimulation (n=4 independent hepatocyte isolations). **(D)** Relative occupancy of ChREBP at *L-Pk* and *Acc* promoters in *Bad* +/+ and -/- primary hepatocytes reconstituted with the indicated adenoviruses and treated with 5 or 25 mM glucose for 4 hrs (n=7 independent hepatocyte isolations). **(E)** Relative occupancy of ChREBP at the promoters of *L-Pk* and *Acc* in livers of *Bad* +/+ and -/- mice reconstituted with the indicated adenoviruses one week prior to being fasted for 24 hrs and refed a HCD for 18 hrs (n=3-4 independent mice per condition).

Error bars in A-E are means ± SEM, *$p < 0.05$; **$p < 0.01$; ***$p < 0.001$; n.s., nonsignificant; one way ANOVA (A,C) or two way ANOVA (B, D, E).

Gene abbreviations in (B): *L-PK*, liver pyruvate kinase; *Acly*, ATP citrate lyase; *Acc1*, acetyl-CoA carboxylase 1; *Fas*, fatty acid synthase; *Elovl6*, Elovl fatty acid elongase 6; *scd-1*, stearoyl-CoA desaturase; *Chrebp*, carbohydrate response element binding protein; *Srebp-1c*, sterol regulatory element-binding protein-1_C; *Pdhk*, pyruvate dehydrogenase kinase.

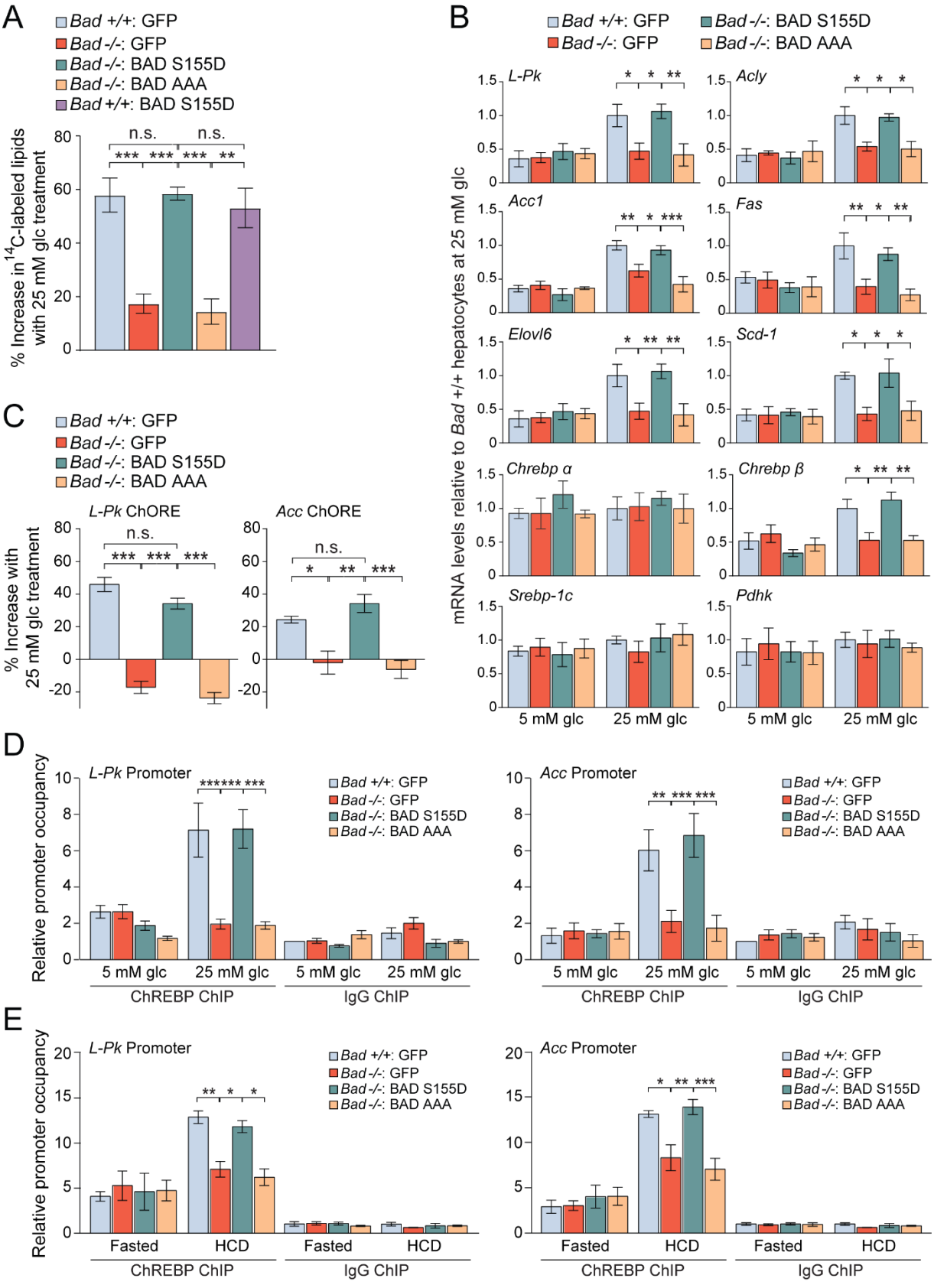


Figure 2.1. (Continued)

A

BAD BH3 Variants	GK-Activating Capacity	Binding to BCL-2 Family Partners
Wild-type L W A A Q R Y G R E L R R M S D E F E G S F K G L	+	+
S155D L W A A Q R Y G R E L R R M D D E F E G S F K G L	+	-
S155A L W A A Q R Y G R E L R R M A D E F E G S F K G L	-	+
AAA (L151A, S155A, D156A) L W A A Q R Y G R E A R R M A A E F E G S F K G L	-	-

B

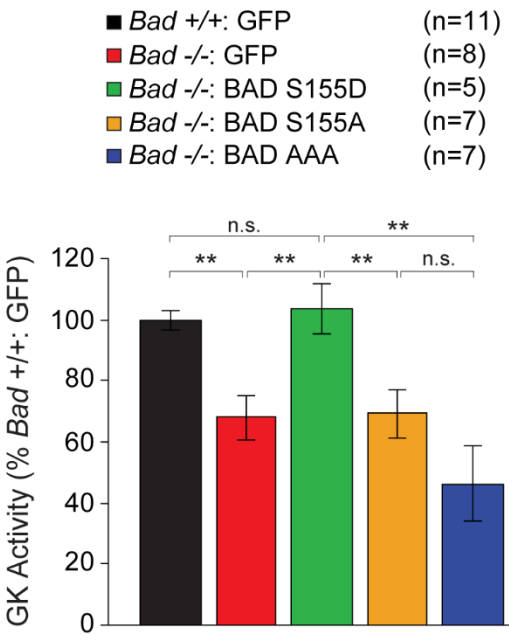


Figure 2.2. BAD's hepatic function is modulated by its phosphorylation status.

(A) BAD phospho-variants used in reconstitution studies. The effect of each mutation on BAD's dual functions or interaction partners is summarized. **(B)** Hepatic GK activity in Bad +/+ and -/- mice after tail vein delivery of the indicated adenoviruses.

Error bars, ± SEM. **p < 0.01; n.s., non-significant.

Figure 2.3. The effect of BAD modifications on lipogenic gene expression

(A) BAD protein levels in *Bad* +/+ and -/- primary hepatocytes after reconstitution with the indicated adenoviruses. **(B)** Time course of changes in *L-Pk* transcription in WT primary hepatocytes treated with 5 or 25 mM glucose (n=4 experimental repeats from hepatocytes derived from 2 mice per genotype). For all subsequent gene expression analyses, glucose treatment was carried out for 20 hrs. **(C-D)** Relative expression of hepatic lipogenic genes in livers of *Bad* +/+ and -/- mice reconstituted with the indicated adenoviruses one week prior to being fasted for 24 hrs and refed a HCD for 18 hrs (C), (n=3-4 mice per condition). Western blots in (D) show protein levels of BAD in livers samples used in (C). **(E)** Relative expression of lipogenic genes in epididymal fat pads of *Bad* +/+ and -/- mice treated as in (C), (n=3 mice per condition). **(F)** Immunoblot analysis and quantification of relative BAD phosphorylation on S155 in liver samples from C57BL/6J mice fasted for 24hrs or fasted then refed a HCD for 18hrs (n=2-3 mice per condition). **(G)** Immunoblot analysis and quantification of relative BAD phosphorylation on S155 in primary hepatocytes from C57BL/6J cultured in 5 or 25 mM glucose for 4 hrs (n=3).

Error bars in B,C, E-G are means ± SEM, *$p < 0.05$; **$p < 0.01$; ***$p < 0.001$; two way ANOVA (B, C, E) or Student's t test (F, G).

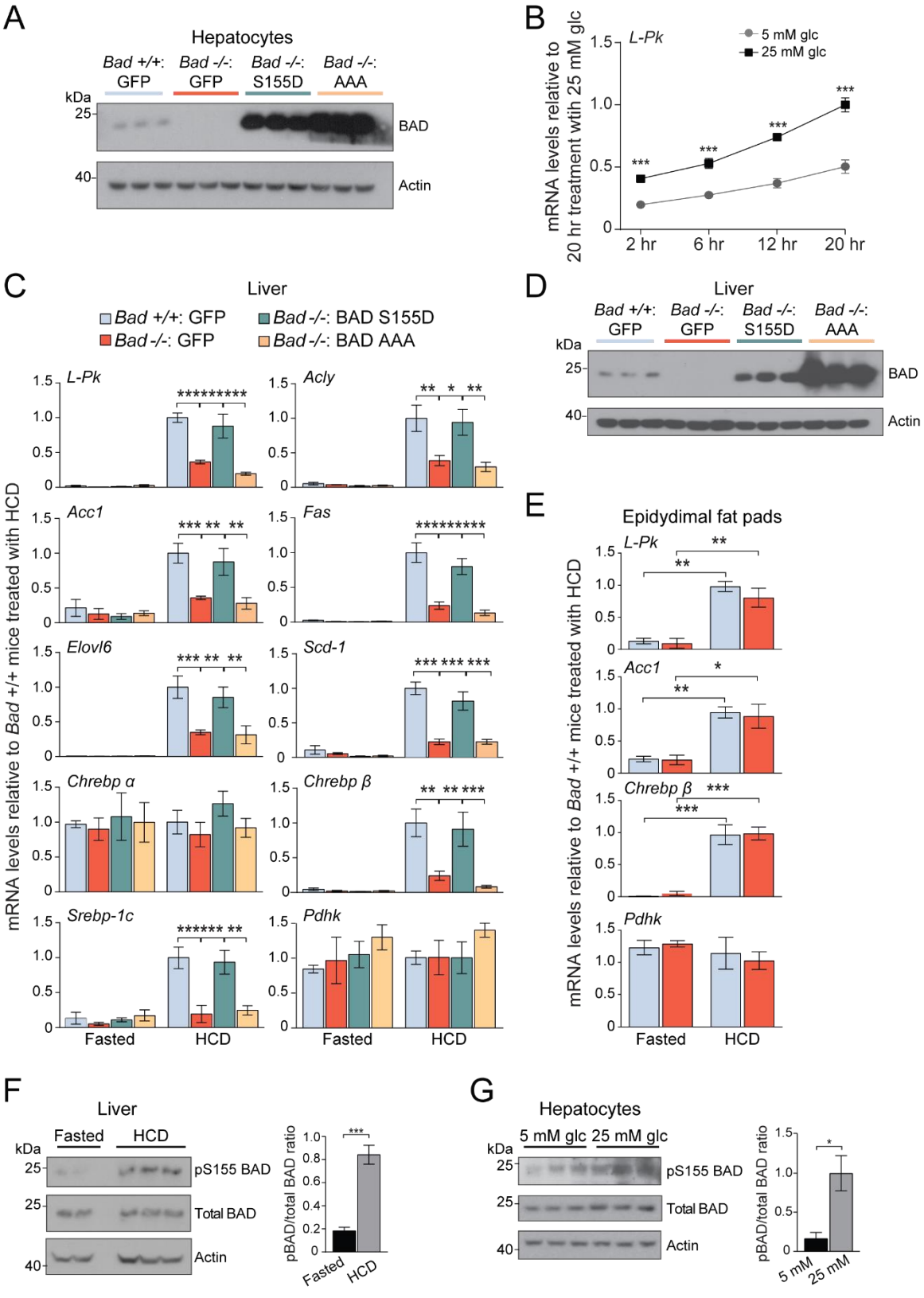


Figure 2.3. (Continued)

alone without insulin stimulation (Ishii et al., 2004; Petrie et al., 2013). As expected, substantial increase in the mRNA abundance of lipogenic genes was observed upon glucose stimulation of WT (*Bad* +/+: GFP) hepatocytes (Figures 2.1B and 2.3B). ChREBPα mRNA levels were not substantially regulated by glucose but those of the ChREBPβ isoform were induced (Figure 2.1B). This is consistent with previous reports that glucose regulates the ChREBPα isoform post translationally, while ChREBPβ expression is regulated by ChREBPα activity (Havula and Hietakangas, 2012; Herman et al., 2012; Stamatikos et al., 2016). In BAD-deficient hepatocytes, glucose induction of mRNAs for lipogenic genes was significantly blunted (Figure 2.1B, *Bad* -/-: GFP, and Table 2.1). However, the expression of other genes whose transcription is not glucose responsive, such as *ChREBPα*, *SREBP-1*$_C$ and pyruvate dehydrogenase kinase (*Pdhk*) (Deng et al., 2002; Stamatikos et al., 2016; Zhang et al., 2015), was comparable in *Bad* +/+ and *-/-* hepatocytes stimulated with glucose (Figure 2.1B). As in lipogenesis assays (Figure 2.1A), BAD S155D but not AAA restored glucose induction of lipogenic gene transcripts in *Bad -/-* hepatocytes (Figure 2.1B).

The observation that BAD modifications affect the transcriptional output in response to glucose warranted examination of ChREBP activity. To this end, we used two complementary functional readouts; luciferase reporters containing the Carbohydrate Response Elements (ChoREs) of *L-Pk* and *Acc* genes and chromatin immunoprecipitation (ChIP) assays to examine promoter occupancy of ChREBP at target genes. Glucose induction of ChoRE reporters and recruitment of ChREBP to endogenous promoters of *L-Pk* and *Acc* genes were significantly lower in *Bad* -/- compared to *Bad* +/+ primary hepatocytes, but were restored to WT levels following genetic rescue with the GK-activating BAD S115D but not the BAD AAA mutant (Figures 2.1C and D). As an *in vivo* correlate to our findings in hepatocyte cultures, we also examined the effect of BAD modifications on hepatic ChREBP activity and the lipogenic gene program in liver biopsies from *Bad* +/+ and -/- mice subjected to short term (18 hr) high-carbohydrate diet (HCD)

Table 2.1. qPCR Primers

Primer Name	Sequence
L-PK F	ctg gaa cac ctc tgc ctt ctg
L-Pk R	cac aat ttc cac ctc cga ctc
Acc1 F	aca gtg gag cta gaa ttg gac
Acc1 R	act tcc cga cca agg act ttg
Scd1 F	ccg gag acc ctt aga tcg a
Scd1 R	tag cct gta aaa gat ttc tgc aaa cc
Elovl6 F	gaa caa gcg agc caa gtt tg
Elovl6 R	tgt aag cac cag ttc gaa gag
Fas F	agc ggc cat ttc cat tgc cc
Fas R	cca tgc cca gag ggt ggt tg
Chrebpα F	ttg ttc agc cgg atc ttg tc
Chrebpα R	agc atc gat ccg aca ctc ac
Chrebpβ F	tct gca gat cgc gtg gag
Chrebpβ R	ctt gtc ccg gca tag caa
Srebp1c F	aac gtc act tcc agc tag ac
Srebp1c R	cca cta agg tgc cta cag agc
Acly F	gaa gct gac ctt gct gaa cc
Acly R	ctg cct cca atg atg agg at
Me F	gcc ggc tct atc ctc ctt tg
Me R	ttt gta tgc atc ttg cac aat ctt t
Pdhk F	tct aac gtc gcc aga att aaa gc
Pdhk R	gga acg tac acg atg tgg att
CycD F	atg gca ctg gcg gca ggt cc
CycD R	ttg cca ttc ctg gac cca aa
L-Pk ChORE F	gtc cca cac ttt gga agc at
L-Pk ChORE R	ccc aac act gat tct acc c
Acc1 ChORE F	gag gcc agt ttc cac tga ct
Acc1 ChORE R	tgg att gcc aat gat cac t

feeding; a treatment known to activate hepatic ChREBP and lipogenesis (Agius, 2016a; Denechaud et al., 2008). In *Bad* -/- liver, both ChREBP binding to *L-Pk* and *Acc* gene promoters and transcriptional induction of lipogenic genes in response to HCD treatment were significantly attenuated (Figures 2.1E, 2.3C and D). These effects were specific to the liver as induction of lipogenic genes by HCD was comparable in *Bad* +/+ and -/- epididymal fat pads in the same animal cohorts (Figure 2.3E). This is consistent with the fact that GK, which is required for hepatic ChREBP activation (Dentin et al., 2004), is not expressed in adipose tissue, indicating that the BAD-GK pathway is irrelevant in this tissue. Hepatic reconstitution of *Bad* -/- mice with adenoviruses encoding BAD S155D or AAA corroborated our findings in primary hepatocytes that BAD phosphorylation is required for full induction of ChREBP activity and expression of lipogenic genes (Figures 2.1E, 2.3C and D). Notably, BAD phosphorylation on S155 within its BH3 domain is normally induced in liver upon HCD feeding or in primary hepatocytes following glucose stimulation (Figures 2.3F and G), garnering further support for the utility of BAD BH3 phospho-mutants in dissecting the physiologic relevance of this post translational modification in nutrient control of DNL.

BAD's effect on lipogenesis is mediated by ChREBP

Attenuation of glucose-induced lipogenesis in BAD-deficient hepatocytes and liver occurs concurrently with diminished ChREBP activity. Likewise, the rescue of lipogenesis by BAD S155D in these settings is associated with restoration of ChRBEP transcriptional activity (Figures 2.1C, D and E). This would be consistent with the GK-activating property of BAD S155D and restoration of glucose signals that are believed to trigger ChREBP activation (Abdul-Wahed et al., 2017). However, these data do not provide evidence for a cause-and-effect relationship between phospho-BAD and ChREBP activity that could account for BAD-dependent changes in DNL. To directly address this possibility, we tested the effects of BAD S155D on DNL in the context of ChREBP deficiency. *Chrebp* knockdown in *Bad* +/+ primary hepatocytes led to diminished DNL and transcriptional induction of lipogenic genes in response to glucose

Figure 2.4. ChREBP is required for BAD's effect on lipogenesis.

(A) Incorporation of glucose carbons into lipids in *Bad* +/+ and -/- hepatocytes co-infected with the indicated adenoviruses and treated with 1μCi of $U^{14}C$-glucose tracer for 4 hrs. Data are presented as percent increase in label incorporation from 5 to 25 mM glucose treatment (n=4 independent hepatocyte isolations). **(B)** Relative mRNA abundance of lipogenic genes in *Bad* +/+ and -/- primary hepatocytes co-infected with the indicated adenoviruses and treated with 5 or 25 mM glucose for 20 hrs (n=4 independent hepatocyte isolations). **(C)** ChREBP protein levels in *Bad* +/+ primary hepatocytes infected with the indicated concentrations of *ChREBP* shRNA-expressing adenovirus. MOI; multiplicity of infection

Error bars are means ± SEM, *p < 0.05; **p < 0.01; ***p < 0.001; n.s., nonsignificant; one way ANOVA (A) or two way ANOVA (B).

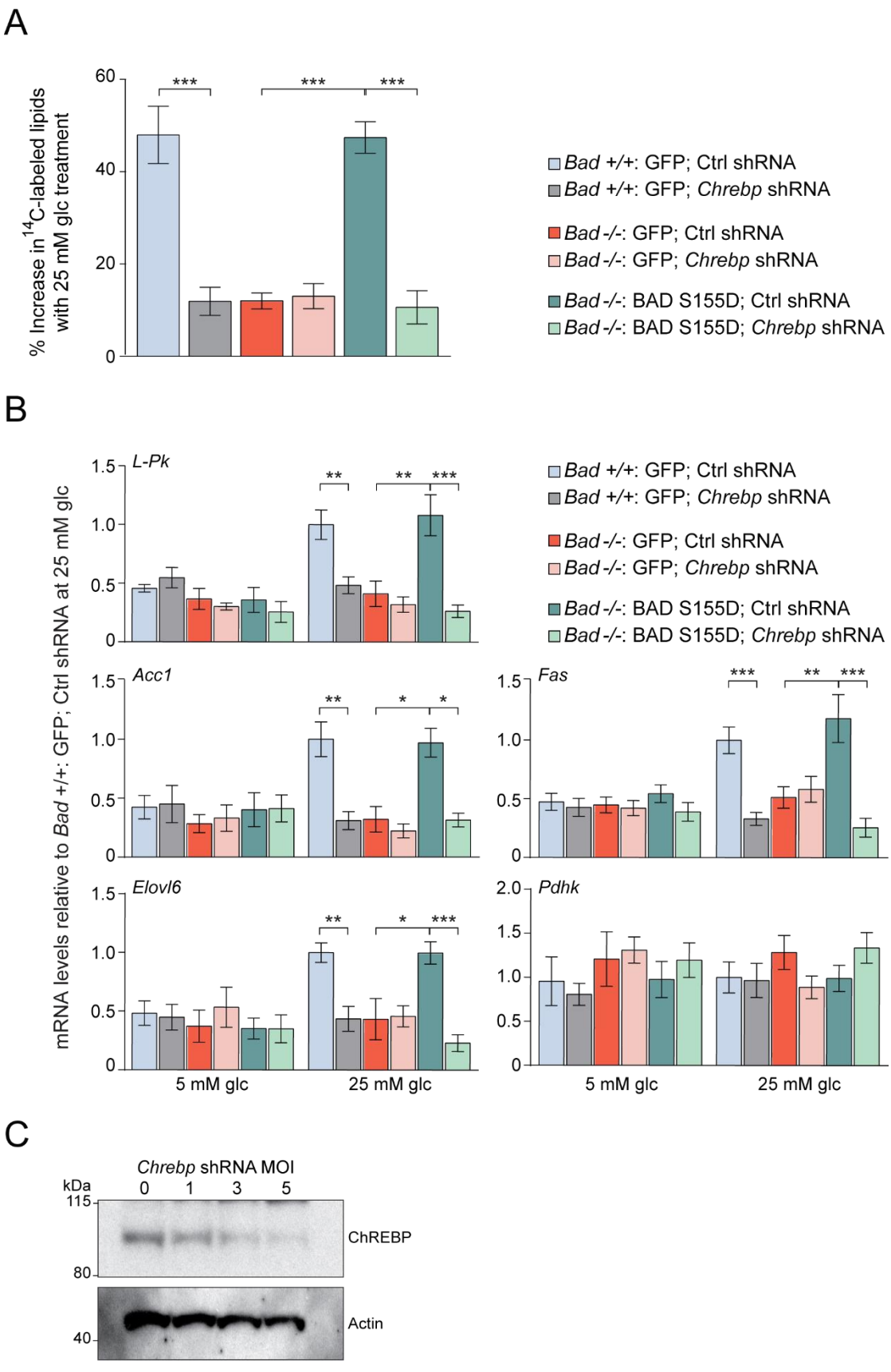


Figure 2.4. (Continued)

consistent with previous reports (Dentin et al., 2006), and completely ablated the ability of BAD S155D to restore lipogenesis in *Bad* -/- hepatocytes (Figures 2.4A, B and C). In *Bad* -/- hepatocytes, ChREBP depletion had no additional effect on reducing DNL (Figures 2.4A and B). Taken together, these data indicate that ChREBP is required for the effect of phospho-BAD on glucose stimulation of lipogenesis.

HCF-1 is a novel ChREBP binding protein that recruits OGT to ChREBP

Given the myriad of mechanisms regulating ChREBP activity (reviewed in (Abdul-Wahed et al., 2017; Agius, 2016a)), we opted for an unbiased approach to determine the possible molecular underpinnings of diminished ChREBP activity in the absence of BAD. To this end, we initially examined changes in ChREBP-containing protein complexes in glucose-stimulated WT hepatocytes compared to BAD-deficient hepatocytes using immunoprecipitation (IP) coupled to mass spectrometry (MS). More significantly, this unbiased approach enabled us to take advantage of the WT and *Bad* -/- hepatocytes, in which glucose induction of ChREBP is preserved or blunted, as a discovery platform to learn about new biochemical mechanisms that can contribute to glucose regulation of ChREBP. To this end, ChREBP was immunoprecipitated from the nuclear fractions of primary *Bad* +/+ and -/- hepatocytes expressing Flag-tagged ChREBP and cultured in 25 mM glucose. Among proteins captured by the anti-Flag antibody in WT hepatocytes, were known ChREBP binding proteins such as Max-like protein X (MLX), a chief partner of ChREBP for transcriptional induction of lipogenic genes (Ma et al., 2006) (Figures 2.5A and B). We then prioritized candidates that were ≥ 3 fold more abundant in ChREBP IPs in WT compared to *Bad* -/- hepatocytes based on spectral counting after normalizing for the efficiency of anti-Flag IP in each genotype, and focused on proteins with direct or indirect functional annotations in gene transcription and glucose signaling using gene ontology, STRING, and DAVID bioinformatic tools. This filtering approach narrowed down our focus to Host Cell Factor (HCF)-1, which was enriched by 3.5 fold in ChREBP IPs of WT

Figure 2.5. Identification of HCF-1 as a novel ChREBP interacting protein

(A) Summary of mass spectrometry (MS) results for ChREBP, Mlx and HCF-1 in anti-Flag immunoprecipates of nuclear fractions from Flag-ChREBP-expressing *Bad* +/+ and -/- hepatocytes treated with 25 mM glucose for 6 hrs. Corrected ratios were calculated by normalizing total peptide spectral counts for each protein to the total peptide spectral counts for ChREBP in each genotype. **(B)** Protein coverage of ChREBP in MS experiment in (A). Sequences underlined in green are peptides captured in the proteomics data set. **(C)** Proteins enriched by 3 fold or more in ChREBP immunoprecipitates from nuclear fractions of *Bad* +/+ and -/- primary hepatocytes treated as in A. **(D)** Representative western blots (left) and quantification of n=3 independent analogous experiments (right) of ChREBP association with HCF-1 and OGT in livers derived from *Bad* +/+ and -/- fasted for 24 hrs and refed with a HCD for 18 hrs.**(E)** Validation of WGA pull down assays for the capture of O-GlcNAcylated ChREBP. O-GlcNAcylated ChREBP capture is competed off following GlcNAc treatment. **(F)** ChREBP protein levels in WT hepatocytes treated with two independent *Hcf-1* siRNAs in the presence of 25 mM glucose.

Error bars in (D) are means ± SEM, *$p < 0.05$; **$p < 0.01$; two way ANOVA.

A

Gene Name	Unique Peptides		Total Peptides		Corrected Ratio *Bad* +/+ to *Bad*-/-	Peptide sequences (*Bad* +/+)
	Bad +/+	*Bad* -/-	*Bad* +/+	*Bad* -/-		
ChREBP	26	26	32	37	1	See panel 2.5B below
Mlx	6	5	6	6	1.6	R.RGAPQLSPESPLLSGAR.G, R.GAPQLSPESPLLSGAR.G, K.VEYAYSDNSLDPGLFVES THK.G, K.KKQEEEVSTLR.K, K.VNYEQIVK.A, K.AHQDNPHEGEDQVSDQVK.F
HCF-1	9	3	9	3	3.5	R.LLVFGGM*VEYGK.Y, R.LGHSFSLVGNK.C, K.VASSPVM*VSNPATR.M, K.VMTSGT GAPAK.I, K.IATGHGQQGVTQVVLK.G, K.GAPGQPGTILR.T, R.TTNTPTVVR.I, K.KQELQPGTAYK.F, R.GPFSEISAFK.T

B

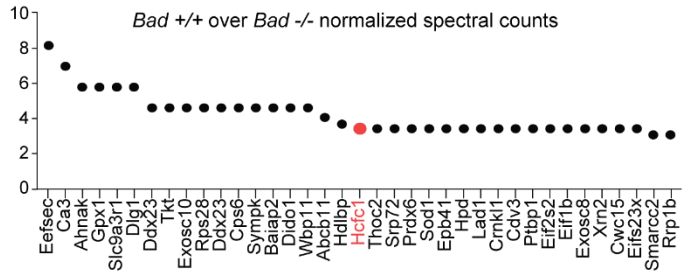
ChREBP Protein coverage in *Bad* +/+ FLAG IP

MARALADLSV NLQVPR**VVPS PDSDSDTDLE DPSPR**RSAGG LHR**SQVIHSG HF MVSSPHSD SLTRRRDQEG PVGLADFGPR** SIDPTLTHLF ECLSLAYSGK LVSPK WKNFK GLKLLCRDKI R**LNNAIWRAW YIQYVQR**RKS PVCGFVTPLQ GSEADEH R**KP EAVILEGNYW KRRIEVVMR**E YHKWRIYYKK RLRKSSREGD FLAPK**QVEG G WPPPER**WCEQ LFSSVVPVLL GGSEEEPGGR QLLDLDCFLS DISDTLFTMT Q PSPSSLQLP PEDAYVGNAD MIQPDLTPLQ PSLDDFMEIS DFFTNYRPPQ TPTS SNYIES PSFGPMADSL FSSGILAPEM PSPASSSSSS GMTPHSGNTR LQARNS CSGP LDPNPFLSSE FLLPEDPKTK IPPAPGPTPL LPFPTPVKVH GLEPCTPSPF PTMAPPPSLL PEESLLSARF PFTSAPPAPG VSTLPAPTTF VPTPQPGPGP VPF SVDHLPH GYLEPVFGPH FTVPQGMQPR CKPSSPSPGG QK**ASPPTLAS ATAS PTATAT AR**DNNPCLTQ LLR**AAKPEQA LEPPTMPGTL LRPPESPQDT VSEIPR**A RAF FPPIPAPTPP RPPPGPATLA PPRSLVVPKA ER**LSPPASSG SER**R**LSGDLN SIQPSGALSV HLSPPQTVLS R**GRVDNNKME NR**RITHISAE QK**RRFNIKLG FDT LHGLVST LSAQPSLK**VS KATTLQK**TAE YILMLQQERA AMQEEAQQLR** DEIEEL NAAI NLCQQQLPAT GVPITHQR**FD QMRDMFDDYV R**TRTLHNWKF WVFSILIRP L FESFNGMVST ASLHSLRQTS LAWLEQYCSL PALRPTVLNS LR**QLSTSTSI LTD PSLVPEQ ATRAVTEGTL GRPL**

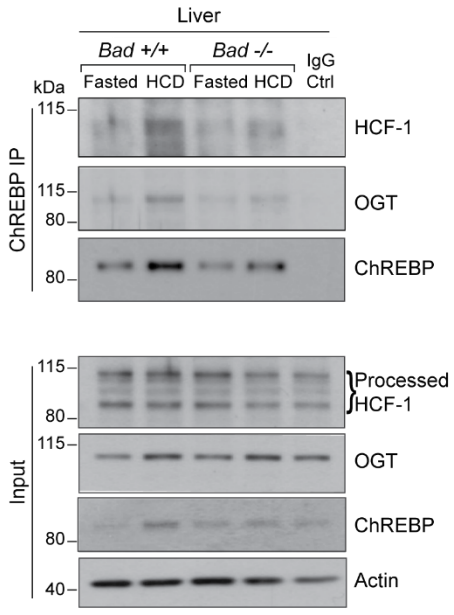
ChREBP Protein coverage in *Bad* -/- FLAG IP

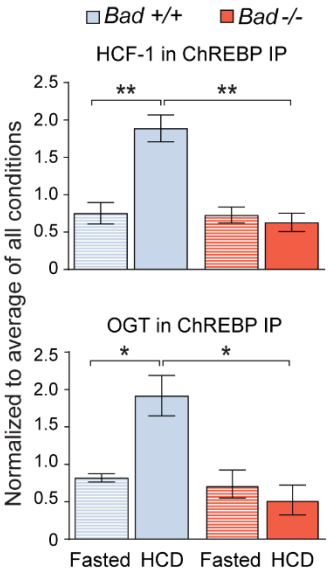
MARALADLSV NLQVPR**VVPS PDSDSDTDLE DPSPR**RSAGG LHR**SQVIHSG HF MVSSPHSD SLTRRRDQEG PVGLADFGPR** SIDPTLTHLF ECLSLAYSGK LVSPK WKNFK GLKLLCRDKI R**LNNAIWRAW YIQYVQR**RKS PVCGFVTPLQ GSEADEH R**KP EAVILEGNYW KRRIEVVMR**E YHKWRIYYKK RLRKSSREGD FLAPK**QVEG G WPPPER**WCEQ LFSSVVPVLL GGSEEEPGGR QLLDLDCFLS DISDTLFTMTQ PSPSSLQLP PEDAYVGNAD MIQPDLTPLQ PSLDDFMEIS DFFTNYRPPQ TPTS SNYIES PSFGPMADSL FSSGILAPEM PSPASSSSSS GMTPHSGNTR LQARNS CSGP LDPNPFLSSE FLLPEDPKTK IPPAPGPTPL LPFPTPVKVH GLEPCTPSPF PTMAPPPSLL PEESLLSARF PFTSAPPAPG VSTLPAPTTF VPTPQPGPGP VPF SVDHLPH GYLEPVFGPH FTVPQGMQPR CKPSSPSPGG QK**ASPPTLAS ATAS PTATAT AR**DNNPCLTQ LLR**AAKPEQA LEPPTMPGTL LRPPESPQDT VSEIPR**A RAF FPPIPAPTPP RPPPGPATLA PPRSLVVPKA ER**LSPPASSG SER**R**LSGDLN SIQPSGALSV HLSPPQTVLS R**GRVDNNKME NRRITHISAE QK**RRFNIKLG FDT LHGLVST LSAQPSLKVS KATTLQK**TAE YILMLQQERA AMQEEAQQLR** DEIEEL NAAI NLCQQQLPAT GVPITHQR**FD QMRDMFDDYV R**TRTLHNWKF WVFSILIRP L FESFNGMVST ASLHSLRQTS LAWLEQYCSL PALRPTVLNS LR**QLSTSTSI LTD PSLVPEQ ATRAVTEGTL GRPL**

C

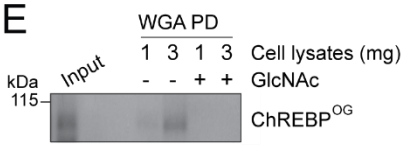


D





E



F

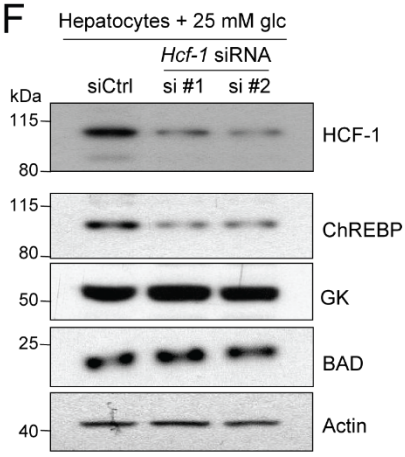


Figure 2.5. (Continued)

compared to *Bad* -/- samples (Figures 2.5A and C). HCF-1 is a transcriptional co-regulator whose interaction with ChREBP or role in DNL has not been previously reported. HCF-1 is activated by its binding to N-Acetylglucosamine (GlcNAc) transferase (OGT), leading to both HCF-1 O-GlcNAcylation and its proteolytic processing and maturation, whereby the N- and C-terminal fragments of HCF-1 remain non-covalently bound, producing a confirmation that enables HCF-1 to interact with its partner proteins (Capotosti et al., 2011; Daou et al., 2011; Lazarus et al., 2013). In addition to being regulated by OGT-dependent proteolytic processing, HCF-1 can function as an adaptor protein that recruits OGT to specific substrates (Han et al., 2017; Ruan et al., 2012).

To ensure that the interaction between ChREBP and HCF-1 is not limited to epitope-tagged and overexpressed ChREBP, we also validated the association of endogenous ChREBP, HCF-1 and OGT in WT hepatocytes and confirmed that it was diminished in the absence of BAD (Figure 2.6A). These experiments were performed in the presence of the proteasome inhibitor MG132 to normalize ChREBP protein stability as previously described (Guinez et al., 2011), because endogenous ChREBP levels were found to be lower in *Bad* -/- hepatocytes and liver compared to WT counterparts (see below). Notably, the association of HCF-1 and ChREBP in WT hepatocytes and liver samples is induced in response to glucose stimulation or HCD treatment, respectively (Figures 2.5D and 2.6A). Moreover, siRNA-mediated depletion of HCF-1 in WT hepatocytes led to diminished capture of OGT in ChREBP immunoprecipitates (Figure 2.6B), indicating that HCF-1 is required for recruitment of OGT to ChREBP. Consistent with these observations, HCF-1 depletion also led to decreased ChREBP O-GlcNAcylation in response to 25 mM glucose as evident from pull down assays using the lectin wheat germ agglutinin (WGA), which primarily binds GlcNAc (Guinez et al., 2011) (ChREBP^{OG}, Figure 2.5E and 2.6C). Reduced ChREBP O-GlcNAcylation in this setting was commensurate with reduced ChREBP protein levels (Figures 2.5F and 2.6D). This is in agreement with the notion that ChREBP stability is regulated by O-GlcNAcylation

Figure 2.6. HCF-1 interacts with ChREBP and is required for its O-GlcNAcylation.

(A) Representative western blots (top) and quantification of n=4 independent analogous experiments (bottom) of ChREBP association with HCF-1 and OGT in *Bad* +/+ and -/- primary hepatocytes cultured in 5 or 25 mM glucose for 6 hrs in the presence of 20 μM MG132. **(B)** Representative western blots (top) and quantification of n=3 independent analogous experiments (bottom) of ChREBP association with HCF-1 and OGT following *Hcf-1* knockdown in WT hepatocytes cultured in 25 mM glucose for 6 hrs in the presence of 20 μM MG132. **(C)** Representative western blot (top) and quantification of n=3 independent analogous experiments (bottom) of O-GlcNAcylated ChREBP ($ChREBP^{OG}$) in WGA pull down (WGA PD) assays in WT hepatocytes subjected to *Hcf-1* knockdown and cultured as in (B). **(D)** Representative western blot (left) and quantification of n=3 independent analogous experiments (right) of ChREBP protein levels in WT hepatocytes subjected to *Hcf-1* knockdown, and cultured in 25 mM glucose for 6 hrs in the absence or presence of 20 μM MG132.

Error bars are means ± SEM, *$p < 0.05$; **$p < 0.01$; two way ANOVA (A, C, D) or one way ANOVA (B).

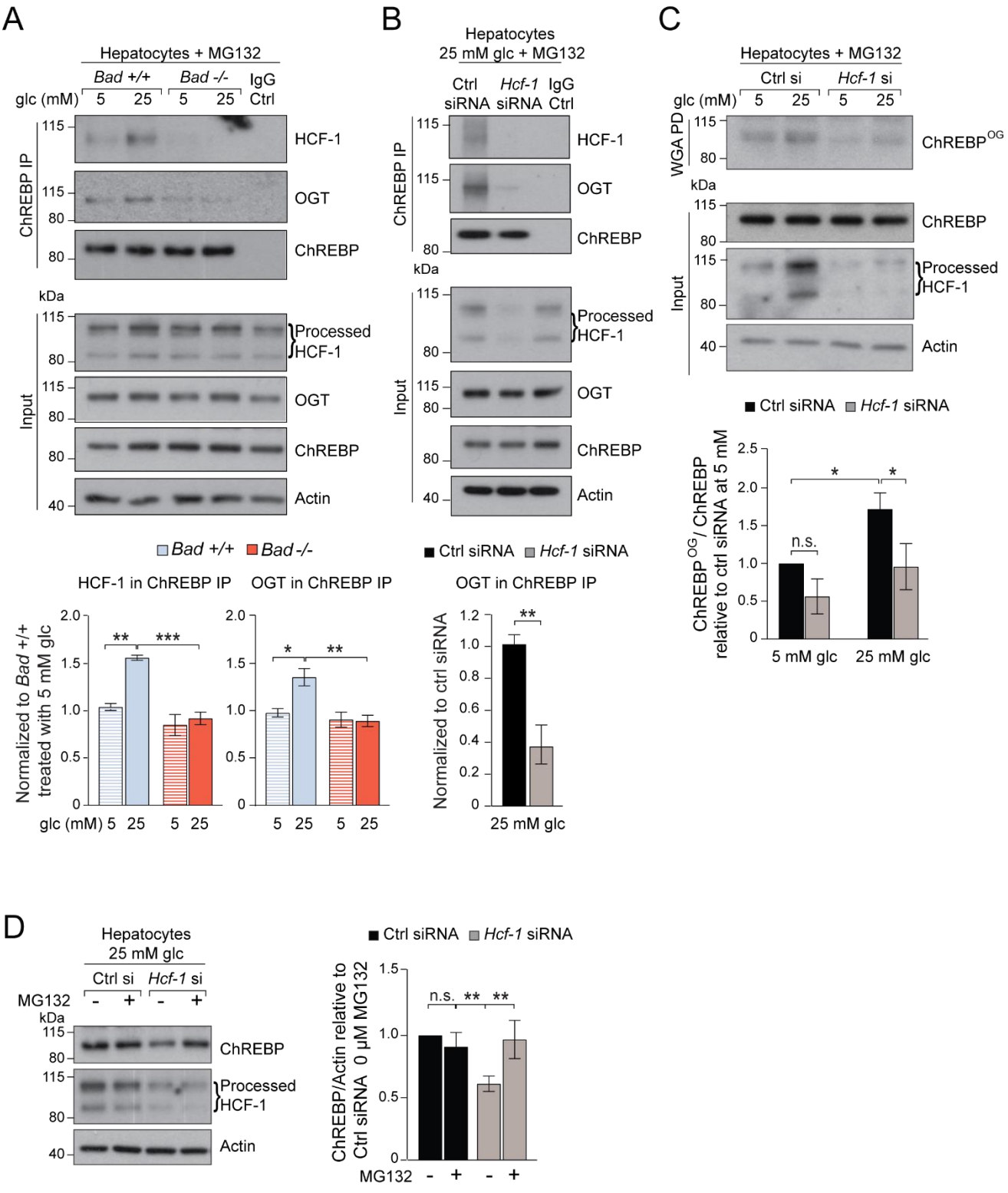


Figure 2.6. (Continued)

(Guinez et al., 2011; Sakiyama et al., 2010). Collectively, these data substantiate HCF-1 as a novel ChREBP binding partner that is required for recruitment of OGT to ChREBP and its O-GlcNAcylation.

Diminished ChREBP, OGT and HCF-1 association in the absence of BAD (Figure 2.6A) prompted examination of whether BAD modifications exert acute effects on ChRBEP O-GlcNAcylation, and whether this is HCF-1 dependent. ChREBP^{OG} was diminished in *Bad* -/- compared to WT hepatocytes treated with control siRNA, and further reduced upon HCF-1 depletion (Figure 2.7A, lanes 1, 2, 5 and 6). Genetic reconstitution with BAD S155D but not BAD AAA was sufficient to rescue ChREBP O-GlcNAcylation (Figure 2.7A, lanes 2-4). However, the effect of BAD S155D on ChREBP O-GlcNAcylation and glucose stimulation of lipogenic gene expression was blunted following *Hcf-1* knockdown (Figures 2.7A, lane 3 vs 7, and 2.7B). BAD-dependent alterations in ChREBP^{OG} are commensurate with corresponding changes in ChREBP protein levels (Figure 2.8A), and were also observed in liver following HCD treatment of *Bad* -/- vs +/+ mice (Figures 2.8B and C). Importantly, high glucose treatment not only stimulates HCF-1 O-GlcNAcylation but also its recruitment to the promoters of lipogenic genes in WT but not *Bad* -/- hepatocytes (Figures 2.7C and D). To our knowledge, this is the first evidence showing that HCF-1 can reside at the promoters of lipogenic genes.

Hexosamine biosynthesis is an intermediate between BAD and ChREBP regulation via HCF-1

Previous studies have indicated that loss of GK blunts ChREBP activity (Dentin et al., 2004), which is consistent with findings that certain glucose-derived phospho-metabolites activate ChREBP (Abdul-Wahed et al., 2017; Agius, 2016a). An additional glucose-derived signal is the OGT substrate, UDP-GlcNAc, which is required for ChREBP O-GlcNAcylation. UDP-GlcNAc also triggers the proteolytic cleavage and activation of HCF-1 (Capotosti et al., 2011; Daou et al., 2011; Lazarus et al., 2013). As such, diminished ChREBP O-GlcNAcylation upon BAD ablation could be due to both reduced binding of OGT to ChREBP (Figure 2.6A), as

Figure 2.7. HCF-1 regulates ChREBP function and lipogenesis downstream of BAD.

(A) Representative western blot (left) and quantification of n=3 independent analogous experiments (right) of O-GlcNAcylated ChREBP in primary *Bad* +/+ and -/- hepatocytes reconstituted with the indicated adenoviruses, subjected to *Hcf-1* knockdown, and cultured in 25 mM glucose for 6 hrs in the presence of 20 μm MG132. **(B)** Relative expression of ChREBP target genes *L-Pk* and *Acc1* in primary *Bad* +/+ and -/- hepatocytes reconstituted with the indicated adenoviruses, subjected to *Hcf-1* knockdown, and cultured in 5 or 25 mM glucose for 8 hrs (n=6 experimental repeats in hepatocytes derived from 3 mice per genotype). **(C)** Representative western blot (top) and quantification of n=3 independent analogous experiments (bottom) of O-GlcNAcylated HCF-1 in *Bad* +/+ and -/- primary hepatocytes cultured in 5 or 25 mM glucose for 6 hrs in the presence of 20 μM MG132. **(D)** Relative occupancy of ChREBP and HCF-1 at *L-Pk* and *Acc* promoters in *Bad* +/+ and -/- primary hepatocytes treated with 5 or 25 mM glucose for 4 hrs (n=9 experimental repeats in hepatocytes derived from 3 mice per genotype).

Error bars in A-D are means ± SEM, *p < 0.05; **p < 0.01; ***p < 0.001; two way ANOVA

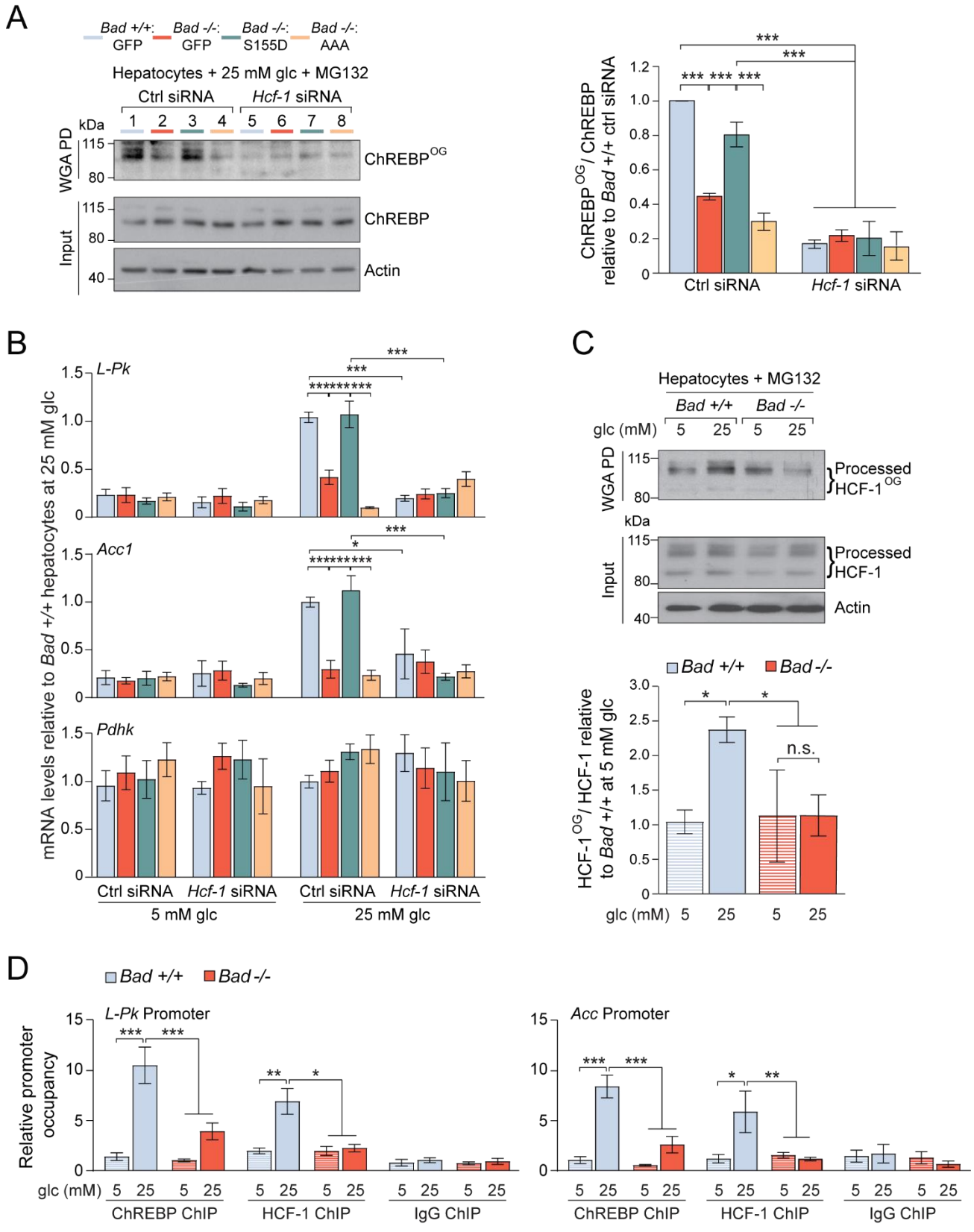


Figure 2.7. (Continued)

Figure 2.8. Regulation of ChREBP protein levels by BAD phosphorylation

(A) Representative western blot (left) and quantification of n=3 independent analogous experiments (right) of ChREBP protein levels in primary *Bad* +/+ and -/- hepatocytes reconstituted with the indicated adenoviruses and cultured in 25 mM glucose for 6 hrs in the presence or absence of 20 μm MG132. **(B)** Representative western blot of O-GlcNAcylated ChREBP in livers from *Bad* +/+ and -/- fasted for 24 hrs and refed a HCD for 18 hrs. **(C)** ChREBP protein levels in *Bad* +/+ and -/- liver samples derived from mice reconstituted with the indicated adenoviruses one week prior to being fasted for 24 hrs and refed a HCD for 18 hrs (n=3 per condition). **(D)** Representative western blot (top) and quantification of n=3 independent analogous experiments (bottom) of O-GlcNAcylated HCF-1 in livers from *Bad* +/+ and -/- mice fasted for 24 hrs and refed a HCD for 18 hrs.

Error bars in A, C and D are means ± SEM, *p < 0.05; **p < 0.01; n.s., non-significant; two way ANOVA (A, D) or one way ANOVA (C).

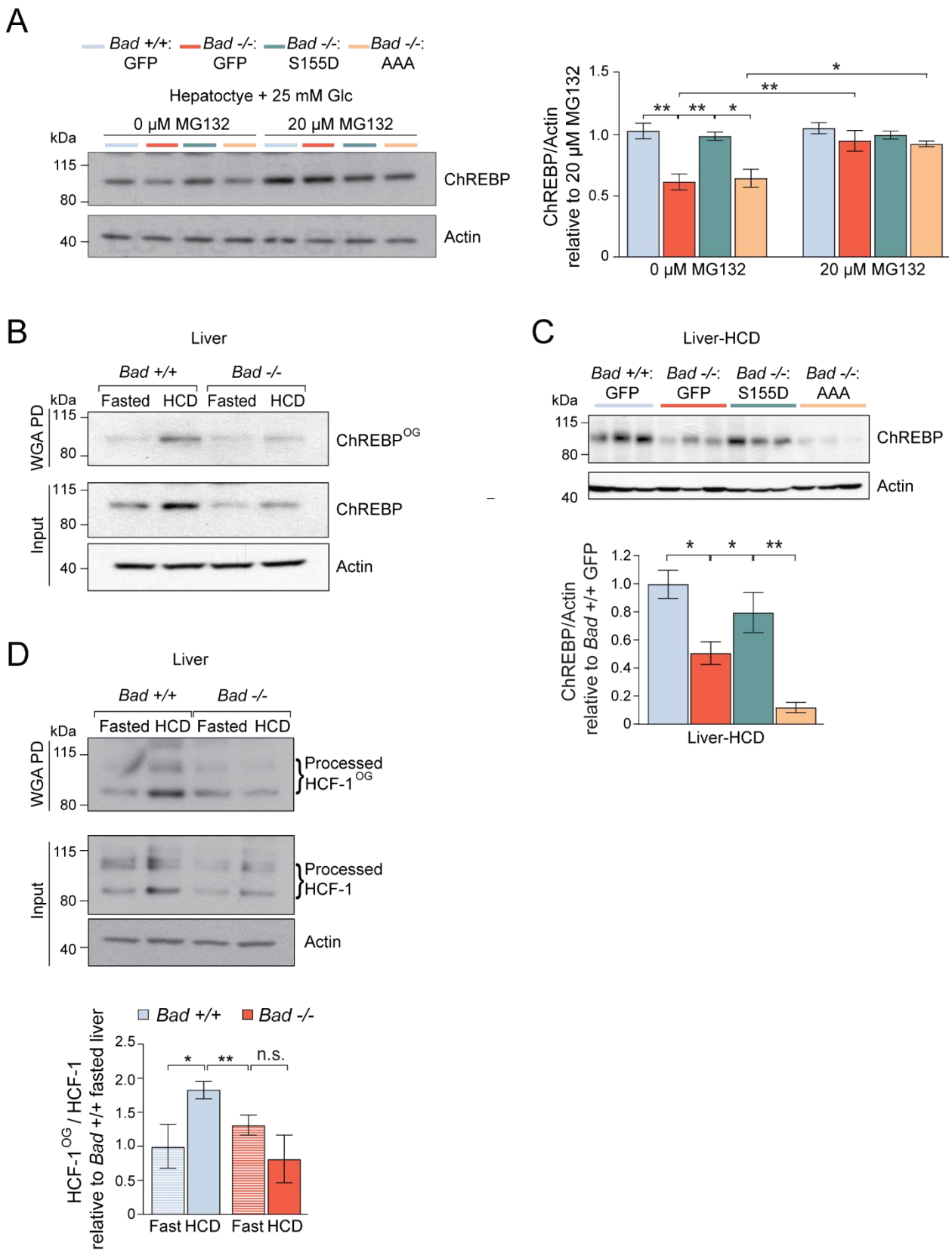


Figure 2.8. (Continued)

well as lower hexosamine biosynthesis pathway (HBP) activity as evident from decreased abundance of HBP metabolites such as UDP-GlcNAc in glucose stimulated *Bad* -/- hepatocytes (Figure 2.9A and Table 2.2). Genetic reconstitution with BAD S155D but not BAD AAA was sufficient to restore the levels of these metabolites in *Bad* -/- hepatocytes (Figure 2.9A). This is in line with phospho-BAD-dependent modulation of GK activity and hepatic glucose metabolism (Giménez-Cassina et al., 2014), and is further corroborated by the observation that acute knockdown of *Bad* or *Gk* in WT hepatocytes similarly reduces HCF-1 O-GlcNAcylation, ChREBP binding to HCF-1 and OGT, and ChREBP O-GlcNAcylation (Figures 2.9B, C, 2.10A and B).

The above observations suggest that, within the context of BAD deficiency or BAD dephosphorylation, the available pool of UDP-GlcNAc may not be sufficient to support O-GlcNAcylation of HCF-1 and ChREBP. If true, then increasing UDP-GlcNAc levels should reverse these effects. To test this prediction, we supplemented *Bad* -/- hepatocytes with GlcNAc or glucosamine (GlcN), the latter bypasses the rate-limiting reaction catalysed by glutamine-fructose-6-phosphate aminotransferase (GFAT), and enters HBP as glucosamine-6-phosphate upon phosphorylation (Guinez et al., 2011; Ryczko et al., 2016). We found that GlcNAc and GlcN rescued HCF-1 and ChREBP O-GlcNAcylation, and ChREBP protein levels under high glucose conditions in the absence of BAD (Figures 2.9D, 2.10C-E). These biochemical changes were commensurate with restored glucose induction of ChREBP target genes (Figure 2.10F). Strikingly, GlcNAc or GlcN supplementation also restored the interaction of ChREBP with HCF-1 and OGT (Figures 2.9E and 2.10G). These results are consistent with the notion that HCF-1 O-GlcNAcylation and proteolytic processing upon O-GlcNAcylation can regulate its capacity to interact with protein partners (Capotosti et al., 2011). As such, the restoration of HCF-1 O-GlcNAcylation in this setting may be conducive to the formation of some HCF-1-containing protein complexes. Furthermore, GlcNAc supplementation led to significant restoration of the biochemical defect in lipogenesis as evident from ^{14}C glucose incorporation into lipids (Figure

Figure 2.9. Hexosamine biosynthesis is an intermediate between BAD and ChREBP regulation via HCF-1.

(A) LC/MS quantification of N-acetyglucosamine-6-phosphate and UDP-GlcNAC in *Bad +/+ and -/-* primary hepatocytes reconstituted with the indicated adenoviruses and cultured in 25 mM glucose for 5 hrs (n=4-8 independent hepatocyte isolations). **(B)** Representative western blot (left) and quantification of n=3 independent analogous experiments (right) of O-GlcNAcylated HCF-1 in WT primary hepatocytes subjected to *Bad* or *Gk* knockdown, and cultured in 25 mM glucose for 6 hrs in the presence of 20 μM MG132. **(C)** Representative western blots (left) and quantification of n=3 independent analogous experiments (right) of ChREBP association with HCF-1 and OGT in primary hepatocytes treated as in (B). **(D)** Representative western blot (left) and quantification of n=3 independent analogous experiments (right) of O-GlcNAcylated HCF-1 in *Bad* +/+ and -/- primary hepatocytes cultured in 25 mM glucose (glc) and 20 μM MG132 in the absence or presence of 20 mM GlcNAc or 5 mM GlcN for 6 hrs. **(E)** Representative western blots (left) and quantification of n=3 independent analogous experiments (right) of ChREBP association with HCF-1 and OGT in *Bad* +/+ and -/- primary hepatocytes cultured in the presence of GlcNAc as in (D). **(F)** Incorporation of glucose into lipid fraction in *Bad* +/+ and -/- hepatocytes cultured in the absence or presence of 20 mM GlcNAc and treated with 1μCi of $U^{14}C$-glucose tracer for 4 hrs. Data are represented as percent increase in label incorporation from 5 to 25 mM glucose treatment (n=4 independent hepatocyte isolations).

Error bars are means ± SEM, *p < 0.05; **p < 0.01; ***p < 0.001; n.s., non-significant; two way ANOVA (A, D-F) or one way ANOVA (B-C).

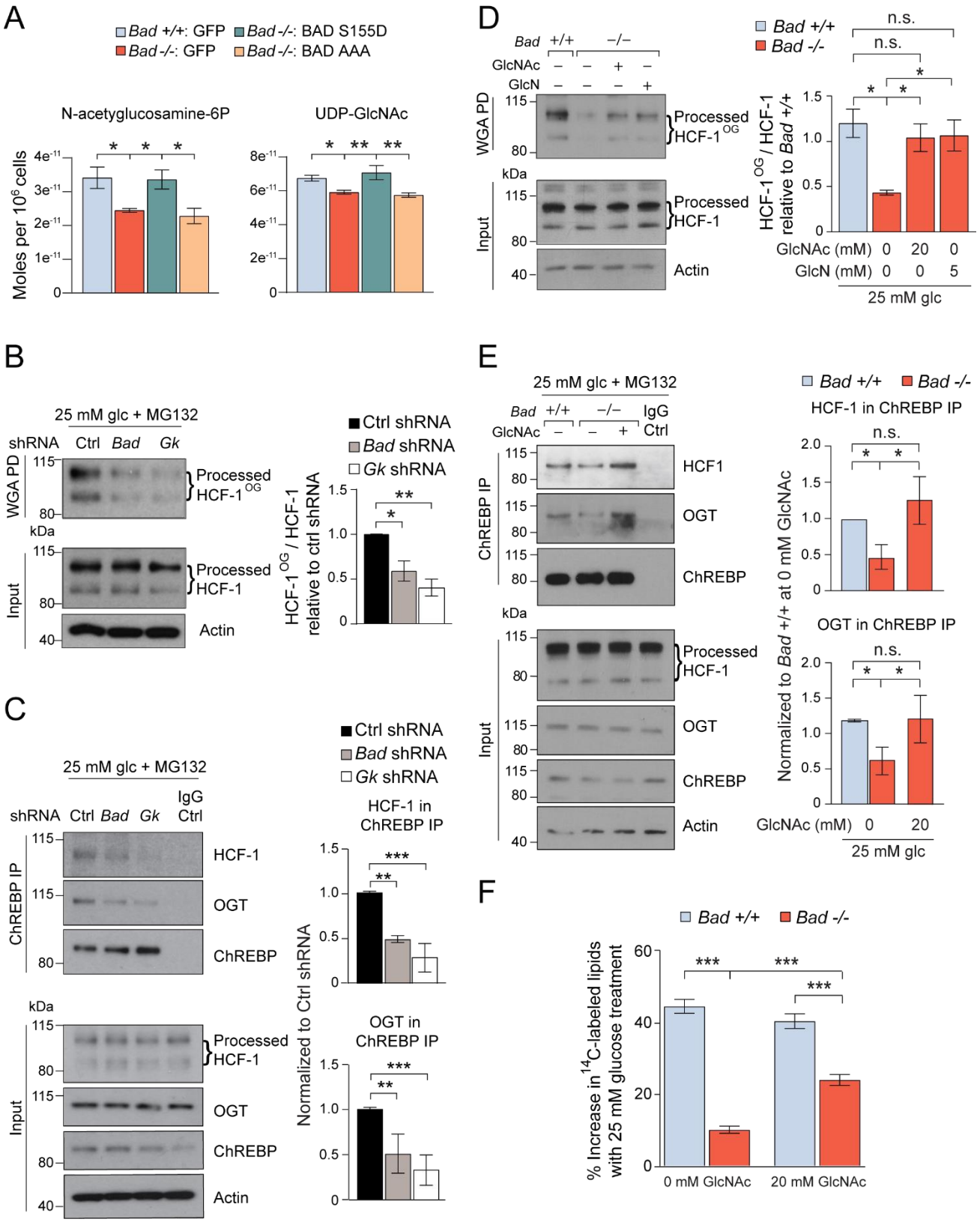


Figure 2.9. (Continued)

Figure 2.10. Rescue of the HCF-1-ChREBP regulatory module in *Bad* -/- hepatocytes following supplementation with glucosamine

(A) BAD and GK protein levels in primary hepatocytes subjected to shRNA-mediated knockdown of *Bad* or *Gk*. **(B)** Representative western blot (left) and quantification of n=6 independent analogous experiments (right) of O-GlcNAcylated ChREBP in WGA pull down assays in WT primary hepatocytes subjected to shRNA-mediated knockdown of *Bad* or *Gk*, and cultured in 25 mM glucose for 6 hrs in the presence of 20 μM MG132. **(C-D)** Representative western blot (left) and quantification of n=3 independent analogous experiments (right) of O-GlcNAcylated HCF-1 (C) and ChREBP (D) in *Bad* +/+ and -/- primary hepatocytes cultured in 25 mM glucose and 20 μM MG132 in the absence or presence of 5 mM GlcN for 6 hrs. **(E)** Representative western blots (left) and quantification of n=4 analogous experiments (right) of ChREBP protein levels in *Bad* +/+ and -/- primary hepatocytes cultured in 25 mM glucose for 6 hrs in the absence or presence of 5 mM GlcN. **(F)** Relative expression of ChREBP target genes *L-Pk* and *Acc1* in *Bad* +/+ and -/- primary hepatocytes cultured in 5 mM or 25 mM glucose in presence or absence of 5 mM GlcN for 20 hrs (n=9 experimental repeats in hepatocytes derived from 3 mice per genotype). **(G)** Representative western blots (left) and quantification of n=3 independent analogous experiments (right) of ChREBP association with HCF-1 and OGT in *Bad* +/+ and -/- primary hepatocytes cultured in the presence of 5 mM GlcN.

Error bars in B-G are means ± SEM, *$p < 0.05$; **$p < 0.01$; ***$p < 0.001$; one way ANOVA (B) or two way ANOVA (C-G).

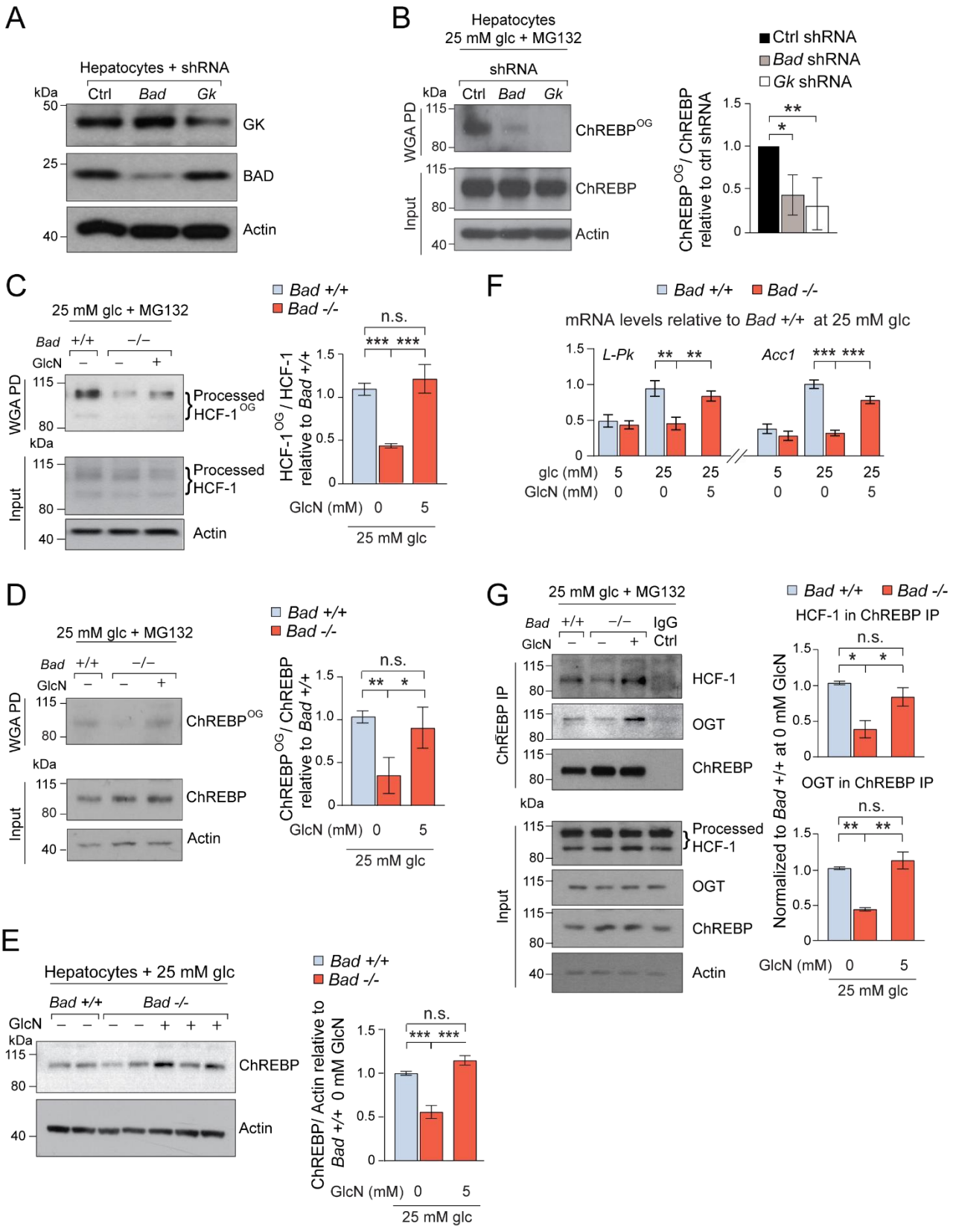


Figure 2.10. (Continued)

Table 2.2. Retention times and MRM transitions for hexosamines (Quantifying transition is indicated in bold letters)

Metabolite	MRM Transitions	Retention time (min)	Polarity
N-acetyl-glucosamine-6-phosphate	**302→284** 302→168 302→126 302→108	11.0	Pos
UDP-N-acetyl-glucosamine	**608→204** 608→138	9.1	Pos

2.9F). While significant, the rescue of actual lipogenesis was partial despite full restoration of ChREBP O-GlcNAcylation (Figure 2.10D). This is expected because, in addition to transcriptional regulation, multiple metabolic branch points downstream of glucose and GK are required for glucose stimulation of DNL. These include malonyl-CoA produced downstream of the glycolytic and oxidative arms of glucose metabolism, as well as NADPH generated through the pentose phosphate pathway, which are not expected to be restored by GlcNAc treatment (Alves-Bezerra and Cohen, 2017; Sanders and Griffin, 2016).

HCF-1 levels and BAD BH3 domain phosphorylation in NASH liver biopsies

Non alcoholic fatty liver disease (NAFLD) is characterized by increased hepatic lipid accumulation in the absence of increased alcohol consumption (Than and Newsome, 2015), which is due, in part, to increased hepatic DNL (Donnelly et al., 2005). The relevance of ChREBP in fatty liver disease is highlighted by studies showing that ChREBP overexpression in mice leads to hepatic steatosis and that ChREBP proteins levels are elevated in the livers of humans with NAFLD (Benhamed et al., 2012; Dentin et al., 2006; Hurtado del Pozo et al., 2011). Our findings that ChREBP activity is modulated by phospho-BAD and HCF-1, prompted assessment of BAD BH3 domain phosphorylation and HCF-1 levels in a pathologic setting of excessive hepatic DNL as in human patients with fatty liver. Consistent with previous reports, ChREBP protein levels were higher in NASH (non alcoholic steatohepatitis) patients compared to healthy liver donors (Figure 2.11 and Table 2.3). Remarkably, BAD phosphorylation on S118 within the BH3 domain (equivalent to S155 in the mouse BAD sequence) and HCF-1 levels were significantly enriched in NASH liver biopsies (Figure 2.11). These data, in conjunction with our findings that HCF-1 binds ChREBP, modulating its transcriptional activity and hepatic lipogenesis in a phospho-BAD dependent manner, suggest that the BAD:HCF-1:ChREBP axis may be relevant in physiologic control of hepatic fat content and, potentially, in the pathophysiology of fatty liver disease.

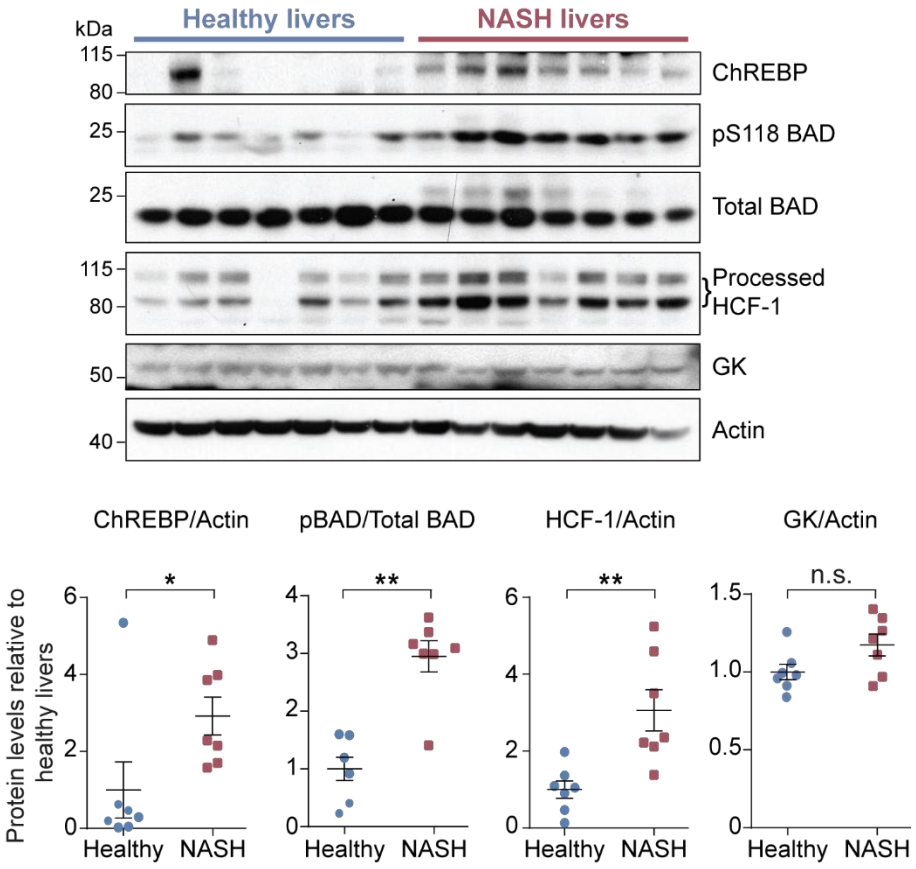


Figure 2.11. Increased BAD phosphorylation and HCF-1 levels in livers of human NASH patients

Immunoblot analysis (top) and quantification (bottom) of the indicated proteins in liver biopsies from healthy subjects and NASH patients (n=7).

Error bars are means ± SEM, *p < 0.05; **p < 0.01; Student's t test.

Table 2.3. List of Human Liver Specimens

Sample ID	Diagnoses	Sex	Age	COD
HH 1142	Normal	M	19	HT/MVA
HH 1170	Normal	F	49	ICH
HH 1174	Normal	F	72	ICH
HH 1202	Normal	F	67	CVA
HH 1211	Normal	M	79	Anoxia
HH 1227	Normal	M	34	CVA
HH 1249	Normal	M	59	CVA
UMN 1098	NASH-Fatty	F	59	N/A
UMN 1152	NASH-Fatty	F	41	N/A
UMN 1228	NASH-Fatty	M	62	N/A
UMN 1242	NASH-Fatty	F	43	N/A
UMN 1249	NASH-Fatty	F	55	N/A
UMN 1305	NASH-Fatty	F	48	N/A
UMN 1370	NASH-Fatty	M	53	N/A

COD: Cause of death; HT/MVA: Head trauma/ motor vehicle accident; ICH: Intracerebral hemorrhage; CVA: Cerebrovascular accident.

DISCUSSION

Our integrative genetic, biochemical and functional studies characterize BAD and identify HCF-1 as two previously unappreciated molecular players in ChREBP regulation and hepatic lipogenesis. The findings reported here, together with previous work (Giménez-Cassina et al., 2014; Szlyk et al., 2014), are consistent with the idea that BAD phosphorylation and the attendant activation of GK are required for glucose modulation of ChREBP O-GlcNAcylation and incorporation of glucose-derived carbons into lipids. In light of the known lipogenic effects of GK activation, a role for the BAD-GK pathway in this setting might have been expected. However, given the multiple regulatory mechanisms that converge on hepatic GK activity, including other GK binding proteins (Agius, 2016b), the relevance of BAD in DNL was neither clear nor certain. The multiple gain- and loss-of-function approaches utilized here to interrogate the consequences of BAD phosphorylation in hepatocytes and liver in response to glucose and HCD now provide solid support for the relevance of this BCL-2 family protein in hepatic DNL. Importantly, taking advantage of BAD-deficiency as a genetic system where glucose induction of ChREBP activity is blunted compared to WT hepatocytes, our unbiased comparative ChREBP interactome studies led to the identification of HCF-1 as a novel ChREBP-interacting protein and modulator of ChREBP function in glucose-stimulation of lipogenesis. We provide multiple lines of evidence that HCF-1 recruits OGT to ChREBP in response to glucose stimulation of WT hepatocytes, regulating ChREBP O-GlcNAcylation and lipogenic gene transcription (Figure 2.12). We further show that this regulatory module is not operational in the absence of GK or BAD, and is required for BAD phosphorylation to exert its effect on DNL.

Multiple post translational mechanisms regulate ChREBP activity (Abdul-Wahed et al., 2017; Agius, 2016a). Among these, O-GlcNAcylation regulates ChREBP DNA binding and transcriptional activity, as well as protein stability (Guinez et al., 2011; Sakiyama et al., 2010; Yang and Qian, 2017). However, a specific mechanism for regulation of ChREBP O-GlcNAcylation has not been previously reported. Protein O-GlcNAcylation is the outcome of the

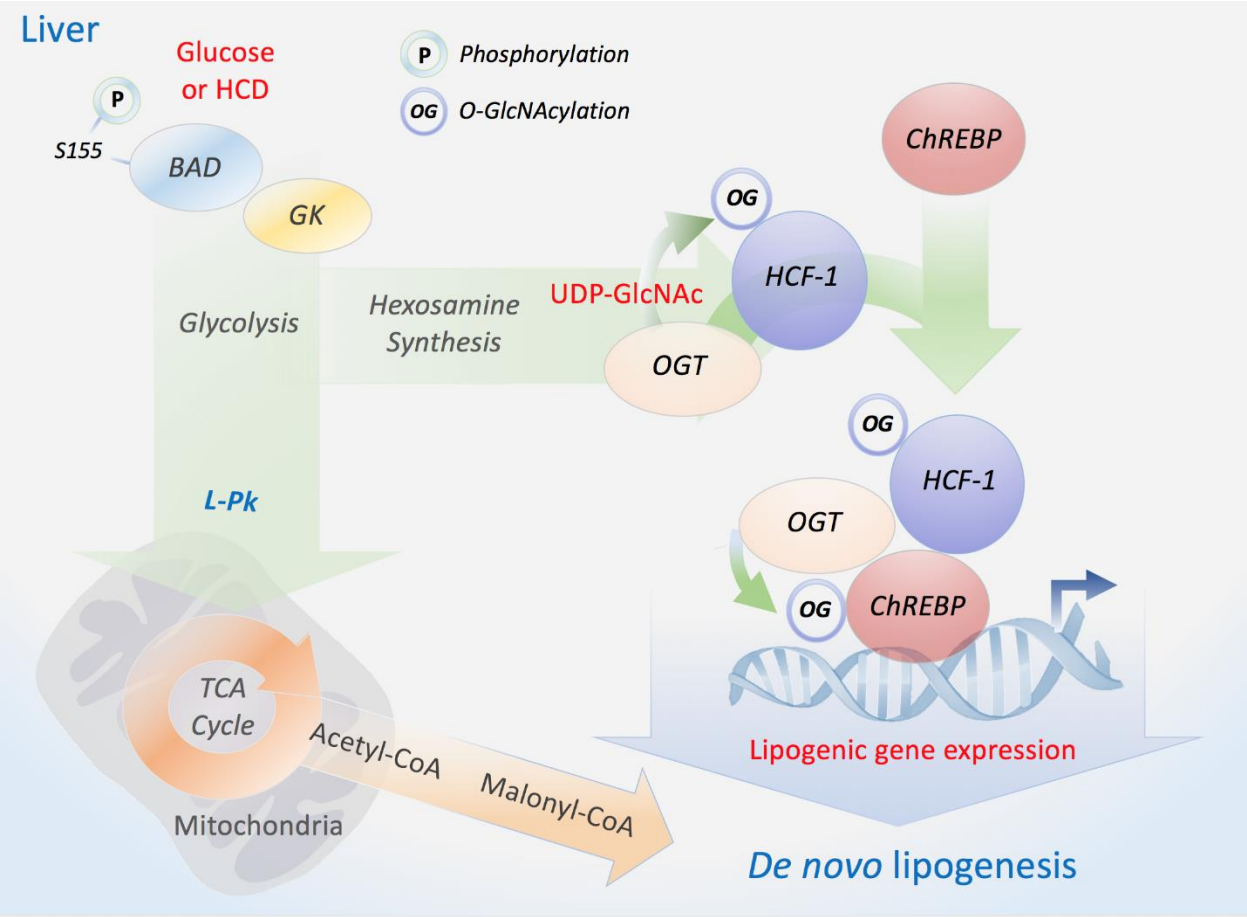


Figure 2.12. Proposed model of biochemical modulation of *de novo* lipogenesis by BAD and HCF-1

Activation of the BAD:GK pathway promotes *de novo* lipogenesis both by providing biosynthetic precursors and stimulating lipogenic gene expression through ChREBP. Full induction of the ChREBP transcriptional program by glucose requires hexosamine biosynthesis and HCF-1-dependent recruitment of OGT to ChREBP, which increases ChREBP O-GlcNAcylation, stability and activity.

net balance between OGT and O-GlcNAcase (OGA) activities, which transfer and remove the sugar modification, respectively. Remarkably, OGT and OGA are each encoded by a single gene, yet the pair regulates O-GlcNAcylation of a multitude of substrates. Several scenarios have been proposed as to how a single *OGT* gene can specifically O-GlcNAcylate hundreds of substrates. Substrate specificity may be achieved, in part, by specific subcellular localization of different OGT splice variants, the capacity of OGT tetratricopeptide repeats (TPRs) to control substrate access to the active site, differential sensitivity of OGT substrates to intracellular UDP-GlcNAc concentrations, and adaptor proteins that recruit the enzyme to specific substrates (Yang and Qian, 2017). We provide evidence that HCF-1 is an adaptor that recruits OGT to ChREBP in response to glucose stimulation, and that this process is GK- and BAD-dependent.

The role of HCF-1 in hepatic substrate utilization, production and storage has not been extensively studied, and is likely to be context-dependent. For example, under low (5 mM) glucose conditions and in the fasted state, HCF-1 is recruited to PGC1α, leading to increased PGC1α stability and gluconeogenic gene expression (Lin et al., 2002; Ruan et al., 2012). In comparison, the HCF-1:ChREBP complex is not abundant at 5 mM glucose concentrations or in fasted liver but is significantly enriched in response to high glucose and HCD treatment, activating the lipogenic gene expression program. This suggests additional mechanisms are at play to direct the specific and context-dependent outcomes of HCF-1 association with transcription factors under select nutrient conditions. For example, beyond glycosylation, other signalling inputs may be required to “licence” active transcription from promoters occupied by HCF-1. In addition, studies in other cell types show that HCF-1 can impact the activity of epigenetic modifiers such as histone methyl transferases and acetyl transferases in OGT-containing promoter complexes (Deplus et al., 2013; Tyagi et al., 2007; Wysocka et al., 2003; Zhou et al., 2013). Within this context, the finding that HCF-1 can reside at lipogenic gene promoters is noteworthy, and points to more complex effects on gene expression beyond ChREBP O-GlcNAcylation. Notably, this occurs predominantly at stimulatory (25 mM) but not basal (5 mM) glucose concentrations

consistent with nutrient conditions associated with active lipogenic gene transcription. Additional studies are required to characterize the potential contribution of HCF-1 to epigenetic regulation of lipogenic gene loci. Furthermore, given the broad range of ChREBP targets beyond lipogenic genes, it also remains to be determined whether HCF-1 is relevant to other ChREBP-dependent transcriptional programs.

Under normal physiological conditions, human hepatic DNL is kept at low levels (Alves-Bezerra and Cohen, 2017; Sanders and Griffin, 2016). However, excessive DNL can contribute to hepatic steatosis (Donnelly et al., 2005; Softic et al., 2016). Hepatic steatosis in response to high carbohydrate overload and in NAFLD reflects net alterations in the balance of hepatic substrate metabolism, including lipid synthesis, oxidation, secretion, uptake, and hepatic glucose production (Diraison et al., 2003; Donnelly et al., 2005; Sunny et al., 2011). Although hepatic DNL is elevated in response to carbohydrate load and in patients with NAFLD, studies in humans show that, under these conditions, the flux through this pathway is relatively small so that triacylglycerol derived from DNL is a minor fraction of total triacylglycerol content (Diraison et al., 2003; Donnelly et al., 2005; Schwarz et al., 1995). These observations indicate that DNL is less likely a quantitative sink for excess carbohydrates and argue for a broader regulatory role of DNL in hepatic fuel selection by controlling fatty acid esterification versus oxidation via modulation of hepatic malonyl-CoA content (Savage et al., 2006; Schwarz et al., 1995). Consistent with this notion, it is possible that reduced DNL in the absence of GK or BAD, or upon BAD dephosphorylation, reflects a shift in the balance of lipid oxidation and synthesis. This possibility is in line with the observation that hepatic fatty acid oxidation is exaggerated when hepatic GK or BAD is depleted, or upon BAD dephosphorylation (Giménez-Cassina et al., 2014).

Diets high in simple sugars including sucrose and high fructose corn syrup can cause increased hepatic DNL, at least in part, through increased ChREBP activity (Softic et al., 2016). Additionally, modulation of ChREBP can affect the development of hepatic steatosis in mouse models of fatty liver, underscoring the importance of ChREBP in the pathophysiology of hepatic

steatosis (Benhamed et al., 2012; Dentin et al., 2006; Iizuka et al., 2006). Our studies uncover a previously unappreciated regulatory pathway of ChREBP activity that is dependent on phosphorylated BAD and HCF-1, adding new mechanistic insights into how ChREBP activity and DNL are regulated in the liver. Importantly, hepatic BAD phosphorylation is upregulated under conditions where ChREBP is active such as short term (18 hr) high carbohydrate (70% sucrose) diet treatment in mice, and liver biopsies of patients with hepatic steatosis show increased BAD phosphorylation and HCF-1 levels. Collectively, our observations suggest that this newly uncovered ChREBP regulatory axis may be relevant for the physiological and pathophysiological regulation of hepatic DNL.

METHODS

List of Reagents

REAGENT or RESOURCE	SOURCE	IDENTIFIER
Antibodies		
Rabbit polyclonal anti-ChREBP	Novus Biologicals	NB400135 lots Q1-Q3
Rabbit polyclonal anti-HCF-1	Bethyl laboratories	A301-400A
Rabbit monoclonal anti-OGT	Cell Signaling	24083
Rabbit polyclonal anti-GCK	Santa Cruz	sc7908
Rabbit monoclonal anti-BAD	abcam	ab32445
Rabbit polyclonal anti-phospho BAD(S155)	Cell Signaling	9297
Mouse monoclonal anti-Actin	Sigma-Aldrich	A5316
Rabbit IgG Isotype Control	Invitrogen	31235
Mouse monoclonal anti FLAG M2- Peroxidase	Sigma-Aldrich	A8592
Mouse Anti-rabbit IgG (Conformation Specific)	Cell Signaling	5127S
Goat anti-rabbit IgG HRP	Jackson ImmunoResearch Laboratories	111-035-003
Goat anti-mouse IgG HRP	Jackson ImmunoResearch Laboratories	115-035-003
Bacterial and Virus Strains		
BAD SD Adenovirus	Gimenez-Cassina et al, 2014	PMID: 24506868
BAD AAA Adenovirus	Gimenez-Cassina et al, 2014	PMID: 24506868
Gk shRNA Adenovirus	Gift of Dr. Christopher Newgard (Duke University) Bain et al., 2004	PMID:15331526
Bad shRNA Adenovirus	Gimenez-Cassina et al, 2014	PMID: 24506868
Chrebp shRNA Adenovirus	Designed from sequence in Dentin et al, 2006	PMID: 16873678
Ctrl shRNA Adenovirus	Gimenez-Cassina et al, 2014	PMID: 24506868
FLAG-ChREBP Adenovirus	Gift from Dr. Donald Scott (Mount Sinai) (Metukuri et al, 2012)	PMID: 22586588
Biological Samples		
Human Liver Tissues Healthy and NASH Patients	Liver Tissue Cell Distribution System, Minneapolis, Minnesota	NIH Contract # HHSN276201200017C
Chemicals, Peptides, and Recombinant Proteins		
Phosphatase Inhibitor Cocktail 2 aqueous solution	Sigma-Aldrich	P5726
Protein Phosphatase Inhibitor Cocktail 3	Sigma-Aldrich	P0044
Phosstop, Phosphatase Inhibitor	Sigma-Aldrich	4906837001

Complete™, EDTA-free Protease Inhibitor Cocktail	Sigma-Aldrich	11873580001
PuGNAC	Sigma-Aldrich	A7229
Thiamet G	Sigma-Aldrich	SML 0244
Sodium Orthovanadate	Sigma-Aldrich	S6508
Western Lightning Plus-ECL	Thermo Fisher Scientific	509049325
SuperSignal West Femto	Thermo Fisher Scientific	PI34095
NuPAGE LDS Sample Buffer (4X)	Life Technologies	NP0008
FLAG Peptide	Sigma-Aldrich	F3290
N-Acetyl-D-glucosamine	Sigma-Aldrich	A8625-5G
Proteinase K	Life technologies	25530015
CHELEX 100 200-400 MB	Bio-Rad Laboratories	1421253
Formaldehyde (37% solution)	Santa Cruz	sc-203049
Collagenase	Sigma-Aldrich	C5138
Insulin	Sigma-Aldrich	I6634
Dexamethasone	Sigma-Aldrich	D-2915
Percoll	Sigma-Aldrich	P4937
MG132	Sigma-Aldrich	C2211
BSA Fraction IV Fatty acid free	Fischer Scientific	NC9227912
Glucosamine hydrochloride	Sigma-Aldrich	G4875
Ammonium Formate	Sigma-Aldrich	17843
Acetonitrile	Sigma-Aldrich	AX0145-1
HPLC grade water	Sigma-Aldrich	WX0008
Ammonium Acetate	Sigma-Aldrich	5330040050
U14C labeled glucose	American Radiolabled Chemical	ARC-122
Critical Commercial Assays		
Dual luciferase reagent	Promega	E1910
Targefect hepatocyte	Targeting systems	HEP-01
Trizol	Life Technologies	15596026
Syber Green Master Mix	Life Technologies	
Superscript III 1st Strand Synthesis	Life Technologies	18080051
Lipofectamine RNAiMax	Life Technologies	13778150
Experimental Models: Organisms/Strains		
C57BL/6J: WT		
C57BL/6J-KO(BAD)		
Oligonucleotides		
Ctrl siRNA: siGenome Non-targeting siRNA #1	Dharmacon	D-001210
Hcf1 siRNA-1 sense sequence: GGA GCU UAU AGU GGU GUU U	Dharmacon	N/A
Hcf1 siRNA-2 sense sequence: AGA ACA ACA UUC CGA GGU A	Dharmacon	N/A

Primers for qPCR: See Table 2.1 for sequence	IDT	N/A
Recombinant DNA		
L-Pk ChORE firefly luciferase reporter	Gift from Dr. Howard Towle: Lou D-Q et al, 1999	PMID: 10497199
Acc ChORE firefly luciferase reporter	Gift from Dr. Howard Towle: O'Callaghan BL et al, 2001	PMID: 11340083
pCMV-Green *Renilla* Luciferase control plasmid:	Thermo Fisher Scientific	PI16153
Software and Algorithms		
ImageJ	https://imagej.nih.gov/ij/	N/A
Prism	Graph Pad	N/A
SDS 2.4 (for Q-PCR)	Applied Biosystems	N/A
MassHunter Quant	Agilent Technologies	N/A
Sequest	Thermo Fischer Scientific	N/A
Other		
Serum	Gemini	100-106 lot A16E00E
High Carbohydrate Diet (70% sucrose)	Envigo	TD.150694
WGA Beads	Vector Laboratories	AL-1023
Anti-FLAG® M2 Magnetic Beads	Sigma-Aldrich	M8823
Protein G Agarose	Sigma-Aldrich Aldrich	11719416001
DynaBeads Protein A	Thermo Fisher Scientific	10001D
Amicon Ultra Centrifugal Filters	Millipore	UFC500324

EXPERIMENTAL MODEL AND SUBJECT DETAILS

Mice

Bad -/- mice have been previously described (Giménez-Cassina et al., 2014). Mice received a standard chow diet unless otherwise indicated and were housed in a barrier facility with 12 hr light and dark cycles. Unless otherwise indicated, male mice at 8-12 weeks of age were used. For high carbohydrate diet experiments, mice were fasted for 24 hrs and refed a high carbohydrate diet (70% sucrose) (TD.150694) for 18 hrs. All animal procedures were approved by the Institutional Animal Care and Use Committee at the Dana Farber Cancer Institute.

Human Liver Tissue

Frozen human liver biopsies classified as normal (n = 7) or fatty liver (NASH) (n = 7) were provided by the Liver Tissue Cell Distribution System (LTCDS, Minneapolis, Minnesota), which was funded by the National Institutes of Health Contract # HSN276201200017C (**Table 2.3**). This study used collected specimen that had been de-identified by the LTCDS and was exempted by the Dana-Farber Cancer Institute Institutional Review Board (IRB) because it was determined that the project activities do not meet the definition of human subjects research set forth at 45 CFR 46.102 (protocol # 16-324).

Hepatocyte Isolation and Culture Conditions

Primary hepatocyte isolation and cultures were carried out as previously described with a two-step digestion process (Matsumoto et al., 2007). Briefly, livers from 8-12 week old male mice were drained of blood by perfusion via vena cava with 42°C perfusion buffer (0.4 g/L KCl, 1.0 g/L Dextrose, 1.8 g/L $NaHCO_3$, 0.2 g/L EDTA) for 3 min. Connective tissue within the liver was digested by perfusion of 42°C liver digest media (0.4 g/L KCl, 1.0 g/L Dextrose, 1.8 g/L $NaHCO_3$, 0.5 g/L CaCl2, 10 g/L BSA, 30 mg/L Collagenase) for 10 min. The liver was mechanically dissociated in plating media (DMEM: 10% FBS, 2 mM Sodium Pyruvate, 2% Pen/Strep, 1 μM Dexamethasone, 0.1 μM Insulin) at 4°C, strained through 70 micron cell strainer, and hepatocytes were collected by centrifugation at 50 g for 3 min. Hepatocytes were further isolated from other cells on a percoll gradient with centrifugation at 650 RPM for 5 min. The cell pellet was washed and resuspended in plating media, and cells were plated in plating media at a density of $8X10^5$ cells/well in 6 well plate or $4X10^6$ cells/10 cm dish unless otherwise indicated and cultured with 5% CO_2 at 37°C. Cells were starved in serum-free M199 media supplemented with 0.2% BSA (2% Pen/Strep, 2 mM Sodium pyruvate) for 12-16 hrs prior to experimental treatments.

For glucosamine (GlcN) and N-acetylglucosamine (GlcNAc) treatments, primary hepatocytes were treated with 5 mM glucosamine hydrochloride (Sigma) or 20 mM N-

acetylglucosamine (Sigma) in high glucose M199 serum free media pH 7.4 for the indicated length of time.

For MG132 treatment, primary hepatocytes treated with the indicated adenoviruses and/or siRNAs were cultured in low (5 mM) or high (25 mM) glucose for 6 hrs. After 3.5 hrs, the cells were treated with MG132 to a final concentration of 20 μM for the remaining 2.5 hrs of the 6 hr treatment.

METHOD DETAILS

Adenovirus Production and Viral Transduction

Recombinant GFP, BAD S155D, and BAD AAA adenoviruses were generated using the pAdEasy system (Stratagene) (Giménez-Cassina et al., 2014). Adenoviruses carrying *Bad* shRNA or scrambled control were constructed using the Adeno-X Expression Systems 2 with Creator Technology (Clontech) (Giménez-Cassina et al., 2014). Adenoviruses carrying *Gk* shRNA were a kind gift of Dr. Christopher Newgard (Duke University) (Bain et al., 2004). Adenoviruses carrying FLAG-ChREBP were a kind gift of Dr. Donald Scott (Mount Sinai) (Metukuri et al., 2012) Adenoviruses containing the *Chrebp* shRNA were created using the following sequence **gatcc**GTGTTGGCAATGCTGACATGttcaagagaCATGTCAGCATTGCCAACAttttttgga**g** against ChREBP from Dentin *et al*. (Dentin et al., 2012). The shRNAs were ligated into pSIREN-DNR-DsRed express plasmid at BamH1 and EcoRI RE sites. The construct was excised at SalI and Spe1 sites to shuttle the hU6 promoter with the *Chrebp* shRNA sequence and ligated into pAdTrack-promoterless at the SalI and EcoRV RE sites. The adenovirus was generated using pAdEasy system (Stratagene). All virus amplification, purification, titration and verification were done using the services of ViraQuest Inc.

Adenoviral transduction of hepatocyte cultures was carried out during plating at a viral dose of 3 pfu/cell for 2-4 hrs followed by 2-4 hr recovery in maintenance media (DMEM: 8 mM Glucose, 1 nM Insulin, 0.1 M Dexamethasone, 2 mM Sodium Pyruvate, 2% Pen/Strep, 10% FBS) before overnight serum starvation in M199 media (0.2% BSA) unless otherwise noted. For

knockdown experiments, hepatocytes were cultured for an additional 24 hrs in maintenance media before serum starvation in M199 media.

For hepatic reconstitution assays, mice were injected with a viral dose of $3x10^8$ pfu/g of body weight via tail vein, and livers were harvested 1 week after injection.

Primary Hepatocyte siRNA Transfection

Reverse siRNA transfection was performed with Lipofectamine RNAi Max (Life Technologies) per the manufacturer's protocol. In brief, 150 pmol of control or HCF-1 RNA duplex and 15 µL Lipofectamine RNAi max were gently mixed in 1 mL Opti-MEM and incubated for 10 min at RT before adding to freshly plated hepatocytes. For experiments that combined HCF-1 siRNA treatment and adenoviral expression of BAD variants, cells treated with HCF-1 siRNA, were left to recover for 2 hrs in maintenance media (DMEM: 8 mM Glucose, 1 nM Insulin, 0.1 M Dexamethasone, 2 mM Sodium Pyruvate, 2% Pen/Strep, 10% FBS) prior to infection with adenoviruses Cells were then harvested for analysis after 30 hrs.

De Novo Lipogenesis Assay

Hepatocytes were plated at 10^6 cells per well in 6 well plates. After overnight serum starvation, hepatocytes were pretreated in 0.8 mL low (5 mM) or high (25 mM) glucose serum free M199 media for 30 min and then spiked with 1 µCi of ^{U14}C labeled glucose (American Radiolabeled Chemicals) for 4 hrs. Lipids were extracted in methanol with a modified Folch method. Briefly, cells were washed with PBS and then harvested in 200 µL of 0.5% Triton in PBS, and 500 µL of 2:1 chloroform:methanol was added to 150 µL of before vortexing at high speed for 20-30 sec and incubating on ice for 1 hr. The remaining protein lysate was used for protein quantification and normalization. The samples were vortexed, and 125 µL of dH_2O was added before vortexing again and centrifuging for 15 min at 1000 RPM at 4°C. The bottom phase was transferred to a large 20 mL glass scintillation vial containing 3 mL of scintillation fluid. Incorporation of ^{14}C carbons into the lipid fraction was measured using a Tri-Carb 2900 TR liquid scintillation counter (Packard), and all reads were normalized to protein content.

Dual Luciferase Assay

Hepatocytes were transfected with 3 µg/mL *Acc* (O'Callaghan et al., 2001) or *L-Pk* (Lou et al., 1999) ChoRE firefly luciferase reporters (kind gift from Dr. Howard Towle) and 10 ng/mL of cmv-*Renilla* luciferase control plasmids using the Targefect hepatocyte (Targeting Systems) transfection reagent. Briefly, transfection complexes were formed in 1 mL serum free high glucose DMEM without antibiotics by first adding 3 µg of DNA followed by 7.5 µL of targefect reagent and 10 µL of virofect reagent per well. The transfection complexes were formed during 20 min incubation at 37°C. The cells were washed in antibiotic free media, and 1 mL of the transfection complex was added per well in 6 well plate. Hepatocytes were cultured in maintenance media without antibiotics (DMEM: 8 mM Glucose, 1 nM Insulin, 0.1 M Dexamethasone, 2 mM Sodium Pyruvate, 10% FBS) for 4 hrs for recovery and then infected with 2 pfu/cell of indicated adenoviruses for 2 hrs before being cultured in serum free (0.2% BSA) M199 media with 5 mM glucose overnight. Hepatocytes were then treated for an additional 20 hrs in either low (5 mM) or high (25 mM) glucose M199 media. ChREBP transcriptional activity was measured by performing Promega dual luciferase assay. Briefly, cells were lysed in 500 µL of 1X passive lysis buffer (Promega), and 20 µL of lysate for each condition was transferred to a 96 well white plate. The samples were analyzed using a Berthold Technologies Mithras LB 940 instrument to inject 100 µL of LAR II reagent, measure firefly luciferase activity followed by 100 µL of Stop & Glo reagent. Renilla luciferase activity for each well was then measured individually.

RNA Preparation and Quantitative Real-Time PCR

mRNA was isolated from hepatocytes plated at a density of $8X10^5$ cells/well in 6 well plate using 0.5 mL of Trizol (Life Technologies) per well, and 1 µg of RNA was used to make cDNA using the Superscript III reverse transcriptase reagents (Life Technologies). cDNA was diluted to 200 µL (1:10 dilution), and qPCR was performed using Syber Green reagents (Life Technologies) to a final volume of 10 µL in 384 well qPCR plates with 3 µL of diluted cDNA (1.5 µL for cyclophilin D control primers) and 300 µM primers for the indicated genes. The qPCR was performed in an

Applied Biosystems 7900HT Fast Real-Time PCR instrument. Gene expression levels were normalized to Cyclophilin D (CycD) using the $2^{-\Delta\Delta Ct}$ method and are presented as relative transcript levels. The sequence of primers is available in Table 2.1.

Chromatin Immunoprecipitation

After overnight serum starvation, primary hepatocytes were treated with low (5 mM) or high (25 mM) glucose for 4 hrs and washed with PBS before incubation in 1% formaldehyde (in PBS) for 10 min at 37°C. Cells were washed once in 0.125 M glycine in PBS and collected in 1 mL of PBS before centrifugation at 2000 g for 5 min at 4°C, resuspended in 500 µL of SBAR (50 mM HEPES pH 7.4, 140 mM NaCl, 1 mM EDTA, 1% Triton, 0.1% NaDOC, 0.1% SDS, 0.5 mM PMSF, Complete™ EDTA-free Protease Inhibitor Cocktail), and passed through an insulin syringe several times.

Cells in SBAR buffer were sonicated in a Biorupter sonicator at middle intensity 3 times for 5 min with a 30 sec ON 30 sec OFF cycle at 4°C. Lysates were centrifuged at max speed for 20 min and the supernatant was transferred to a new tube. DNA concentration was measured and the equivalent of 75 µg of DNA was used per ChIP in a total volume of 200 µL of SBAR (10 µL was kept for input). Samples were incubated with 1 µg of the indicated antibody at 4°C overnight, and 10 µL of dynabeads Protein A (Invitrogen) pre-blocked with salmon sperm DNA were added to the sample and rotated for 1.5 hr at 4°C. Consecutive washes were performed in the following buffers: Buffer I (1% Triton, 0.1% NaDOC, 150 mM NaCl, 10 mM Tris.Cl pH 8), Buffer II (1% NP-40, 1% NaDOC, 150 mM KCL, 10 mM TrisCl), Buffer III (0.5% Triton, 0.1% NaDOC, 500 mM NaCl, 10mM TrisCl), Buffer IV (0.5% NP-40, 0.5% NaDOC, 250 mM LiCl, 20 mM TrisCl, 1 mM EDTA), Buffer V (0.1% NP-40, 150 mM NaCl, 20 mM TrisCl, 1 mM EDTA), and TE for 5 min each. 100 µL of 10% Chelex resin was added to all samples to recover eluates, and 5 µL of 2 mg/mL proteinase K was added to the eluates (20 mg/mL for inputs) followed by 30 min incubation at 55°C. The digestion was then stopped by boiling the samples for 10 min. qPCR was performed using 3 µL per replica for eluates and 1 µL per replica for input. A standard curve was

generated using dilutions of a pooled input sample, and ChIP samples were normalized to their respective inputs. Primers used are available in Table 2.1.

For liver chromatin immunoprecipitation assays, approximately 80% of the liver sample was homogenized in 5 mL of SHB (15 mM HEPES pH 7.9, 15 mM KCl, 1 mM EDTA, 50 µM spermine, 50 µM spermidine, 1.9 M sucrose, 0.5 mM PMSF, Complete™ EDTA-free Protease Inhibitor Cocktail) using low speed motor-driven pestle 3 times up and down. The liver homogenate was layered on top of 7.5 mL of cold SHB in 13.5 mL Beckman Ultra-Clear tubes and centrifuged at 25,000 RPM for 1 hr at 4°C. The pellet was gently resuspended in 400 µL of SucC buffer (15 mM HEPES pH 7.9, 60 mM KCL, 15 mM NaCl, 15 µM β-ME, 0.2 mM $MgCl_2$, 0.34 M sucrose, 0.5 mM PMSF, Complete™ EDTA-free Protease Inhibitor Cocktail), and transferred to a new Eppendorf tube. Formaldehyde was added to a final concentration of 1%, and the tubes was incubated for 13 min at 37°C to crosslink the DNA and protein. Crosslinking was stopped by adding glycine to a final concentration of 0.125 M followed by a 5 min incubation on ice. The homogenate was transferred to a second cushion of SucC buffer with 0.9 M sucrose in a 15 mL centrifuge tube and spun at 4,000 RPM for 15 min at 4°C before resuspending the pellet in 400 uL of SBAR buffer.

Co-Immunoprecipitation and Western Blotting

For immunoprecipitation assays (IPs), cells were lysed in buffer containing (Tris/HCl pH 7.5 20 mM, NaCl, 137 mM, 5% glycerol, 2 mM EDTA, 2 mM Na_3VO_4, Complete™ EDTA-free Protease Inhibitor Cocktail, Phosphatase inhibitor cocktail 3, 2 µM Thiamet-G, 10µM PUGNAc, 1 µM TSA, 0.15% Triton-X100). Cells were mechanically disrupted by passing through an insulin syringe and rotating for 1.5 hr at 4°C, pelleted at maximum speed in a desktop centrifuge, and the supernatant was transferred to a new tube. Immunoprecipitation was carried out with 3 mg of protein lysates and 3 µg of ChREBP antibody (Novus Biologicals, lots Q1-Q3) rotating overnight at 4°C. After overnight incubation with the antibody, 50 µL of protein G agarose beads (Sigma-Aldrich) were added to each sample and rotated for an additional 2 hrs at 4°C. The IPs were washed once in

lysis buffer, and proteins were eluted in 2X LDS sample buffer (Life Technologies) with a 10 min boil.

For western blotting without immunoprecipitation, cells were lysed in RIPA buffer (10 mM Tris/HCl, 150 mM NaCl, 1% Triton X-100 [v/v], 0.5% sodium deoxycholate, 0.1% sodium dodecyl sulfate, 10 μM PUGNAc , and 2 μM Thiamet-G , and protease inhibitors; pH 7.4), and the protein amount was quantified by BCA assay. For western blots 10-30 μg of protein lysate was loaded.

Samples were prepared for western blotting using the NuPAGE 4X sample buffer and NuPAGE gel systems (Life Technologies). Proteins were transferred onto PVDF membrane in Towbin buffer (Tris Base 3.03 g/L, Glycine 7.57 g/L, methanol 20%), and blotted with the indicated antibodies (see key resource table). The ImageJ software was used for quantification of band intensities.

Wheat Germ Agglutinin (WGA) Pull Down

For detecting protein O-GlcNAcylation, wheat germ agglutinin (WGA) pull down assays were performed as previously described by (Guinez et al., 2011). In brief, primary hepatocytes subjected to the indicated genetic manipulations and cell culture conditions were treated with MG132 (20 μM) and lysed in RIPA lysis buffer (10 mM Tris/HCl, 150 mM NaCl, 1% Triton X-100 [v/v], 0.5% sodium deoxycholate, 0.1% sodium dodecyl sulfate, 10 μM PUGNAc , and 2 μM Thiamet-G , and protease inhibitors; pH 7.4) supplemented with or without 0.5 M of GlcNAc for 20 min on ice. Samples were centrifuged at 16,400 RPM for 20 min, and 1.5 mg of protein lysate was incubated with 50 μL of WGA beads (VWR) for 2 hrs at 4°C.

Beads were centrifuged briefly at 2,000 RPM and subsequently washed 3 with the following buffers: I) RIPA buffer; II) 1:1 mixture of RIPA and RIPA containing 500 mM NaCl; III) TNE (10 mM Tris/HCl, 150 mM NaCl, and 1 mM EDTA; pH 7.4). Samples were boiled in 50 μL of 2X LDS sample buffer (Life Technologies) and subjected to SDS-PAGE followed by western blotting with the indicated antibodies.

Hexosamine Pathway Metabolite Measurement

Primary hepatocytes infected with the indicated adenoviruses were serum starved overnight and subsequently treated with high (25 mM) glucose for 5 hrs. For each measurement extracts from three 10 cm dishes were used. Cells were quickly washed twice on ice with cold 150 mM ammonium formate at pH 7.4. Plates were placed on dry ice and scraped in 230 µL of 50% MeOH/ 50% HPLC H_2O solution and transferred to a pre-chilled tube with a metal bead. Plates were then washed with an additional 150 µL of 50% MeOH/ 50% HPLC H_2O solution and tubes vortexed for 10 sec. 220 µL of ice cold acetonitrile was added and the tubes were vortexed for an additional 10 sec. Thawed samples were placed in pre-chilled bead beater racks and beaten for 2-5 min at 30 Hz. 600 µL of dichloromethane and 300 µL of ice cold H_2O were added to the tubes. Tubes were vortexed for 15 sec then incubated on ice for 10 min. The samples were spun down for 5 min at 4,000 RPM at 1^{o}C and the upper aqueous phase was transferred to a new tube on ice. The samples were spun 1 min at 13,000 RPM to remove any remaining contaminants and supernatants were transferred to a new tube on dry ice. The aqueous phase was dried using a chilled speedvac, and samples were stored at -80°C until ready for LC-MS/MS data collection.

Metabolite measurements and tracer analyses were performed at the Rosalind and Morris Goodman Cancer Research Centre Metabolomics Core Facility. For targeted analysis and semi-quantitative concentration determination of the hexosamine metabolites, 5 uL of each sample was re-suspended in 50 µL of water and injected in an Agilent 6430 Triple Quadrupole (QQQ)-LC-MS/MS. Chromatography was performed using a 1290 Infinity ultra-performance LC system (Agilent Technologies) consisting of vacuum degasser, autosampler and a binary pump. The mass spectrometer was equipped with an electrospray ionization (ESI) source and samples were analyzed in negative mode. Multiple reaction monitoring (MRM) transitions were optimized on standards for each quantitated metabolite. MRM transitions and metabolite retention times are shown in Table 2.2. Gas temperature and flow were set at 350°C and 10 L/min respectively, nebulizer pressure was set at 50 psi and capillary voltage was set at ±4000V.

Chromatographic separation was performed on a Unison UK-Amino column 3 µm, 2.0×150mm (Imtakt Corp) maintained at 55°C. The chromatographic gradient started at 90% mobile phase B (acetonitrile) with a 2 min hold followed with a 18 min gradient to 100% mobile phase A (200 mM ammonium acetate in H_2O) and then held at 100% A for 10 min at a flow rate of 0.6 mL/min. This was followed by a 6 min re-equilibration at 100% mobile phase B before the next injection. Relative concentrations were determined from external calibration curves prepared in H_2O. Additional corrections for potential sample ion suppression were not made. Data were analyzed using MassHunter Quant (Agilent Technologies).

Nuclear FLAG-ChREBP IP and LC/MS Analysis

Primary hepatocytes were rinsed once with cold PBS and once with cold H_2O before being scraped in 400 µL of hypotonic lysis buffer (40 mM Tris PH 7.4, 10 mM NaCl, 1 mM EDTA, 2 mM Na_3VO_4, Complete™ EDTA-free Protease Inhibitor Cocktail). Cells were incubated on ice for 20 min and CHAPS was added to a final concentration of 0.5%. Cells were passed up and down in an insulin syringe 4-5 times, and nuclei were pelleted by centrifugation at 1,600 g for 7 min. The nuclei were washed 3 times in hypotonic wash buffer (hypotonic lysis buffer + 0.5% CHAPS) and resuspended in 150 µL of hypertonic lysis buffer (40 mM Tris PH 7.4, 420 mM NaCl, 1 mM EDTA, 0.5 mM DTT, 2 mM Na_3VO_4, 0.5 mM PMSF, Complete™ EDTA-free Protease Inhibitor Cocktail, 0.5% CHAPS) using hand held pestle homogenizer. Nuclei were incubated on ice for an additional 30 min with periodic vortexing and spun at 10,000 g for 30 min followed by transferring the nuclear fraction (supernatant) to a new tube.

For Co-IP experiments, nuclear fractions were concentrated using Amicon Ultra centrifugal filter units with a 3K cut off, and samples were diluted such that the final buffer concentrations was the same as Co-IP lysis buffer (20 mM Tris/HCL pH 7.4, 137 mM NaCl, 5% glycerol, 2 mM EDTA, 2 mM Na_3VO_4, Complete™ EDTA-free Protease Inhibitor Cocktail, 0.5% CHAPS). Anti-FLAG® M2 magnetic beads (Sigma-Aldrich) were washed 3 times in Co-IP lysis buffer and the equivalent of 20 µL of initial slurry was added to 3.5 mg of nuclear lysate. Samples

were rotated for 8 hrs at 4°C, and cells were washed 3 times in Co-IP lysis buffer. After the 3rd wash, proteins were eluted by resuspending the beads in 50 µL of Co-IP buffer with 15 µg of FLAG peptides followed by incubation on a vortex platform for 30 min at 4°C. The eluate was transferred to a centrifugal filter prewashed with Co-IP buffer, and the elution step was repeated. Eluates were then pooled in a single tube, TCA precipitated, and submitted for proteomic analysis at the Taplin Mass Spectrometry Facility at Harvard Medical School.

For proteomics analysis, the TCA-precipitated samples were reduced in a solution of 1 mM DTT and 50 mM ammonium bicarbonate for 30 min at 60°C. The samples were then cooled to room temperature (RT) and iodacetamide was added to a concentration of 5 mM for 15 min in the dark at RT. DTT was then added to a 5 mM concentration to quench the reaction. Sequence grade trypsin was added at a concentration of 5 ng/ µL followed by overnight incubation at 37°C. The samples were then desalted by an in house-made desalting column, dried in a speed vac, and stored at 4°C until analysis.

On the day of analysis, the samples were reconstituted in 5-10 µl of HPLC solvent A (2.5% acetonitrile, 0.1% formic acid). A nano-scale reverse-phase HPLC capillary column was created by packing 2.6 µm C18 spherical silica beads into a fused silica capillary (100 µm inner diameter x ~30 cm length) with a flame-drawn tip (Shevchenko et al., 1996). After equilibrating the column, each sample was loaded via a Famos auto sampler (LC Packings) onto the column. A gradient was formed, and peptides were eluted with increasing concentrations of solvent B (97.5% acetonitrile, 0.1% formic acid).

As peptides eluted they were subjected to electrospray ionization and then entered into an LTQ Orbitrap Velos Pro ion-trap mass spectrometer (Thermo Fisher Scientific). Peptides were detected, isolated, and fragmented to produce a tandem mass spectrum of specific fragment ions for each peptide. Peptide sequences (and hence protein identity) were determined by matching protein databases with the acquired fragmentation pattern by the software program, Sequest (Thermo Fisher Scientific) (Eng et al., 1994). All databases include a reversed version of all the

sequences, and the data was filtered to between a one and two percent peptide false discovery rate.

The spectral counts for the identified proteins in Flag-ChREBP immunoprecipitates were normalized by ChREBP spectral counts in each IP sample. Proteins that were enriched above 3-fold in WT compared to *Bad -/-* samples were prioritized for analysis using online databases, including DAVID, Panther, and UniProt. Proteins with exclusively mitochondrial or endoplasmic reticulum localization were excluded from the list.

QUANTIFICATION AND STATISTICAL ANALYSIS

Data are presented as mean ± SEM of the indicated number of independent hepatocyte isolations or mice per genotype in the figure legend. Statistical significance among the groups was tested with unpaired or paired Student's t test and ANOVA when appropriate using GraphPad Prism software. Differences were considered significant at $p < 0.05$.

CONTRIBUTIONS

Elizabeth Lane, Dong Wook Choi and Nika Danial conceived this project, Elizabeth Lane performed the majority of the experiments presented in this chapter. Dong Wook Choi worked with Elizabeth Lane on CO-IP experiments and performed WGA experiments; Meghan Tedoldi and Luisa Garcia-Haro helped with the harvest of organs from HCD fed mice; Luisa Garcia Haro helped with liver ChREBP ChIP experiments. Taplin Mass Spectrometry Facility at Harvard Medical School performed proteomic analysis of FLAG-ChREBP IPs; Daina Avizonis and Gaëlle Bridon performed metabolite measurements at the Rosalind and Morris Goodman Cancer Research Centre Metabolomics Core Facility at McGill University.

REFERENCES

Abdul-Wahed, A., Guilmeau, S., and Postic, C. (2017). Sweet Sixteenth for ChREBP: Established Roles and Future Goals. Cell Metab 26, 324-341.

Agius, L. (2016a). Dietary carbohydrate and control of hepatic gene expression: mechanistic links from ATP and phosphate ester homeostasis to the carbohydrate-response element-binding protein. Proc Nutr Soc 75, 10-18.

Agius, L. (2016b). Hormonal and Metabolite Regulation of Hepatic Glucokinase. Annu Rev Nutr 36, 389-415.

Alves-Bezerra, M., and Cohen, D.E. (2017). Triglyceride Metabolism in the Liver. Compr Physiol 8, 1-8.

Arden, C., Tudhope, S., Petrie, J., Al-Oanzi, Z., Cullen, K., Lange, A., Towle, H., and Agius, L. (2012). Fructose 2,6-bisphosphate is essential for glucose-regulated gene transcription of glucose-6-phosphatase and other ChREBP target genes in hepatocytes. The Biochemical journal 443, 111-123.

Bain, J.R., Schisler, J.C., Takeuchi, K., Newgard, C.B., and Becker, T.C. (2004). An adenovirus vector for efficient RNA interference-mediated suppression of target genes in insulinoma cells and pancreatic islets of langerhans. Diabetes 53, 2190-2194.

Benhamed, F., Denechaud, P.-D.D., Lemoine, M., Robichon, C., Moldes, M., Bertrand-Michel, J., Ratziu, V., Serfaty, L., Housset, C., Capeau, J., et al. (2012). The lipogenic transcription factor ChREBP dissociates hepatic steatosis from insulin resistance in mice and humans. The Journal of clinical investigation 122, 2176-2194.

Bricambert, J., Miranda, J., Benhamed, F., Girard, J., Postic, C., and Dentin, R. (2010). Salt-inducible kinase 2 links transcriptional coactivator p300 phosphorylation to the prevention of ChREBP-dependent hepatic steatosis in mice. J Clin Invest 120, 4316-4331.

Capotosti, F., Guernier, S., Lammers, F., Waridel, P., Cai, Y., Jin, J., Conaway, J.W., Conaway, R.C., and Herr, W. (2011). O-GlcNAc transferase catalyzes site-specific proteolysis of HCF-1. Cell 144, 376-388.

Danial, N., Walensky, L., Zhang, C.-Y., Choi, C., Fisher, J., Molina, A., Datta, S., Pitter, K., Bird, G., Wikstrom, J., et al. (2008). Dual role of proapoptotic BAD in insulin secretion and beta cell survival. Nature medicine 14, 144-153.

Danial, N.N., Gramm, C.F., Scorrano, L., Zhang, C.Y., Krauss, S., Ranger, A.M., Datta, S.R., Greenberg, M.E., Licklider, L.J., Lowell, B.B., et al. (2003). BAD and glucokinase reside in a mitochondrial complex that integrates glycolysis and apoptosis. Nature 424, 952-956.

Daou, S., Mashtalir, N., Hammond-Martel, I., Pak, H., Yu, H., Sui, G., Vogel, J.L., Kristie, T.M., and Affar el, B. (2011). Crosstalk between O-GlcNAcylation and proteolytic cleavage regulates the host cell factor-1 maturation pathway. Proc Natl Acad Sci U S A 108, 2747-2752.

Davies, M.N., O'Callaghan, B.L., and Towle, H.C. (2008). Glucose activates ChREBP by increasing its rate of nuclear entry and relieving repression of its transcriptional activity. J Biol Chem 283, 24029-24038.

Denechaud, P.D., Bossard, P., Lobaccaro, J.M., Millatt, L., Staels, B., Girard, J., and Postic, C. (2008). ChREBP, but not LXRs, is required for the induction of glucose-regulated genes in mouse liver. J Clin Invest 118, 956-964.

Deng, X., Cagen, L.M., Wilcox, H.G., Park, E.A., Raghow, R., and Elam, M.B. (2002). Regulation of the rat SREBP-1c promoter in primary rat hepatocytes. Biochem Biophys Res Commun 290, 256-262.

Dentin, R., Benhamed, F., Hainault, I., Fauveau, V., Foufelle, F., Dyck, J.R., Girard, J., and Postic, C. (2006). Liver-specific inhibition of ChREBP improves hepatic steatosis and insulin resistance in ob/ob mice. Diabetes 55, 2159-2170.

Dentin, R., Pégorier, J.-P., Benhamed, F., Foufelle, F., Ferré, P., Fauveau, V., Magnuson, M., Girard, J., and Postic, C. (2004). Hepatic glucokinase is required for the synergistic action of ChREBP and SREBP-1c on glycolytic and lipogenic gene expression. The Journal of biological chemistry 279, 20314-20326.

Dentin, R., Tomas-Cobos, L., Foufelle, F., Leopold, J., Girard, J., Postic, C., and Ferré, P. (2012). Glucose 6-phosphate, rather than xylulose 5-phosphate, is required for the activation of ChREBP in response to glucose in the liver. Journal of hepatology 56, 199-209.

Deplus, R., Delatte, B., Schwinn, M.K., Defrance, M., Mendez, J., Murphy, N., Dawson, M.A., Volkmar, M., Putmans, P., Calonne, E., et al. (2013). TET2 and TET3 regulate GlcNAcylation and H3K4 methylation through OGT and SET1/COMPASS. EMBO J 32, 645-655.

Diraison, F., Moulin, P., and Beylot, M. (2003). Contribution of hepatic de novo lipogenesis and reesterification of plasma non esterified fatty acids to plasma triglyceride synthesis during non-alcoholic fatty liver disease. Diabetes Metab 29, 478-485.

Donnelly, K.L., Smith, C.I., Schwarzenberg, S.J., Jessurun, J., Boldt, M.D., and Parks, E.J. (2005). Sources of fatty acids stored in liver and secreted via lipoproteins in patients with nonalcoholic fatty liver disease. J Clin Invest 115, 1343-1351.

Eng, J.K., McCormack, A.L., and Yates, J.R. (1994). An approach to correlate tandem mass spectral data of peptides with amino acid sequences in a protein database. J Am Soc Mass Spectrom 5, 976-989.

Gimenez-Cassina, A., and Danial, N.N. (2015). Regulation of mitochondrial nutrient and energy metabolism by BCL-2 family proteins. Trends Endocrinol Metab 26, 165-175.

Giménez-Cassina, A., Garcia-Haro, L., Choi, C.S., Osundiji, M.A., Lane, E.A., Huang, H., Yildirim, M.A., Szlyk, B., Fisher, J.K., Polak, K., et al. (2014). Regulation of hepatic energy metabolism and gluconeogenesis by BAD. Cell metabolism 19, 272-284.

Guinez, C., Filhoulaud, G., Rayah-Benhamed, F., Marmier, S., Dubuquoy, C., Dentin, R., Moldes, M., Burnol, A.F., Yang, X., Lefebvre, T., et al. (2011). O-GlcNAcylation increases ChREBP protein content and transcriptional activity in the liver. Diabetes 60, 1399-1413.

Han, J.W., Valdez, J.L., Ho, D.V., Lee, C.S., Kim, H.M., Wang, X., Huang, L., and Chan, J.Y. (2017). Nuclear factor-erythroid-2 related transcription factor-1 (Nrf1) is regulated by O-GlcNAc transferase. Free Radic Biol Med 110, 196-205.

Havula, E., and Hietakangas, V. (2012). Glucose sensing by ChREBP/MondoA-Mlx transcription factors. Semin Cell Dev Biol 23, 640-647.

Herman, M.A., Peroni, O.D., Villoria, J., Schon, M.R., Abumrad, N.A., Bluher, M., Klein, S., and Kahn, B.B. (2012). A novel ChREBP isoform in adipose tissue regulates systemic glucose metabolism. Nature 484, 333-338.

Hurtado del Pozo, C., Vesperinas-Garcia, G., Rubio, M.A., Corripio-Sanchez, R., Torres-Garcia, A.J., Obregon, M.J., and Calvo, R.M. (2011). ChREBP expression in the liver, adipose tissue and differentiated preadipocytes in human obesity. Biochim Biophys Acta 1811, 1194-1200.

Iizuka, K., Miller, B., and Uyeda, K. (2006). Deficiency of carbohydrate-activated transcription factor ChREBP prevents obesity and improves plasma glucose control in leptin-deficient (ob/ob) mice. Am J Physiol Endocrinol Metab 291, E358-364.

Iizuka, K., Wu, W., Horikawa, Y., and Takeda, J. (2013). Role of glucose-6-phosphate and xylulose-5-phosphate in the regulation of glucose-stimulated gene expression in the pancreatic beta cell line, INS-1E. Endocr J 60, 473-482.

Ishii, S., Iizuka, K., Miller, B.C., and Uyeda, K. (2004). Carbohydrate response element binding protein directly promotes lipogenic enzyme gene transcription. Proc Natl Acad Sci U S A 101, 15597-15602.

Kabashima, T., Kawaguchi, T., Wadzinski, B.E., and Uyeda, K. (2003). Xylulose 5-phosphate mediates glucose-induced lipogenesis by xylulose 5-phosphate-activated protein phosphatase in rat liver. Proc Natl Acad Sci U S A 100, 5107-5112.

Kim, M.S., Krawczyk, S.A., Doridot, L., Fowler, A.J., Wang, J.X., Trauger, S.A., Noh, H.L., Kang, H.J., Meissen, J.K., Blatnik, M., et al. (2016). ChREBP regulates fructose-induced glucose production independently of insulin signaling. J Clin Invest 126, 4372-4386.

Kooner, J., Chambers, J., Aguilar-Salinas, C., Hinds, D., Hyde, C., Warnes, G., Gómez Pérez, F., Frazer, K., Elliott, P., Scott, J., et al. (2008). Genome-wide scan identifies variation in MLXIPL associated with plasma triglycerides. Nature genetics 40, 149-151.

Lazarus, M.B., Jiang, J., Kapuria, V., Bhuiyan, T., Janetzko, J., Zandberg, W.F., Vocadlo, D.J., Herr, W., and Walker, S. (2013). HCF-1 is cleaved in the active site of O-GlcNAc transferase. Science 342, 1235-1239.

Lin, J., Puigserver, P., Donovan, J., Tarr, P., and Spiegelman, B.M. (2002). Peroxisome proliferator-activated receptor gamma coactivator 1beta (PGC-1beta), a novel PGC-1-related transcription coactivator associated with host cell factor. J Biol Chem 277, 1645-1648.

Lou, D.Q., Tannour, M., Selig, L., Thomas, D., Kahn, A., and Vasseur-Cognet, M. (1999). Chicken ovalbumin upstream promoter-transcription factor II, a new partner of the glucose response element of the L-type pyruvate kinase gene, acts as an inhibitor of the glucose response. J Biol Chem 274, 28385-28394.

Ma, L., Robinson, L.N., and Towle, H.C. (2006). ChREBP*Mlx is the principal mediator of glucose-induced gene expression in the liver. J Biol Chem 281, 28721-28730.

Matschinsky, F.M. (2009). Assessing the potential of glucokinase activators in diabetes therapy. Nat Rev Drug Discov 8, 399-416.

Matsumoto, M., Pocai, A., Rossetti, L., Depinho, R.A., and Accili, D. (2007). Impaired regulation of hepatic glucose production in mice lacking the forkhead transcription factor Foxo1 in liver. Cell Metab 6, 208-216.

Metukuri, M.R., Zhang, P., Basantani, M.K., Chin, C., Stamateris, R.E., Alonso, L.C., Takane, K.K., Gramignoli, R., Strom, S.C., O'Doherty, R.M., et al. (2012). ChREBP mediates glucose-stimulated pancreatic beta-cell proliferation. Diabetes 61, 2004-2015.

Nissim, I., Horyn, O., Nissim, I., Daikhin, Y., Wehrli, S.L., Yudkoff, M., and Matschinsky, F.M. (2012). Effects of a glucokinase activator on hepatic intermediary metabolism: study with 13C-isotopomer-based metabolomics. Biochem J 444, 537-551.

O'Callaghan, B.L., Koo, S.H., Wu, Y., Freake, H.C., and Towle, H.C. (2001). Glucose regulation of the acetyl-CoA carboxylase promoter PI in rat hepatocytes. J Biol Chem 276, 16033-16039.

Perumpail, B.J., Khan, M.A., Yoo, E.R., Cholankeril, G., Kim, D., and Ahmed, A. (2017). Clinical epidemiology and disease burden of nonalcoholic fatty liver disease. World J Gastroenterol 23, 8263-8276.

Petrie, J.L., Al-Oanzi, Z.H., Arden, C., Tudhope, S.J., Mann, J., Kieswich, J., Yaqoob, M.M., Towle, H.C., and Agius, L. (2013). Glucose induces protein targeting to glycogen in hepatocytes by fructose 2,6-bisphosphate-mediated recruitment of MondoA to the promoter. Mol Cell Biol 33, 725-738.

Postic, C., Shiota, M., Niswender, K.D., Jetton, T.L., Chen, Y., Moates, J.M., Shelton, K.D., Lindner, J., Cherrington, A.D., and Magnuson, M.A. (1999). Dual roles for glucokinase in glucose homeostasis as determined by liver and pancreatic beta cell-specific gene knock-outs using Cre recombinase. J Biol Chem 274, 305-315.

Ruan, H.B., Han, X., Li, M.D., Singh, J.P., Qian, K., Azarhoush, S., Zhao, L., Bennett, A.M., Samuel, V.T., Wu, J., et al. (2012). O-GlcNAc transferase/host cell factor C1 complex regulates gluconeogenesis by modulating PGC-1alpha stability. Cell Metab 16, 226-237.

Ryczko, M.C., Pawling, J., Chen, R., Abdel Rahman, A.M., Yau, K., Copeland, J.K., Zhang, C., Surendra, A., Guttman, D.S., Figeys, D., et al. (2016). Metabolic Reprogramming by Hexosamine Biosynthetic and Golgi N-Glycan Branching Pathways. Sci Rep 6, 23043.

Sakiyama, H., Fujiwara, N., Noguchi, T., Eguchi, H., Yoshihara, D., Uyeda, K., and Suzuki, K. (2010). The role of O-linked GlcNAc modification on the glucose response of ChREBP. Biochem Biophys Res Commun 402, 784-789.

Samuel, V.T., and Shulman, G.I. (2018). Nonalcoholic Fatty Liver Disease as a Nexus of Metabolic and Hepatic Diseases. Cell Metab 27, 22-41.

Sanders, F.W., and Griffin, J.L. (2016). De novo lipogenesis in the liver in health and disease: more than just a shunting yard for glucose. Biol Rev Camb Philos Soc 91, 452-468.

Savage, D.B., Choi, C.S., Samuel, V.T., Liu, Z.X., Zhang, D., Wang, A., Zhang, X.M., Cline, G.W., Yu, X.X., Geisler, J.G., et al. (2006). Reversal of diet-induced hepatic steatosis and hepatic insulin

resistance by antisense oligonucleotide inhibitors of acetyl-CoA carboxylases 1 and 2. J Clin Invest 116, 817-824.

Schwarz, J.M., Neese, R.A., Turner, S., Dare, D., and Hellerstein, M.K. (1995). Short-term alterations in carbohydrate energy intake in humans. Striking effects on hepatic glucose production, de novo lipogenesis, lipolysis, and whole-body fuel selection. J Clin Invest 96, 2735-2743.

Shevchenko, A., Wilm, M., Vorm, O., and Mann, M. (1996). Mass spectrometric sequencing of proteins silver-stained polyacrylamide gels. Anal Chem 68, 850-858.

Softic, S., Cohen, D.E., and Kahn, C.R. (2016). Role of Dietary Fructose and Hepatic De Novo Lipogenesis in Fatty Liver Disease. Dig Dis Sci 61, 1282-1293.

Stamatikos, A.D., da Silva, R.P., Lewis, J.T., Douglas, D.N., Kneteman, N.M., Jacobs, R.L., and Paton, C.M. (2016). Tissue Specific Effects of Dietary Carbohydrates and Obesity on ChREBPalpha and ChREBPbeta Expression. Lipids 51, 95-104.

Sunny, N.E., Parks, E.J., Browning, J.D., and Burgess, S.C. (2011). Excessive hepatic mitochondrial TCA cycle and gluconeogenesis in humans with nonalcoholic fatty liver disease. Cell Metab 14, 804-810.

Szlyk, B., Braun, C.R., Ljubicic, S., Patton, E., Bird, G.H., Osundiji, M.A., Matschinsky, F.M., Walensky, L.D., and Danial, N.N. (2014). A phospho-BAD BH3 helix activates glucokinase by a mechanism distinct from that of allosteric activators. Nat Struct Mol Biol 21, 36-42.

Than, N.N., and Newsome, P.N. (2015). A concise review of non-alcoholic fatty liver disease. Atherosclerosis 239, 192-202.

Tsatsos, N., and Towle, H. (2006). Glucose activation of ChREBP in hepatocytes occurs via a two-step mechanism. Biochemical and biophysical research communications 340, 449-456.

Tyagi, S., Chabes, A.L., Wysocka, J., and Herr, W. (2007). E2F activation of S phase promoters via association with HCF-1 and the MLL family of histone H3K4 methyltransferases. Mol Cell 27, 107-119.

Uyeda, K., and Repa, J. (2006). Carbohydrate response element binding protein, ChREBP, a transcription factor coupling hepatic glucose utilization and lipid synthesis. Cell metabolism 4, 107-110.

Velho, G., Petersen, K.F., Perseghin, G., Hwang, J.H., Rothman, D.L., Pueyo, M.E., Cline, G.W., Froguel, P., and Shulman, G.I. (1996). Impaired hepatic glycogen synthesis in glucokinase-deficient (MODY-2) subjects. J Clin Invest 98, 1755-1761.

Wang, Y., Viscarra, J., Kim, S.J., and Sul, H.S. (2015). Transcriptional regulation of hepatic lipogenesis. Nat Rev Mol Cell Biol 16, 678-689.

Wysocka, J., Myers, M.P., Laherty, C.D., Eisenman, R.N., and Herr, W. (2003). Human Sin3 deacetylase and trithorax-related Set1/Ash2 histone H3-K4 methyltransferase are tethered together selectively by the cell-proliferation factor HCF-1. Genes Dev 17, 896-911.

Yang, A.Q., Li, D., Chi, L., and Ye, X.S. (2017). Validation, Identification, and Biological Consequences of the Site-specific O-GlcNAcylation Dynamics of Carbohydrate-responsive Element-binding Protein (ChREBP). Mol Cell Proteomics 16, 1233-1243.

Yang, X., and Qian, K. (2017). Protein O-GlcNAcylation: emerging mechanisms and functions. Nat Rev Mol Cell Biol 18, 452-465.

Yecies, J.L., Zhang, H.H., Menon, S., Liu, S., Yecies, D., Lipovsky, A.I., Gorgun, C., Kwiatkowski, D.J., Hotamisligil, G.S., Lee, C.H., et al. (2011). Akt stimulates hepatic SREBP1c and lipogenesis through parallel mTORC1-dependent and independent pathways. Cell Metab 14, 21-32.

Zhang, P., Kumar, A., Katz, L.S., Li, L., Paulynice, M., Herman, M.A., and Scott, D.K. (2015). Induction of the ChREBPbeta Isoform Is Essential for Glucose-Stimulated beta-Cell Proliferation. Diabetes 64, 4158-4170.

Zhou, P., Wang, Z., Yuan, X., Zhou, C., Liu, L., Wan, X., Zhang, F., Ding, X., Wang, C., Xiong, S., et al. (2013). Mixed lineage leukemia 5 (MLL5) protein regulates cell cycle progression and E2F1-responsive gene expression via association with host cell factor-1 (HCF-1). J Biol Chem 288, 17532-17543.

CHAPTER 3
Regulation of Hepatic Energy Metabolism and Gluconeogenesis by BAD

SUMMARY

The homeostatic balance of hepatic glucose utilization, storage and production is exquisitely controlled by hormonal signals and hepatic carbon metabolism during fed and fasted states. How the liver senses extracellular glucose to cue glucose utilization versus production is not fully understood. Here, we show that the physiologic balance of hepatic glycolysis and gluconeogenesis is regulated by BAD, a dual function protein with roles in apoptosis and metabolism. BAD deficiency reprograms hepatic substrate and energy metabolism towards diminished glycolysis, excess fatty acid oxidation and exaggerated glucose production that escapes suppression by insulin. Genetic and biochemical evidence suggest that BAD's suppression of gluconeogenesis is actuated by phosphorylation of its BH3 domain and subsequent activation of glucokinase. The physiologic relevance of these findings is evident from the ability of a BAD phospho-mimic variant to counteract unrestrained gluconeogenesis and improve glycemia in leptin resistant and high-fat diet models of diabetes and insulin resistance.

INTRODUCTION

Hepatic glucose production (HGP) is central to metabolic adaptation during fasting and its abnormal elevation is a chief determinant of fasting hyperglycemia in diabetes (Lin and Accili, 2011; Rizza, 2010). During short term fasting, glucose is produced by both net glycogenolysis and gluconeogenesis (Rothman et al., 1991), whereas upon prolonged fasting, glucose is synthesized almost exclusively from gluconeogenesis. Gluconeogenesis and glycolysis are competing pathways that are reciprocally regulated by glucagon and insulin during fasted and fed states, respectively. In addition to transcriptional regulation, changes in hepatic carbon flux can exert allosteric effects on gluconeogenic enzymes (Magnuson et al., 2003). Hepatic substrate flux is further intertwined with fatty acid oxidation (FAO), TCA cycle and mitochondrial electron transport chain activity, which supply the gluconeogenic pathway with carbon substrates, reducing equivalents and ATP (Satapati et al., 2012).

We have previously shown that the BCL-2 family protein BAD has an alternative function in glucose metabolism separate from its role in apoptosis (Danial, 2008; Danial et al., 2003; Danial et al., 2008). BAD's metabolic effect is dependent on its ability to activate glucokinase (GK) and modulate glucose oxidation (Danial, 2008; Danial et al., 2008). GK is the product of the maturity onset diabetes of the young type 2 (MODY2) gene that exerts tissue-restricted functions (Matschinsky, 2009). In liver, GK regulates substrate utilization and storage by stimulating glycogen and lipid synthesis while suppressing hepatic glucose production (Postic et al., 1999; Rossetti et al., 1997; Velho et al., 1996). In β-cells, GK is critical for glucose-regulation of insulin secretion (Matschinsky, 2009). We previously reported that in β-cells, GK activation and glucose sensing are attuned to BAD phosphorylation on S155 within an amphipathic α-helical region known as the BCL-2 Homology (BH)-3 domain. BAD S155 is the target of multiple kinases that either phosphorylate S155 directly or modify upstream priming phosphorylation sites, facilitating S155 phosphorylation [reviewed in (Danial, 2008)]. Phosphorylation of the BH3 domain not only triggers BAD's metabolic function but also suppresses its apoptotic activity. Importantly, the

phospho-BAD BH3 helix is both required and sufficient for BAD's metabolic function (Danial et al., 2008). Recent biochemical and structural dissection of the BAD-GK complex has revealed that the phospho-BAD BH3 helix directly engages GK near its active site and increases the Vmax of the enzyme without drastic effects on its glucose affinity (Szlyk et al., 2014).

Beyond β-cell abnormalities, the contribution of altered hepatic metabolism to glucose homeostasis defects associated with loss of BAD has not been examined. This is especially relevant as the regulatory networks that modulate GK activity in liver are distinct from β-cells (Matschinsky, 2009). Here, we use a combination of informative genetic models and BAD mutants to investigate the significance of BAD and its partnership with GK in hepatic substrate utilization and glucose production. Moreover, we probe the physiologic relevance of hepatic BAD in restoring proper control of glucose production in the leptin resistant and high-fat diet models of diabetes and insulin resistance.

RESULTS

BAD-dependent modulation of hepatic glucose metabolism

To define the contribution of altered hepatic metabolism to glucose homeostasis abnormalities in *Bad -/-* mice, we initially focused on glycolytic and gluconeogenic pathways. In primary *Bad -/-* hepatocytes, lactate production in response to glucose was diminished (Figure 3.1A), and gluconeogenesis was significantly exaggerated as apparent from glucose release in response to lactate/pyruvate (Figure 3.1B). These observations suggest that the net balance of glycolysis and gluconeogenesis is shifted towards gluconeogenesis in the absence of BAD. Pyruvate tolerance tests (PTT) confirmed that *Bad -/-* mice display significantly higher gluconeogenic conversion of pyruvate to glucose *in vivo* (Figure 3.1C). Importantly, knockdown of *Bad* in primary wild-type hepatocytes was sufficient to reduce glycolysis and enhance gluconeogenesis (Figures 3.1D and E), indicating an acute and cell autonomous role for BAD in these processes.

Impaired PTT in *Bad -/-* mice is consistent with changes in hepatic glucose metabolism, however, secondary changes due to chronic whole body deletion of *Bad* cannot be excluded. To directly examine the relevance of hepatic BAD *in vivo*, *Bad* was knocked down in the liver of C57BL/6J mice following tail vein delivery of adenoviruses bearing *Bad* shRNA or control (scrambled) sequence (Figure 3.2A). Hepatic depletion of BAD manifested in excess glucose production during PTT and fasting hyperglycemia (Figure 3.1F). In addition, acute hepatic knockdown of *Bad* resulted in impaired glucose tolerance (Figure 3.2B) similar to *Bad -/-* mice (Danial et al., 2003). Notably, hepatic depletion of BAD did not alter insulin secretion in response to a glucose challenge *in vivo* (Figure 3.2C). In addition, fed/fasted insulin levels were comparable in mice treated with *Bad* shRNA versus control shRNA (Figure 3.2D). Collectively, the above *in vitro* and *in vivo* observations indicate that hepatic BAD influences the fate of pyruvate and is relevant for the proper regulation of glucose utilization and production in the liver.

Figure 3.1. Hepatic glucose metabolism in the absence of BAD

(A) Glucose-stimulated lactate production by primary *Bad* +/+ and -/- hepatocytes (n=5-8). **(B)** Glucose release by *Bad* +/+ and -/- hepatocytes treated with lactate/pyruvate (n=6). **(C)** PTT in *Bad* +/+ and -/- mice (n=14-20). **(D)** Lactate production in *Bad* knockdown hepatocytes 8 hr after glucose stimulation (n=9). **(E)** Glucose production in *Bad* knockdown hepatocytes treated with lactate/pyruvate (n=3-5). **(F)** PTT in C57BL/6J mice after hepatic knockdown of *Bad* (n=12-17). **(G-H)** Relative hepatic mRNA levels of *Pck1* (G) and *L-Pk* (H) in fed and overnight fasted C57BL/6J mice after hepatic knockdown of *Bad* (n=10). **(I)** PTT in C57BL/6J mice after hepatic knockdown of *Gk* (n=8-12). **(J-K)** Relative hepatic mRNA levels of *Pck1* (J) and *L-Pk* (K) in fed and overnight fasted C57BL/6J mice after hepatic knockdown of *Gk* (n=5).

Error bars, ± SEM. *$p < 0.05$; **$p < 0.01$, ***$p < 0.001$.

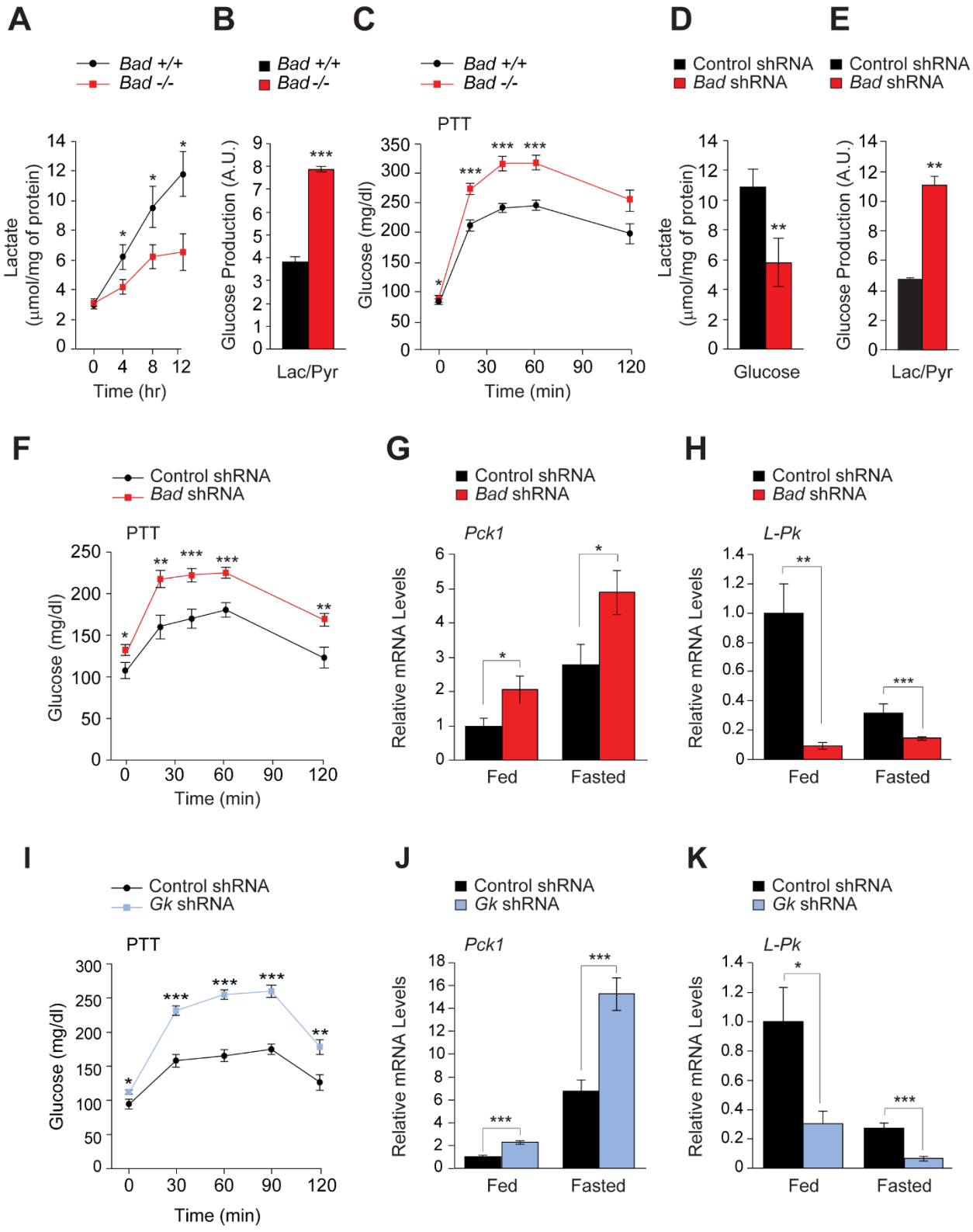


Figure 3.1. (Continued)

Figure 3.2. BAD-modulation of hepatic glucose metabolism.

(A) Hepatic BAD protein levels in C57BL/6J mice 5 days after tail vein delivery of control or *Bad* shRNA adenoviruses. **(B-C)** Blood glucose **(B)** and insulin levels **(C)** during i.p. GTT in C57BL/6J mice treated as in **(A)** (n=5-8). **(D)** Serum insulin levels in fed and overnight-fasted C57BL/6J mice after hepatic knockdown of *Bad* (n=10). **(E)** Relative hepatic mRNA levels of glycolytic (*L-Pk, Gk*) and gluconeogenic (*Pck1, Fbp1, G6pc*) genes in fed and overnight-fasted *Bad* +/+ and -/- mice (n=5). **(F-G)** Relative levels of *Pck1* (F) and *L-Pk* (G) mRNAs in primary hepatocytes incubated with high or low glucose concentrations for 24 hr after *Bad* knockdown (n=4-5 independent hepatocyte cultures). **(H)** Hepatic GK protein levels in C57BL/6J mice 5 days after tail vein delivery of control or *Gk* shRNA adenoviruses. **(I)** Blood glucose during i.p. GTT in C57BL/6J mice treated as in (H) (n=5).

Error bars, ± SEM. *p < 0.05; **p < 0.01; ***p < 0.001.

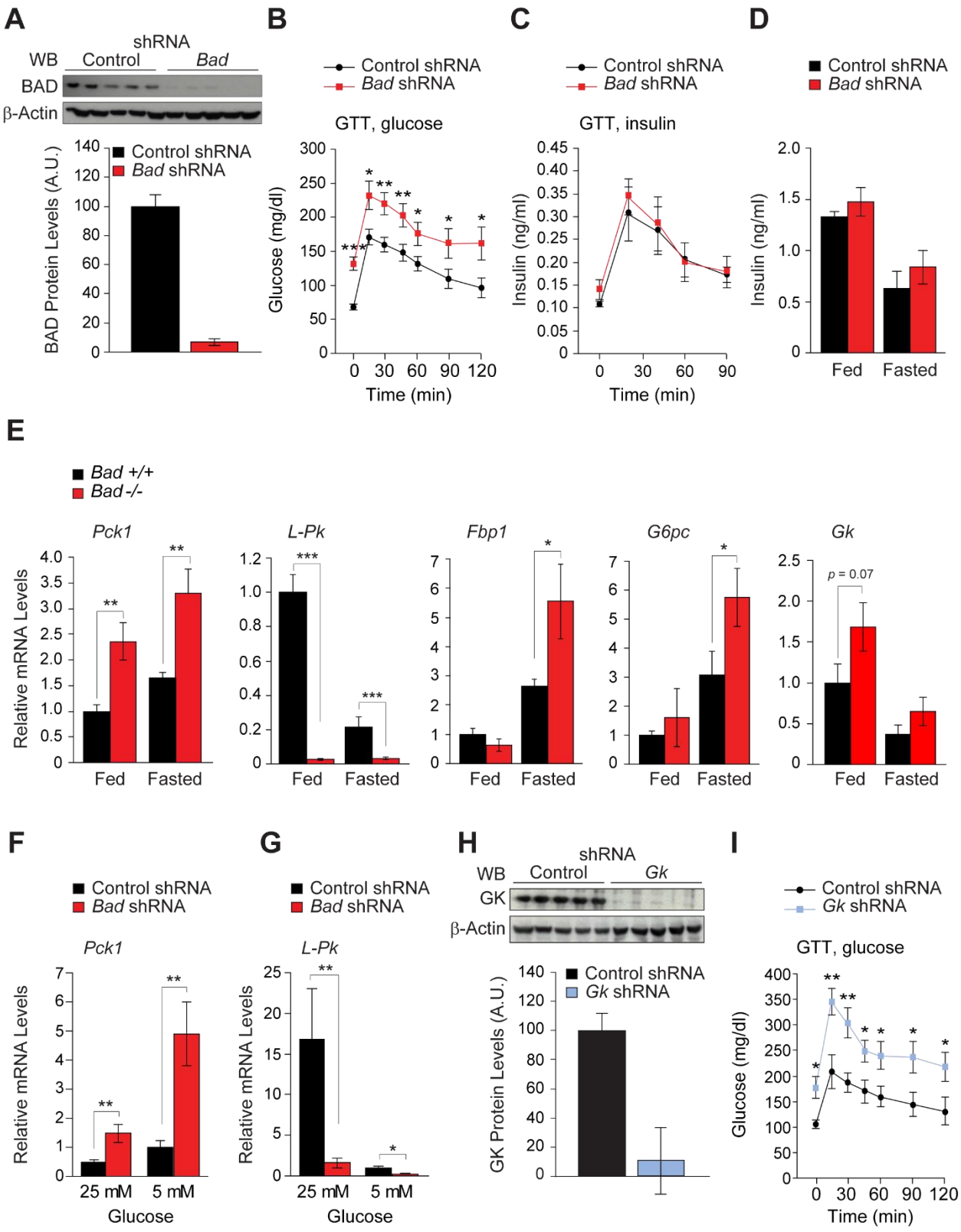


Figure 3.2. (Continued)

Hepatic pyruvate metabolism is regulated, at least in part, at the transcriptional level downstream of hormonal and nutrient signaling (Lin and Accili, 2011). Initial examination of gluconeogenic and glycolytic genes in fed and fasted *Bad -/-* and *Bad* knockdown liver indicated changes in several genes. In particular, mRNA levels of the gluconeogenic enzyme phosphoenolpyruvate carboxykinase (*Pck*) 1 were significantly elevated, while mRNA levels of the glycolytic enzyme liver-type pyruvate kinase (*L-Pk*) were significantly diminished (Figures 3.1G, H, and 3.2E). Other gluconeogenic genes [fructose 1,6-bisphosphatase (*Fbp*) 1 and glucose 6-phosphatase (*G6Pase*)] were also increased in *Bad -/-* liver (Figure 3.2E). This is further consistent with BAD-dependent reciprocal changes in hepatic glycolysis and gluconeogenesis.

In addition to transcriptional control during fed/fasted states, *L-Pk* and *Pck1* expression can be regulated by glucose. Specifically, the promoters of both genes are glucose-sensitive in that increased glucose metabolism through GK stimulates *L-Pk* transcription and represses that of *Pck1* (Cournarie et al., 1999; Scott et al., 1998; Yamada and Noguchi, 1999). Based on these reports, we predicted that glucose-modulation of *L-Pk* and *Pck1* transcription may be altered upon hepatic depletion of BAD and the attendant diminution of glucose metabolism. This was indeed the case. In wild-type hepatocytes, *L-Pk* mRNA levels were elevated at high compared to low glucose concentrations (25 mM versus 5 mM), whereas *Pck1* mRNA levels showed the opposite profile (Figures 3.2F and G). *Bad* knockdown, however, resulted in higher *Pck1* mRNA levels that were especially exaggerated at low glucose (Figure 3.2F). In comparison, glucose-stimulation of *L-Pk* transcripts was significantly reduced (Figure 3.2G).

The above observations in both cultured hepatocytes and whole animals using a combination of biochemical and transcriptional readouts suggest that BAD is required for proper interpretation of glucose signals. Notably, the metabolic outcome of BAD depletion in the liver was phenocopied in mice treated with *Gk* shRNA (Figure 3.2H). This is evident from exaggerated glucose levels during PTT, significant elevation of hepatic *Pck1* mRNA levels and diminution of

L-Pk transcripts, as well as impaired glucose tolerance (Figures 3.1I, J, K, and 3.2I). Given the biochemical interaction between BAD and GK (Danial et al., 2003; Danial et al., 2008; Szlyk et al., 2014), these shared metabolic outcomes suggest their functional partnership may be relevant for the proper control of glycolysis and gluconeogenesis in the liver (see below).

We have previously reported that BAD's capacity to activate GK in β-cells is triggered by S155 phosphorylation (aa enumeration based on the mouse sequence of BAD) (Danial et al., 2008). Importantly, S155 phosphorylation is sensitive to nutrient status in both β-cells (Danial et al., 2008) and in liver (Figure 3.3A). Specifically, BAD S155 phosphorylation is induced upon re-feeding. In addition, the phosphorylation of two priming serine residues upstream of the BAD BH3 domain, S112 and S136, is similarly increased upon re-feeding (Figure 3.3A). These observations suggest that BAD phosphorylation and metabolic activity may be integrated with nutritional states. Consistent with this idea, interference with BAD phosphorylation through a *Bad* S155A non-phosphorylatable knock-in allele was associated with fasting hyperglycemia and excess glucose release during PTT (Figure 3.3B).

To interrogate the direct significance of BAD phosphorylation specifically in the liver, we carried out whole animal liver reconstitution assays in *Bad -/-* mice using adenoviruses expressing wild-type or defined phosphorylation mutants within the BAD BH3 domain. Hepatic reconstitution with wild-type BAD lowered the glucose values during PTT, indicating that exaggerated gluconeogenesis in *Bad -/-* is directly related to the loss of BAD function in the liver (Figure 3.3C). Given BAD's dual capacity to engage GK and influence glucose metabolism on one hand, and to bind select BCL-2 protein (BCL-2, BCL-XL and BCL-w) and influence the sensitivity of cells to apoptosis on the other, a definitive role for BAD's metabolic function in regulation of gluconeogenesis could not be inferred solely based on the phenotype of wild-type BAD in these assays. Therefore, we examined three separate BAD phosphorylation

Figure 3.3. The effect of BAD phosphorylation on gluconeogenesis

(A) Immunoblot analysis and quantification of relative BAD phosphorylation on S155, S136 and S112 in liver samples derived from C57BL/6J mice fasted overnight and re-fed for 6 hr after overnight fasting. **(B)** PTT in *Bad* +/+ and S155A knock-in mice (n=10-11). **(C)** PTT in *Bad* +/+ and -/- mice following hepatic reconstitution with the indicated adenoviruses (n=16-24). Asterisks in (C) compare *Bad* -/-: BAD S155D versus *Bad* -/-: GFP and the symbols # compare *Bad* -/-: BAD WT versus *Bad* -/-: GFP. **(D)** Glucose production in primary *Bad* -/- hepatocytes reconstituted with the indicated adenoviruses and treated with lactate/pyruvate (n=7-12).

Error bars, ± SEM. *p < 0.05; **p < 0.01, ***p < 0.001; n.s., non-significant.

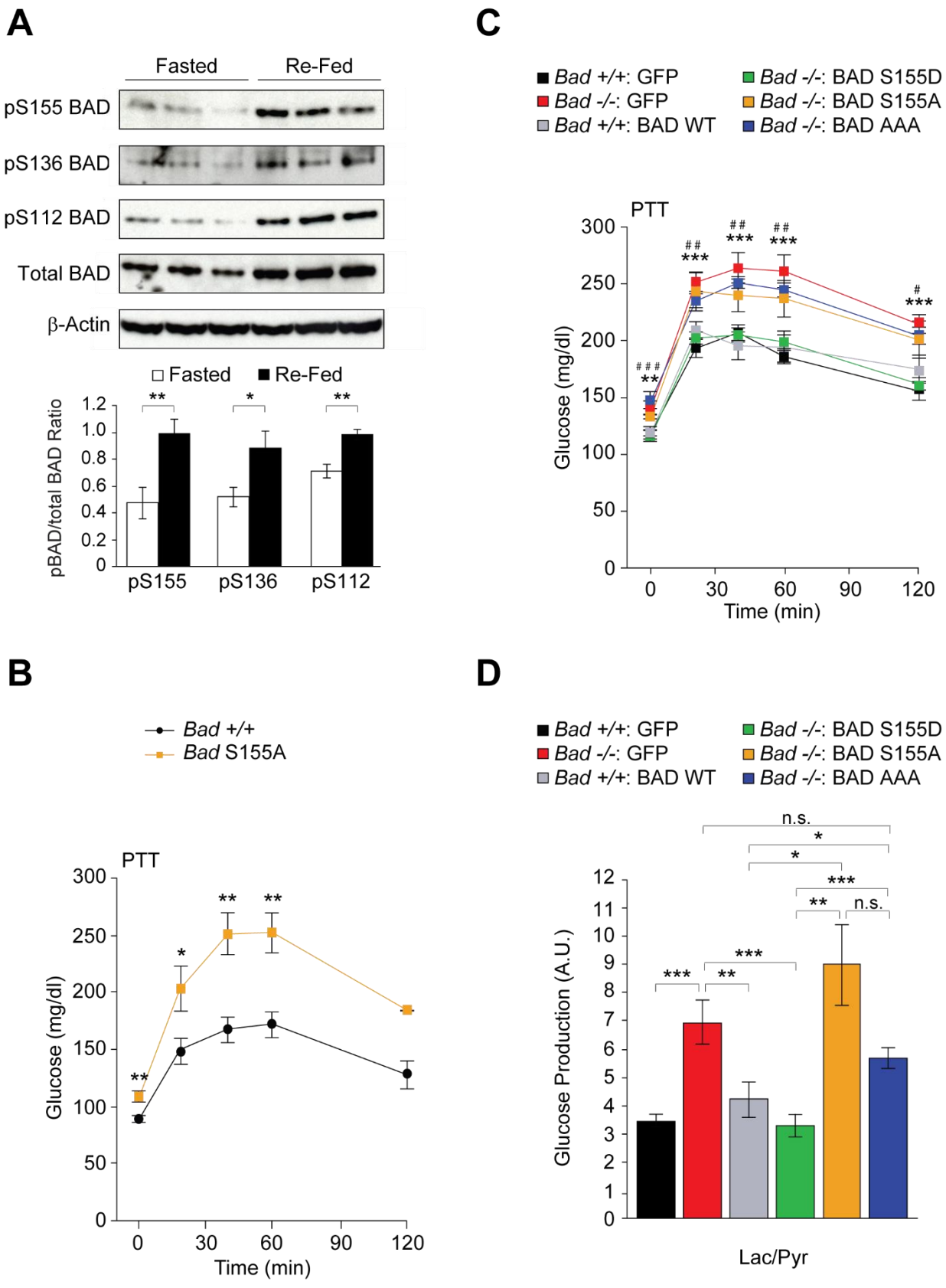


Figure 3.3. (Continued)

mutants that are competent or deficient in activating GK (Figure 3.4A). The phospho-mimic S155D mutation triggers BAD's capacity to activate GK while blocking its interaction with BCL-2 protein partners (Danial et al., 2008). Hepatic reconstitution with this mutant was sufficient to restore GK activity and correct the PTT profile of *Bad -/-* mice (Figures 3.3C and 3.4B). The corresponding phospho-deficient variant, BAD S155A, which is compromised in its capacity to restore hepatic GK activity in *Bad -/-* mice (Figure 3.4B), did not correct the glucose values during PTT (Figure 3.3C). Although diminished in its ability to activate GK, BAD S155A retains its capacity to interact with BCL-2 family partners (Danial, 2008), and is therefore not a direct control for S155D GK-activating variant, which does not bind to BCL-2 family proteins (Figure 3.4A). For these reasons, we used a second phospho-deficient BAD variant that has diminished GK-activating capacity but cannot bind BCL-2 family partners (BAD L151A, S155A, and D156A triple mutant referred to as BAD AAA) (Figures 3.4A and B) (Danial et al., 2008). Parallel comparison of this mutant with BAD S155D allowed assessment of BAD's capacity to engage and activate GK separate from its ability to bind BCL-2 family partners. Unlike BAD S155D, BAD AAA did not restore the PTT profile in *Bad -/-* mice (Figure 3.3C). Furthermore, *in vitro* genetic reconstitution studies using these variants were consistent with the above observations in that BAD S155D, but not BAD S155A or BAD AAA corrected gluconeogenesis in *Bad -/-* hepatocytes to levels comparable to GFP-expressing *Bad +/+* controls (Figure 3.3D). Thus *in vivo* and *in vitro* interference with BAD S155 phosphorylation is associated with unrestrained gluconeogenesis and phenocopies the changes in hepatic metabolism observed in *Bad -/-* and *Bad* knockdown liver.

BAD's effect on mitochondrial energy metabolism in hepatocytes

Mitochondria play a pivotal role in gluconeogenesis through provision of carbon substrates, reducing equivalents, and ATP (Burgess et al., 2007; Satapati et al., 2012). Metabolic flux analysis has also uncovered a tight connection between PCK1, mitochondrial

A

BAD BH3 Variants	GK-Activating Capacity	Binding to BCL-2 Family Partners
Wild-type L W A A Q R Y G R E L R R M S D E F E G S F K G L	+	+
S155D L W A A Q R Y G R E L R R M D D E F E G S F K G L	+	-
S155A L W A A Q R Y G R E L R R M A D E F E G S F K G L	-	+
AAA (L151A, S155A, D156A) L W A A Q R Y G R E A R R M A A E F E G S F K G L	-	-

B

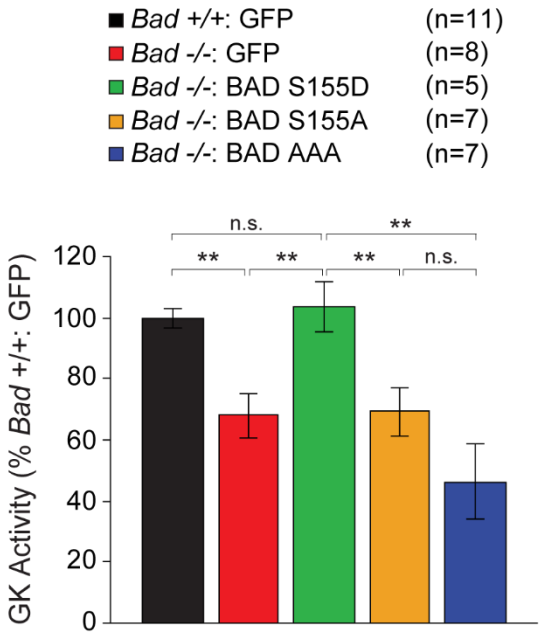


Figure 3.4. BAD's hepatic function is modulated by its phosphorylation status.

(A) BAD phospho-variants used in reconstitution studies. The effect of each mutation on BAD's dual functions or interaction partners is summarized. **(B)** Hepatic GK activity in *Bad* +/+ and -/- mice after tail vein delivery of the indicated adenoviruses.

Error bars, ± SEM. **p < 0.01; n.s., non-significant.

bioenergetics and TCA cycle (Burgess et al., 2007; Hakimi et al., 2005; Satapati et al., 2012). To assess how *Bad -/-* hepatocytes derive the ATP required to support excess gluconeogenesis, we focused on mitochondrial energy metabolism. We reasoned that gluconeogenesis from exogenous lactate/pyruvate would create a state of energy demand driving ATP production by mitochondrial oxidative phosphorylation, which can be deduced from the fraction of mitochondrial oxygen consumption rate (OCR) that is sensitive to the mitochondrial ATP-synthase inhibitor oligomycin. In the presence of lactate/pyruvate, *Bad -/-* hepatocytes showed a significantly higher induction of mitochondrial ATP production (Figure 3.5A and Table 3.1), which was restored to wild-type values after genetic introduction of the BAD S155D variant but not the BAD AAA mutant (Figure 3.5A and Table 3.1).

Gluconeogenesis and mitochondrial FAO are interdependent. For example, fatty acids augment flux through pyruvate carboxylase leading to significant stimulation of OCR and gluconeogenesis in the presence of lactate/pyruvate (Gustafson et al., 2001; Pryor et al., 1987). Importantly, inhibition of carnitine palmitoyl transferase (CPT1), which is required for mitochondrial import of long-chain fatty acids, or interference with mitochondrial electron transport chain activity reverse these effects (Pryor et al., 1987), indicating the importance of mitochondria in energetic and substrate coupling between FAO and gluconeogenesis. This prompted examination whether increased gluconeogenesis in the absence of BAD is linked to elevated FAO. Indeed, mitochondrial OCR in response to palmitate was significantly higher in primary *Bad -/-* hepatocytes compared with controls (Figure 3.5B and Table 3.1). Similar results were also obtained in *Bad* knockdown hepatocytes (data not shown). As predicted, the rise in OCR normally seen upon treatment with lactate/pyruvate was inhibited by the mitochondrial FAO inhibitor etomoxir (Etx) in both *Bad* +/+ and -/- hepatocytes (Figure 3.5C). However, the etomoxir inhibitable portion of this respiratory rate was significantly larger in *Bad -/-* than control hepatocytes (Figure 3.5C and Table 3.1), which is in agreement with higher FAO in *Bad -/-*

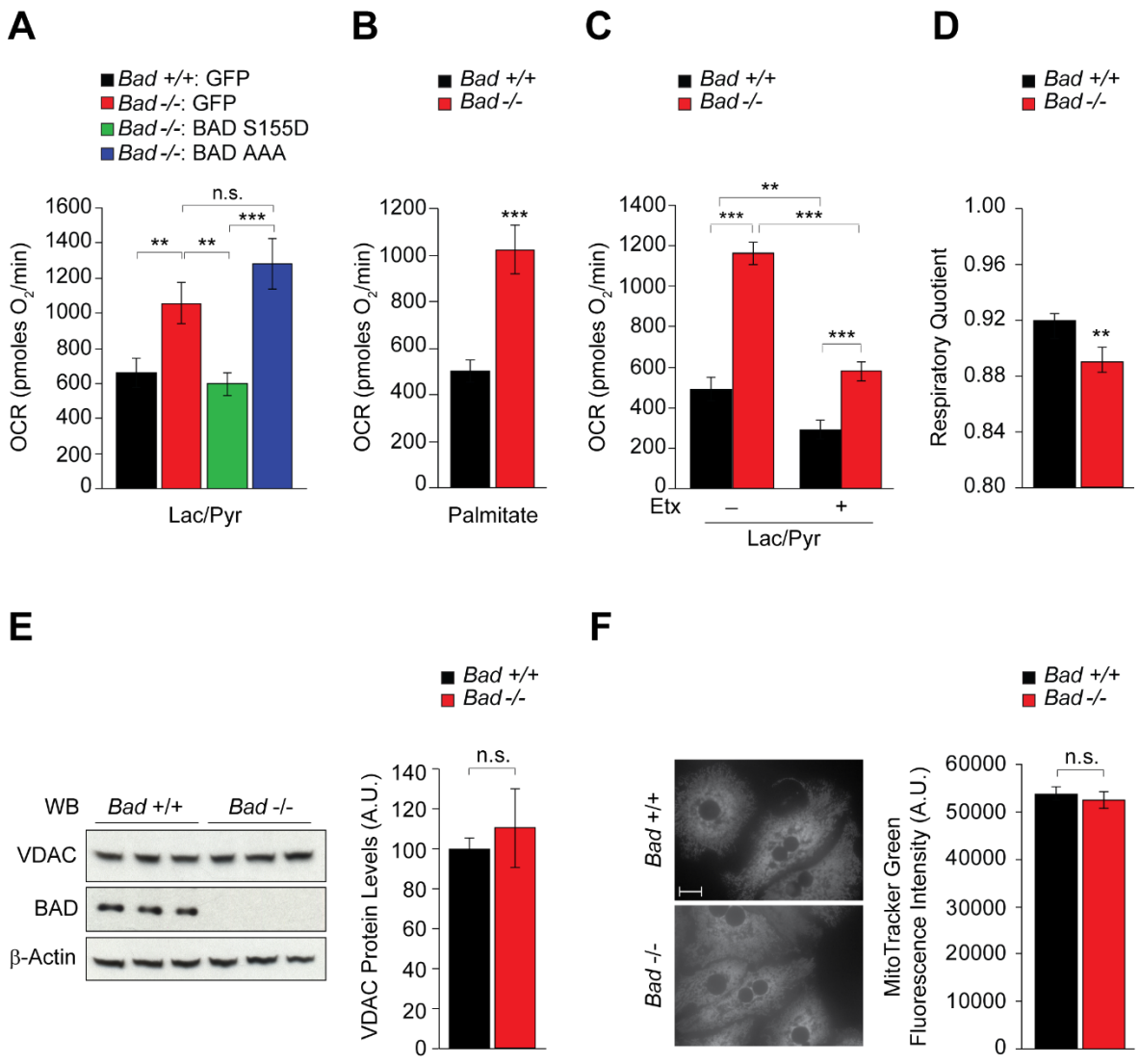


Figure 3.5. BAD-dependent modulation of hepatic energy metabolism

(A) Mitochondrial OCR in primary *Bad* +/+ and -/- hepatocytes transduced with the indicated adenoviruses and treated with lactate/pyruvate (n=4). **(B)** Mitochondrial OCR in primary *Bad* +/+ and -/- hepatocytes treated with palmitate (n=10). **(C)** Etomoxir (Etx) inhibition of OCR in primary hepatocytes treated with lactate/pyruvate (n=5). **(D)** Respiratory quotient in *Bad* +/+ and -/- mice (n=8). **(E-F)** Comparison of mitochondrial mass as examined by the protein levels of Voltage Dependent Anion Channel (VDAC) using western blot analysis (E) and by the fluorescence signal intensity of MitoTracker Green in *Bad* +/+ and -/- primary hepatocytes (F) (n=3). Scale bar in F, 10 μm.

Error bars, ± SEM. **p < 0.01, ***p < 0.001; n.s., non-significant.

Table 3.1. Summary of oligomycin-inhibitable portion of OCR in the absence and presence of ADP

OCR values in the absence and presence of ADP are shown for all substrates and genotypes tested in Figures 3.5 and 3.7. As expected, the OCR values were lower in the absence of ADP than in its presence, however, statistical significance held across comparisons regardless of the absence or presence of ADP. Figures 3.5 and 3.7 show OCR values in the presence of ADP. *p < 0.05; **p < 0.01; ***p < 0.001; n.s., non-significant.

		Mean ± SEM			p value	
Figure	**Genotype**	**Without ADP**	**With ADP**		**Without ADP**	**With ADP**
3A (Lac/Pyr)	*Bad* +/+: GFP	408.69 ± 57.89	655.23 ± 84.88	*Bad* +/+: GFP vs. *Bad* -/-: GFP	*	**
	Bad -/-: GFP	620.44 ± 73.4	1021.85 ± 125.08	*Bad* -/-: GFP vs. S155D	**	**
	Bad -/-: BAD S155D	380.44 ± 45.28	582.28 ± 65.49	*Bad* -/-: GFP vs. BAD AAA	n.s.	n.s.
	Bad -/-: BAD AAA	761.07 ± 90.66	1250.34 ± 148.32	*Bad* -/-: BAD S155D vs. BAD AAA	***	***
3B (Palmitate)	*Bad* +/+	259.25 ± 25.46	501.34 ± 45.54	*Bad* +/+ vs. *Bad* -/-	***	***
	Bad -/-	597.32 ± 58.60	1022.36 ± 105.05			
3C (Lac/Pyr)	*Bad* +/+	431.21 ± 74.93	488.97± 57.24	*Bad* +/+ vs. *Bad* -/-	*	***
	Bad -/-	679.27 ± 55.92	1161.25 ± 54.51	*Bad* +/+: minus vs. plus Etx	*	**
	Bad +/+ plus Etx	226.06 ± 39.39	289.34 ± 46.63	*Bad* -/-: minus vs. plus Etx	***	***
	Bad -/- plus Etx	416.56 ± 46.71	578.46 ± 45.26	*Bad* +/+ plus Etx vs. *Bad* -/- plus Etx	**	***
4A (Lac/Pyr)	$GK^{lox/lox}$	285.01 ± 21.29	358.92 ± 28.49	$GK^{lox/lox}$ vs. $GK^{lox/lox}$; *Alb-cre*	**	**
	$GK^{lox/lox}$; *Alb-cre*	1385.08 ± 384.75	1479.88 ± 383.79			
4A (Palmitate)	$GK^{lox/lox}$	231.22 ± 19.79	326.97 ± 20.58	$GK^{lox/lox}$ vs. $GK^{lox/lox}$; *Alb-cre*	**	**
	$GK^{lox/lox}$; *Alb-cre*	815.01 ± 201.08	1127.75 ± 247.84			
4B (Lac/Pyr)	$GK^{lox/lox}$: GFP	616.83 ± 71.09	805.96 ± 145.87	$GK^{lox/lox}$ vs. $GK^{lox/lox}$; *Alb-cre*: GFP	***	***
	$GK^{lox/lox}$; *Alb-cre*: GFP	1510.14 ± 197.23	2470.43 ± 276.37			
	$GK^{lox/lox}$; *Alb-cre*: BAD S155D	1737.45 ± 234.959	2539.64 ± 277.88			

hepatocytes (Figure 3.5B). This is also consistent with lower respiratory quotient (RQ) in *Bad -/-* mice (Figure 3.5D), which reflects preferential utilization of fatty acids as energy source. Overall, these results suggest that loss of BAD is associated with an altered program of mitochondrial substrate and energy metabolism that matches excess gluconeogenesis. Notably, these alterations do not appear to be linked to changes in mitochondrial mass in the absence of BAD (Figures 3.5E and 3.5F).

The functional increase in FAO in the absence of BAD warranted examination of hepatic genes involved in fatty acid metabolism. Comparison of microarray expression profiles using gene set enrichment analysis (GSEA) identified the mitochondrial β-oxidation pathway as the top gene set enriched in fasted *Bad -/-* liver compared to *Bad +/+* controls (Figure 3.6A). Quantitative real-time PCR provided independent evidence for augmented mRNA abundance of the FAO genes in *Bad -/-* liver (Figure 3.6B). Conversely, transcription of the lipogenic gene acetyl-CoA carboxylase (*Acc*) was markedly down-regulated in *Bad -/-* liver (Figure 3.6B). Examination of key transcriptional regulators of FAO also indicated significant induction of *Pparα* mRNA in *Bad -/-* liver (Figure 3.6B). Importantly, these transcriptional changes were also observed following acute hepatic knockdown of *Bad* (Figure 3.6C), and were further phenocopied by acute hepatic knockdown of *Gk* (Figure 3.6D) or liver-specific deletion of *Gk*, ($Gk^{lox/lox}$ versus $Gk^{lox/lox}$; *Alb-cre*,, Figure 3.6E). These observations suggest a potential link between BAD- and GK-dependent metabolic signaling and hepatic gene expression.

Hepatic function of BAD is mediated by GK

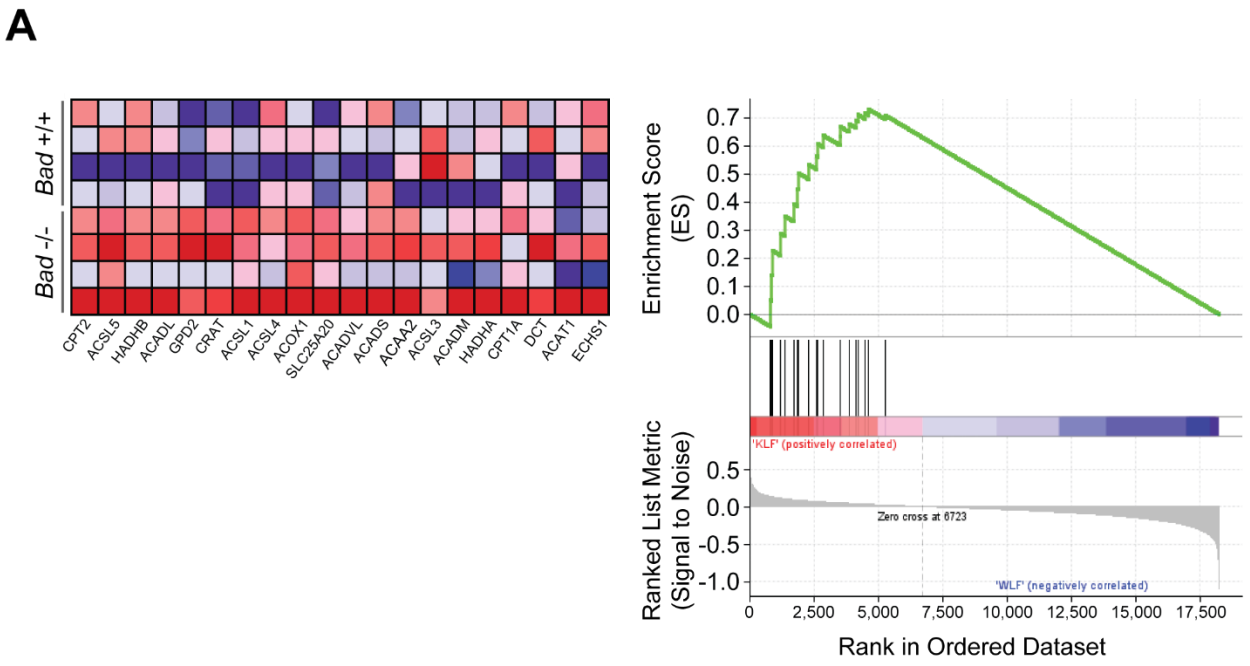
The differential effect of BAD S155D and AAA variants in genetic reconstitution assays suggests that BAD's influence on glycolysis and gluconeogenesis is coordinated with its ability to activate GK. In addition, the common phenotype of exaggerated gluconeogenesis and FAO when either BAD or GK are acutely depleted in the liver suggests that the functional interaction of these two proteins is relevant for hepatic substrate metabolism This predicts that loss of GK would phenocopy loss of BAD in mitochondrial energy metabolism and handling of.

Figure 3.6. Changes in the expression of genes involved in fatty acid metabolism following hepatic manipulation of BAD and GK.

(A) Gene set enrichment analysis of mitochondrial β-oxidation in 24 hr fasted *Bad* +/+ and -/- liver (n=4-5). **(B-C)** mRNA abundance of fatty acid metabolism genes in liver samples derived from fed and fasted *Bad* +/+ and -/- mice (B) and mice subjected to hepatic knockdown of *Bad* (C) (n=4-5). **(D-E)** mRNA abundance of β-oxidation genes in liver samples derived from mice treated with *Gk* shRNA (D) and liver-specific *Gk* null mice (E) (n=5).

Error bars, ± SEM. *$p < 0.05$; **$p < 0.01$; ***$p < 0.001$.

Abbreviations: *Cpt*, carnitine palmitoyl transferase; *Scad, Mcad, Lcad* and *Vlcad*, short-, medium, long-, very long-acyl-CoA dehydrogenase; *Hadh*, hydroxyacyl-CoA dehydrogenase (component of the mitochondrial trifunctional protein); *Acc*, acetyl-CoA carboxylase; *Hmgcs2*, mitochondrial 3-hydroxy-3-methylglutaryl-CoA synthase 2; *Ppara*, peroxisome proliferator-activated receptor alpha.



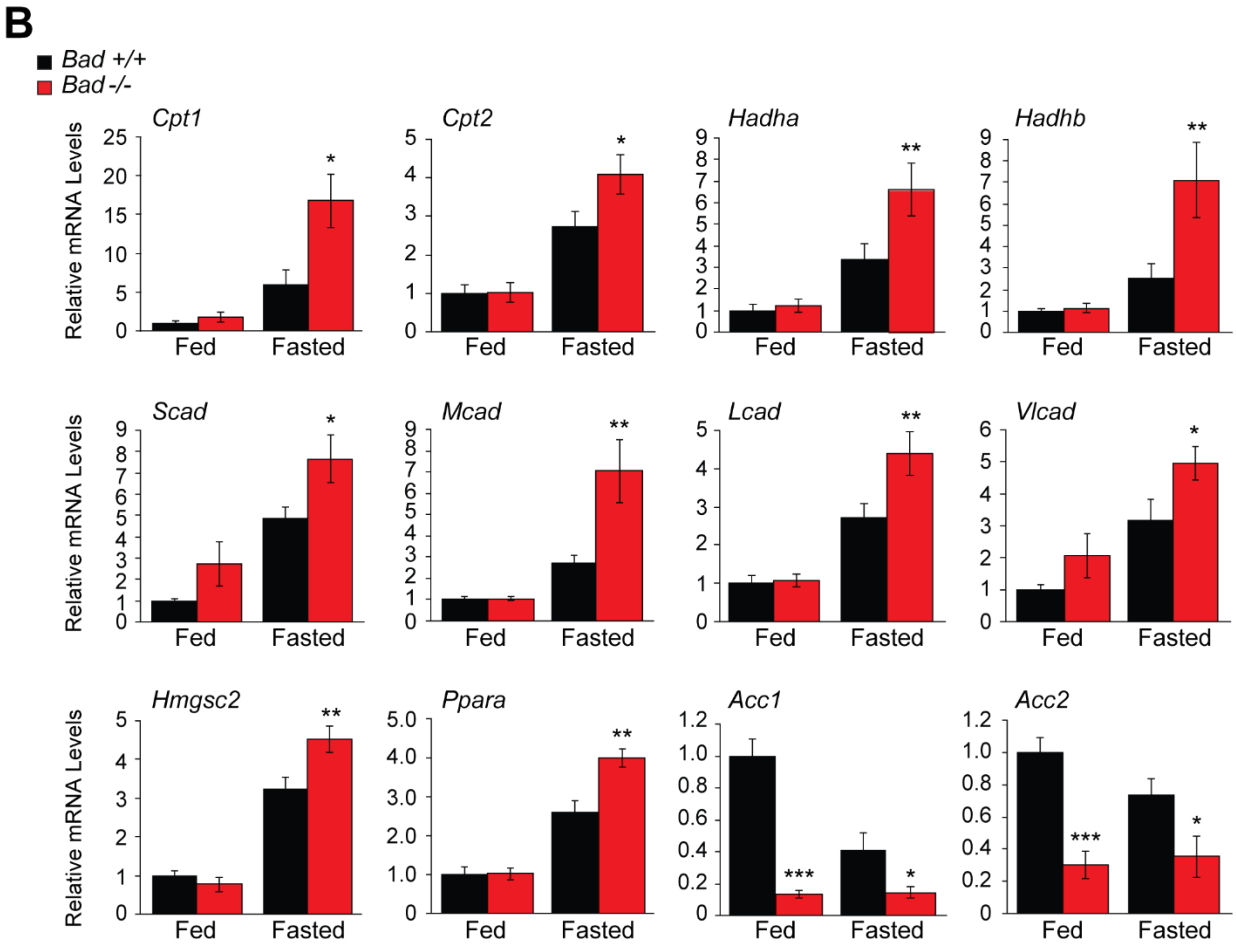


Figure 3.6. (Continued)

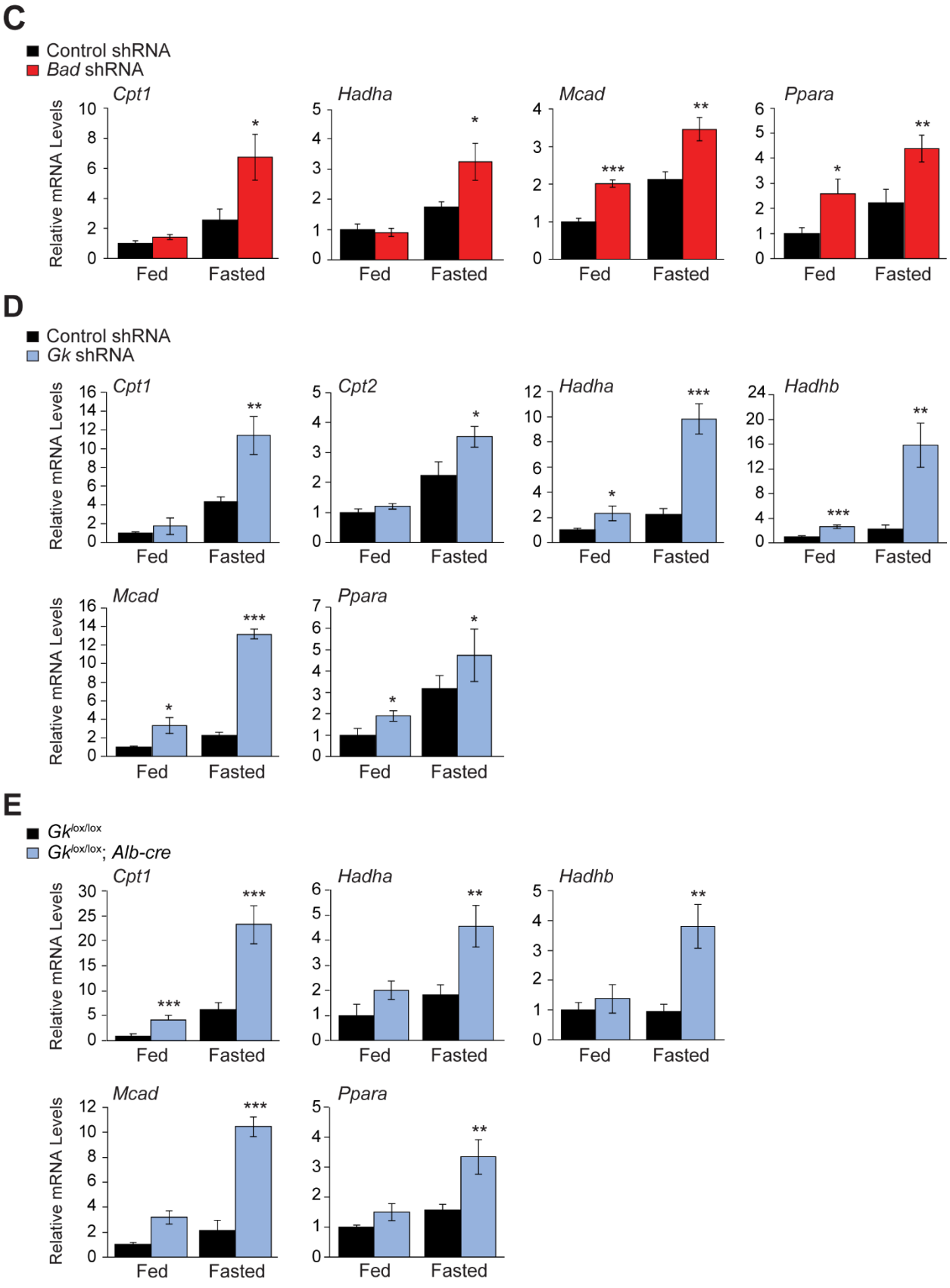


Figure 3.6. (Continued)

gluconeogenic substrates; and that BAD's effect on hepatic substrate utilization would be abrogated in the genetic background of *Gk* deficiency. We next tested each of these predictions. Primary *Gk -/-* hepatocytes display marked stimulation of mitochondrial OCR when cultured with lactate/pyruvate or palmitate ($Gk^{lox/lox}$ versus $Gk^{lox/lox}$; *Alb-cre*, Figures 3.7A and B; Table 3.1) analogous to *Bad -/-* hepatocytes. Gluconeogenesis was also significantly higher in *Gk*-null hepatocytes (Figure 3.7C). However, expression of BAD S155D in *Gk -/-* hepatocytes was ineffective in curtailing excess mitochondrial OCR and glucose production in the presence of lactate/pyruvate (Figures 3.7B and C). This contrasts with the capacity of BAD S155D to correct these parameters in *Bad -/-* hepatocytes (Figures 3.3D and 3.5A). These data provide genetic and mechanistic evidence consistent with GK as a downstream mediator of BAD's effect on hepatic substrate and energy metabolism.

Hepatic insulin resistance in *Bad -/-* mice

Insulin is a critical regulator of hepatic glucose metabolism through transcriptional and post-translational mechanisms, as well as modulation of substrate supply (Lin and Accili, 2011; Saltiel and Kahn, 2001). It stimulates transcription of several glycolytic genes, including *Gk*, and represses that of gluconeogenic genes *Pck1, Fbp1* and *G6p*. In addition, insulin stimulates BAD phosphorylation in the liver (Figure 3.8A). Given the effect of BAD phosphorylation on GK activity and hepatic substrate utilization, these observations predict that BAD's hepatic function may be subject to insulin regulation. To test the physiologic relevance of BAD in the context of insulin action, we performed euglycemic-hyperinsulinemic clamp analysis. While glucose was maintained at basal concentration (~6.7 mM) throughout the analysis (Figure 3.8B), *Bad -/-* mice displayed a small but statistically significant reduction in glucose infusion rates (GIR) (Figure 3.8C, 51.5 ± 2.5 versus 43.4 ± 2.6 mg/kg/min, $p < 0.05$, *Bad +/+* versus *Bad -/-*) consistent with whole body insulin resistance. As reduced GIR can derive from impaired suppression of HGP by insulin and/or its diminished capacity to enhance glucose uptake in peripheral tissues, hepatic

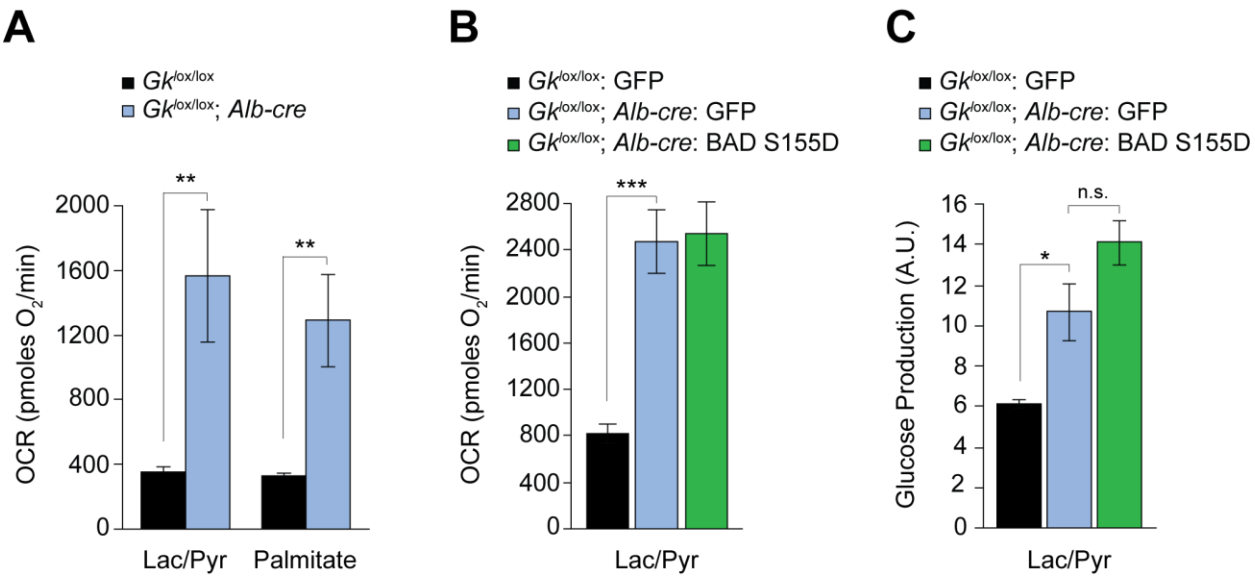


Figure 3.7. Hepatic function of BAD is GK-dependent.

(A) Mitochondrial OCR in GK-deficient hepatocytes treated with lactate/pyruvate or palmitate (n=8-10). **(B-C)** Mitochondrial OCR (B) and glucose production (C) in GK-deficient hepatocytes transduced with the indicated adenoviruses (n=9).

Error bars, ± SEM. *p < 0.05; **p < 0.01, ***p < 0.001; n.s., non-significant.

Figure 3.8. Hepatic insulin resistance in the absence of BAD

(A) Modulation of hepatic BAD phosphorylation by insulin *in vivo*. Immunoblot analysis and quantification of relative BAD phosphorylation on S155, S136 and S112 in liver samples derived from C57BL/6J mice fasted overnight and injected with saline or insulin. **(B-G)** Euglycemic-hyperinsulinemic clamp analysis in *Bad -/-* and *Bad +/+* mice (n=7-9), showing plasma glucose (B), glucose infusion rate (GIR) (C), hepatic glucose production (HGP) (D), relative mRNA abundance of hepatic gluconeogenic genes (E), hepatic glycogen synthesis rates (F), and peripheral insulin sensitivity (G).

Error bars, ± SEM. *$p < 0.05$; **$p < 0.01$, *Bad* -/- versus *Bad* +/+ mice.

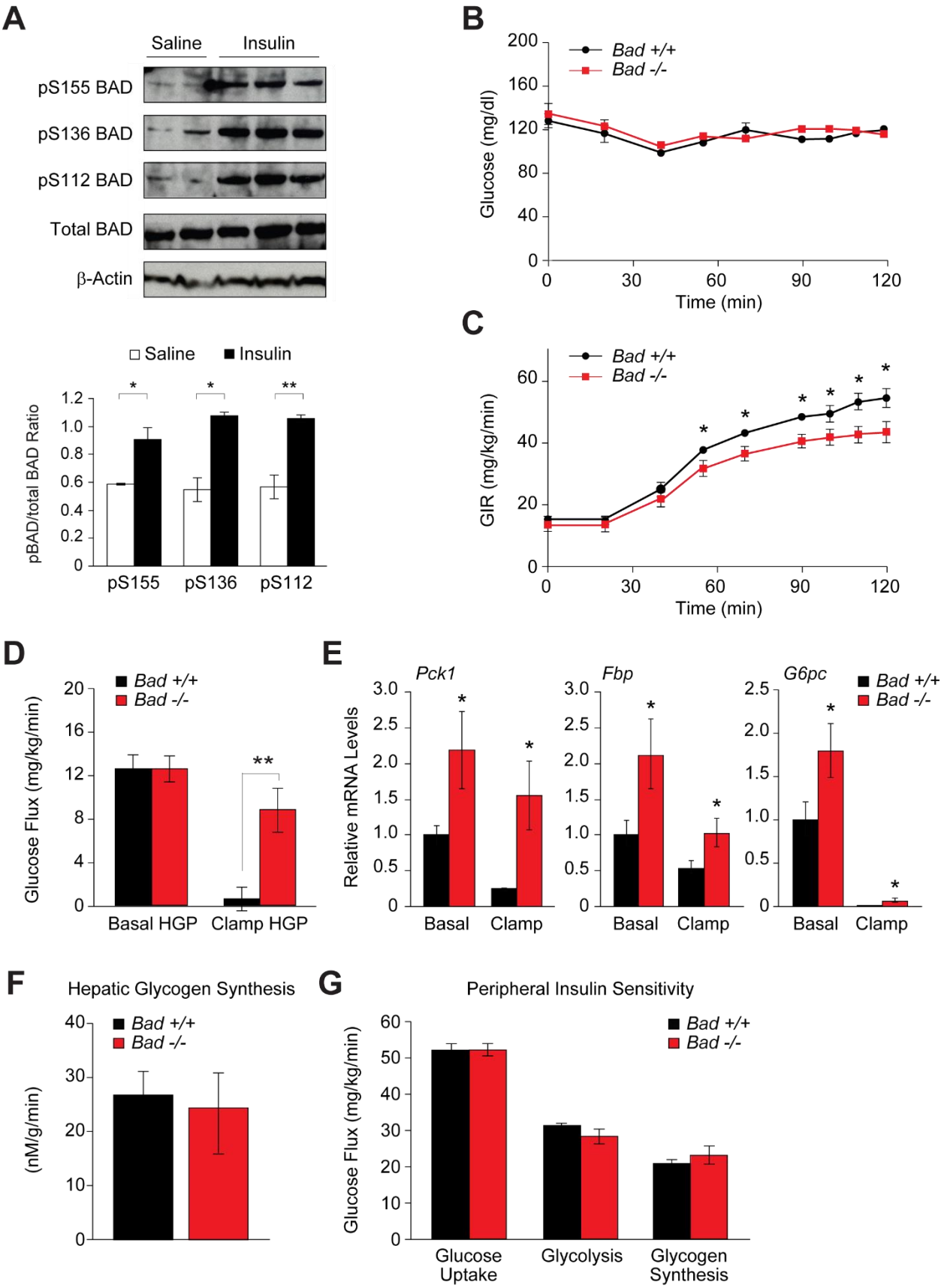


Figure 3.8. (Continued)

and peripheral insulin sensitivities were measured separately. Suppression of HGP by insulin in *Bad -/-* mice was markedly impaired consistent with hepatic insulin resistance (Figure 3.8D, 94.7 ± 14.7% versus 32.1 ± 14.0%, $p < 0.008$, *Bad* +/+ versus *Bad -/-*). This was further consistent with diminished capacity of insulin to fully inhibit the transcription of *Pck1, Fbp1* and the catalytic subunit of *G6p* (*G6pc*) in *Bad -/-* liver (Figure 3.8E).

To determine if hepatic insulin resistance in BAD-deficient mice extends to abnormalities in glucose storage, the net hepatic glycogen synthesis rates were also measured and found to be comparable in *Bad* +/+ and -/- mice (Figure 3.8F). These rates reflect the net balance of direct and indirect pathways of glycogen synthesis (Agius, 2008). While diminished hepatic glucose utilization in *Bad -/-* mice (Figure 3.1A) would predict lower glycogen synthesis via the direct pathway, increased gluconeogenesis in these animals may lead to a larger contribution from the indirect pathway. It is possible that a relative increase in the indirect pathway of glycogen synthesis may have offset any differences in the direct pathway, rendering total glycogen synthesis in *Bad -/-* mice comparable to controls. Notably, a prominent contribution of the gluconeogenic pathway to hepatic glycogen synthesis in glucokinase-deficient (MODY2) subjects has been reported (Velho et al., 1996).

Insulin resistance in *Bad -/-* mice is restricted to liver as insulin-mediated glucose uptake in skeletal muscle and white adipose tissues was not altered (Figures 3.9A and B). Whole body glucose uptake, glycolysis and glycogen synthesis did not reveal any differences in the two genotypes (Figure 3.8G). Other metabolic parameters such as fat and lean mass, energy expenditure, activity, as well as fasted serum levels of glucagon, FFA and triglycerides were comparable in both genotypes (Figures 3.9C-H). Overall, these results indicate that peripheral insulin sensitivity is preserved in *Bad -/-* mice and that diminished GIR in this genetic model can be chiefly attributed to impaired suppression of HGP.

Figure 3.9. Peripheral insulin action and additional metabolic parameters in *Bad* +/+ and -/- mice.

(A-B) Peripheral insulin action as measured by glucose uptake in skeletal muscle (A) and white adipose tissues (B) in *Bad* +/+ and -/- mice subjected to euglycemic-hyperinsulinemic clamp analysis as in Figure 3.8 (n=7-9). **(C-E)** Body weight, lean and fat mass (C), energy expenditure (D), and activity (E) in *Bad* +/+ and -/- mice (n=7-9). **(F-H)** Fasting levels of serum glucagon (F), FFA (G), and Triglycerides (H) in *Bad* +/+ and -/- mice (n=5-9).

Error bars, ± SEM.

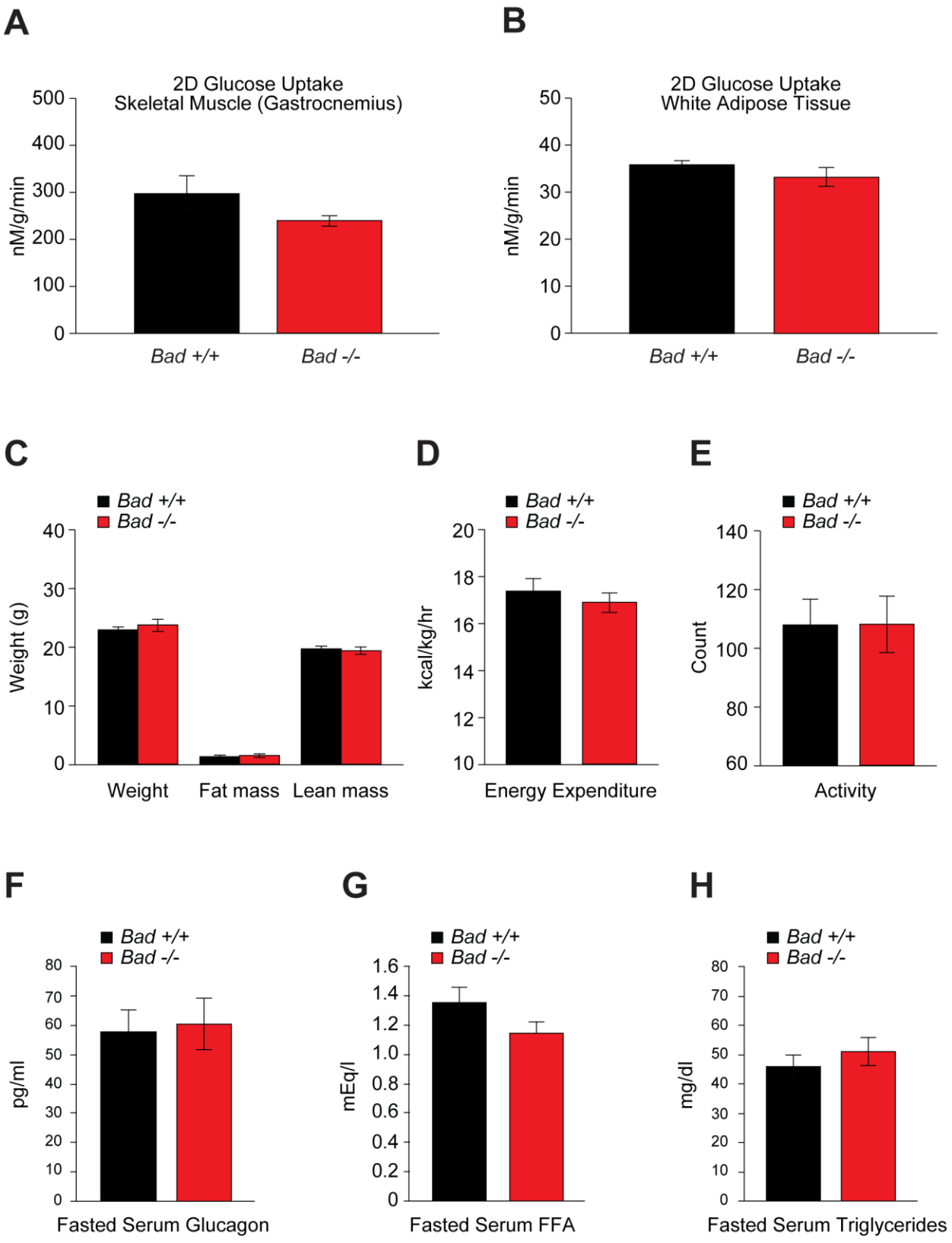


Figure 3.9. (Continued)

Hepatic insulin signaling in the absence of BAD

Impaired hepatic insulin action in *Bad -/-* mice warranted examination of insulin signaling. Insulin stimulation of PI3K activity was significantly diminished in *Bad -/-* liver but not in *Bad -/-* gastrocnemius muscle (Figures 3.10A and 3.11A). Lower hepatic PI3K activity in *Bad -/-* was consistent with reduced stimulation of AKT phosphorylation by insulin but could not be explained by changes in insulin receptor (IR) phosphorylation (Figure 3.10B). Importantly, insulin stimulation of AKT phosphorylation was not altered in muscle (Figure 3.11B), which is in agreement with selective loss of insulin action in liver but not in muscle (Figures 3.8D and 3.9A). Reduced AKT phosphorylation in response to insulin was further evident in primary *Bad -/-* hepatocytes treated with insulin (Figure 3.11C), indicating a cell autonomous effect of BAD deficiency on insulin signaling. Moreover, attenuated insulin signaling in *Bad -/-* mice was recapitulated in mice treated with *Bad* shRNA (Figure 3.10C). Reduced PI3K-AKT signaling without alterations in insulin receptor phosphorylation predicts inhibition at the level of IRS-1 through negative feedback loops (Copps and White, 2012). Examination of several IRS-1 inhibitory kinases revealed comparable hepatic JNK and ERK phosphorylation but diminished GSK-3 phosphorylation in *Bad* shRNA liver (Figure 3.10C and data not shown). Because phosphorylation inactivates GSK-3, these results indicate increased hepatic GSK-3 activity in BAD-depleted liver. However, GSK-3 phosphorylation is itself regulated by insulin similar to several other IRS-1 inhibitory kinases (Copps and White, 2012), and whether GSK-3 activity is the cause or consequence of reduced insulin signaling in these mice remains to be determined. Importantly, an analogous decline in hepatic insulin signaling was also observed in mice treated with *Gk* shRNA (Figure 3.10D). This is consistent with published reports that loss of GK or inhibition of its activity is associated with blunted suppression of HGP and hepatic insulin resistance (Barzilai et al., 1996; Clement et al., 1996; Rossetti et al., 1997). In aggregate, our findings indicate that, similar to hepatic depletion or inhibition of GK, loss of BAD and the

Figure 3.10. Altered insulin signaling upon hepatic manipulation of BAD and GK

(A) IRS-1-associated PI3K activity in liver of *Bad* +/+ and -/- mice injected with saline or insulin after an overnight fast (n=10 per genotype). **(B)** Phosphorylation of the insulin receptor (IR) and AKT in liver of *Bad* +/+ and -/- mice treated as in (A). Bar graphs quantitate relative insulin induction of IR and AKT phosphorylation (n=4). **(C-D)** Insulin signaling in liver samples isolated from C57BL/6J mice following hepatic knockdown of *Bad* (C) and *Gk* (D). Bar graphs quantitate relative insulin induction of IR, AKT, and GSK-3 phosphorylation (n=4).

Error bars, ± SEM. *$p < 0.05$; **$p < 0.01$, ***$p < 0.001$.

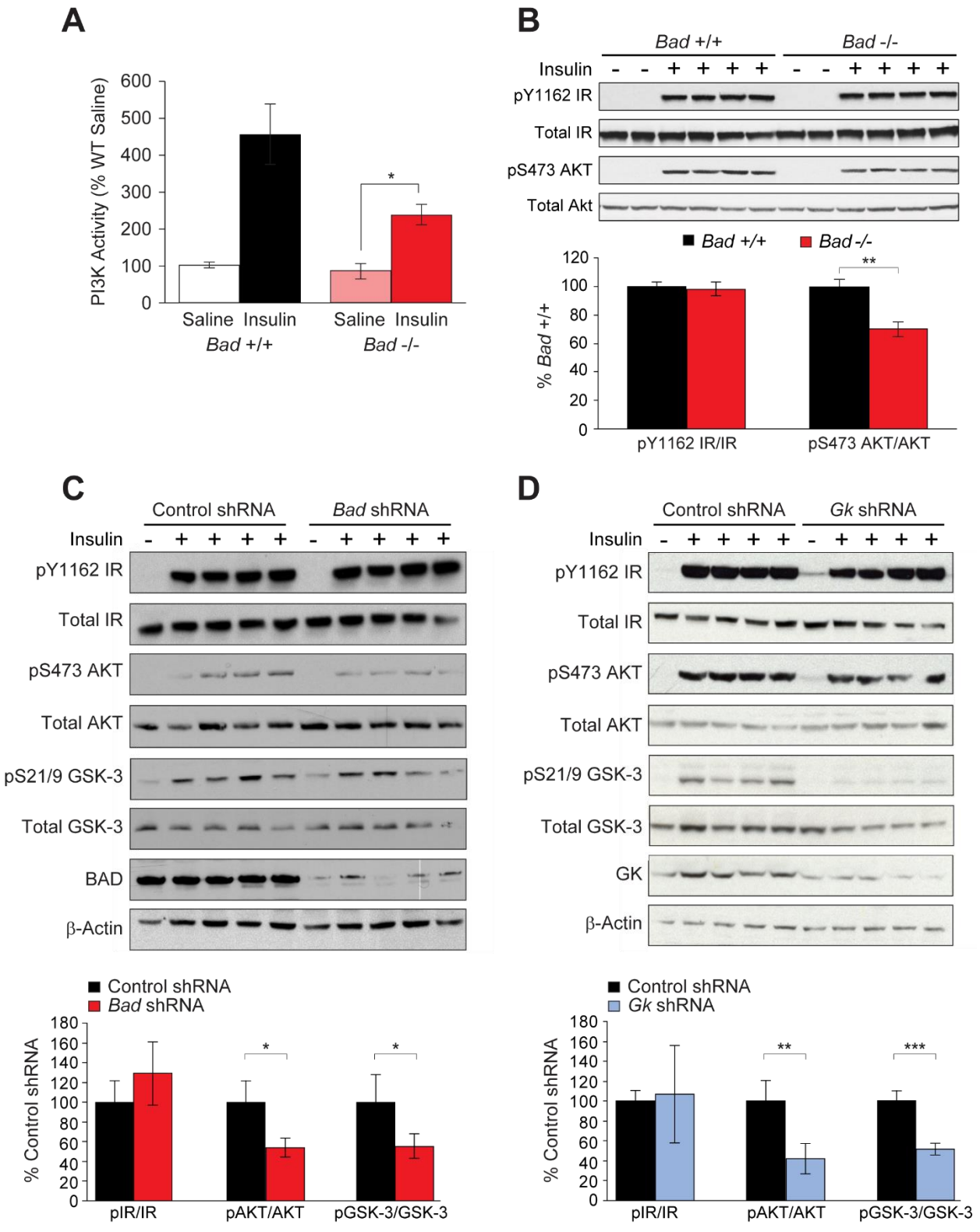


Figure 3.10. (Continued)

Figure 3.11. Insulin signaling in the absence of BAD.

(A) IRS-1-associated PI3K activity in muscle of *Bad* +/+ and -/- mice injected with saline or 0.1 U/g insulin after an overnight fast (n=10 mice per genotype). **(B)** Phosphorylation of the insulin receptor (IR) and AKT in skeletal muscle of *Bad* +/+ and -/- mice treated as in (A) (n=4). **(C)** Insulin signaling in primary *Bad* +/+ and -/- hepatocyte cultures. Bar graphs quantitate relative insulin-induction of IR and AKT phosphorylation (n=4). **(D-E)** Relative hepatic mRNA abundance of *Srebp1c* (D) and *Gk* (E) in *Bad -/-* and *Bad* +/+ mice subjected to euglycemic-hyperinsulinemic clamp as in Figure 3.8 (n=6 mice per condition).

Error bars, mean ± SEM. *p < 0.05; **p < 0.01; n.s., non-significant.

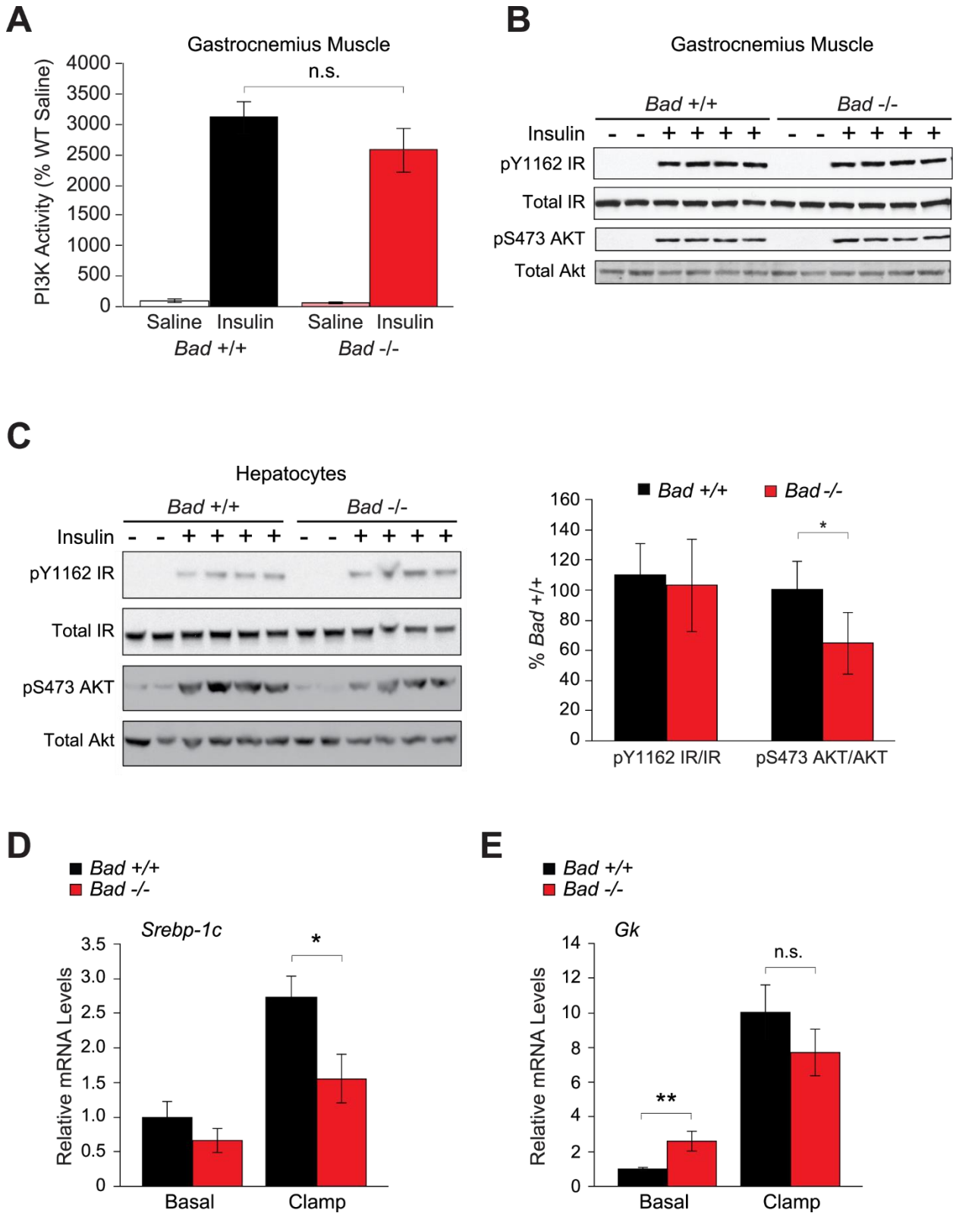


Figure 3.11. (Continued)

attendant diminution of GK activity is associated with reduced hepatic insulin sensitivity and insulin signaling

Hepatic GK and BAD are both regulated by insulin. *Gk* is a transcriptional target of SREBP1c downstream of the PI3K-AKT axis, and BAD phosphorylation, which stimulates GK activity (Figure 3.4B) (Szlyk et al., 2014), is induced by insulin. It is, therefore, possible that BAD may serve as an additional downstream mediator of insulin's effect on GK, whereby insulin stimulates GK activity beyond induction of *Gk* transcription. Given insulin regulation of BAD and GK and reduced insulin signaling in *Bad -/-* mice, two potential scenarios may explain the diminished insulin suppression of HGP in these mice; diminished insulin stimulation of *Gk* expression or diminished capacity of insulin to enhance GK activity through BAD phosphorylation. To determine changes in *Gk* expression in this setting, we examined hepatic *Srebp1c* and *Gk* mRNA levels in *Bad* +/+ and *-/-* mice subjected to euglycemic-hyperinsulinemic clamp. Relative *Srebp1c* mRNA abundance was lower in *Bad -/-* liver (Figure 3.11D), which is consistent with reduced insulin stimulation of PI3K-AKT signaling in these mice. Surprisingly, however, *Gk* mRNA levels were not diminished in these samples (Figure 3.11E), suggesting potential SREBP1c-independent compensatory mechanisms that maintain *Gk* mRNA levels despite reduced insulin signaling in *Bad -/-* liver. Of note, several other transcription factors can directly activate the *Gk* promoter in the absence of SREBP1c (Bechmann et al., 2012; Kim et al., 2009; Oosterveer et al., 2012). Moreover, *Gk* mRNA levels can be regulated by 6-phosphofructo-2-kinase/fructose-2,6-bisphosphatase (PFK2) independent of insulin and SREBP1c (Payne et al., 2005; Wu et al., 2004). Therefore, it is possible that one or more of these mechanisms may stabilize *Gk* expression in *Bad -/-* liver under these conditions. In addition, the potential contribution of residual insulin signaling in these mice cannot be ruled out. Regardless of the mechanisms that may stabilize *Gk* mRNA levels in *Bad -/-* mice, our results indicate that diminished insulin suppression of HGP in these animals cannot be explained by diminished *Gk* transcription. Considering insulin-induction of BAD phosphorylation on S155 and the direct stimulatory effect of the phospho-BAD BH3

domain on GK activity (Szlyk et al., 2014), our data are most consistent with the proposal that defective GK activity in *Bad -/-* liver, despite stabilized *Gk* mRNA levels, may curtail the full effect of insulin on proper modulation of HGP.

Metabolic benefits of BAD in models of diabetes and insulin resistance

The capacity of BAD S155D to counterbalance exaggerated gluconeogenesis in *Bad -/-* liver warranted examination of its effect in models of diabetes and insulin resistance such as *ob/ob* mice. Hepatic BAD protein levels were comparable in *ob/ob* and control *ob/+* mice despite elevated *Bad* mRNA levels in *ob/ob* animals, indicating that increased transcription of the *Bad* gene does not result in higher protein levels in this context (Figures 3.12A and B). Remarkably, however, BAD phosphorylation on S155 and S136 was significantly diminished in *ob/ob* liver (Figure 3.12C). These observations further motivated examination whether expression of a BAD S155D can alter hepatic metabolism in these animals. Hepatic delivery of BAD S155D, but not BAD AAA, significantly ameliorated fasting hyperglycemia in *ob/ob* mice (Figure 3.13A), which was accompanied by diminished fasting *Pck1* mRNA abundance (Figure 3.13B). Importantly, glucose levels during PTT were markedly down-regulated in *ob/ob* mice reconstituted with BAD S155D adenoviruses so that they were comparable to *ob/+* controls treated with GFP viruses (Figure 3.13C). BAD S155D expression further resulted in systemic metabolic benefits marked by improved glucose tolerance in *ob/ob* mice (Figure 3.13D).

We next set out to determine whether the differential effects of BAD S155D and BAD AAA in *ob/ob* liver parallel their GK-activating capacity. Previous studies have reported an age-dependent progressive decline in hepatic *Gk* mRNA and GK activity in leptin resistant rodent models (Torres et al., 2009). Importantly, increased GK activity through chemical or genetic approaches improved glucose homeostasis in these models (Grimsby et al., 2003; Torres et al., 2009). Hepatic expression of BAD S155D or BAD AAA variants did not alter *Gk* mRNA levels in *ob/ob* mice (Figure 3.12D), but had distinct effect on GK activity. Specifically, BAD S155D increased hepatic GK activity whereas the BAD AAA variant was ineffective (Figure 3.12E).

Figure 3.12. Metabolic effects of BAD in *ob*/*ob* liver

(A) Hepatic mRNA abundance of *Bad* in *ob/ob* and *ob/+* mice (n=6). **(B)** Immunoblot analysis of total BAD levels in whole cell lysates prepared from *ob/ob* and *ob/+* liver samples. **(C)** Immunoblot analysis and quantification of relative BAD phosphorylation in liver samples derived from *ob/ob* and *ob/+* mice fasted for 24 hr and refed for 1 hr. BAD was immunoprecipitated with anti-BAD antibody and western blotted with phospho-specific antibodies to pS155 and pS136 BAD. **(D)** Hepatic *Gk* mRNA levels in *ob/ob* mice (~25 wks) after tail vein delivery of the indicated adenoviruses (n=4-8 independent mice per condition). **(E)** Hepatic GK activity in *ob/ob* mice after tail vein delivery of the indicated adenoviruses (n=3-9 mice per condition).

Error bars, ± SEM. *p < 0.05; **p < 0.01; ***p < 0.001.

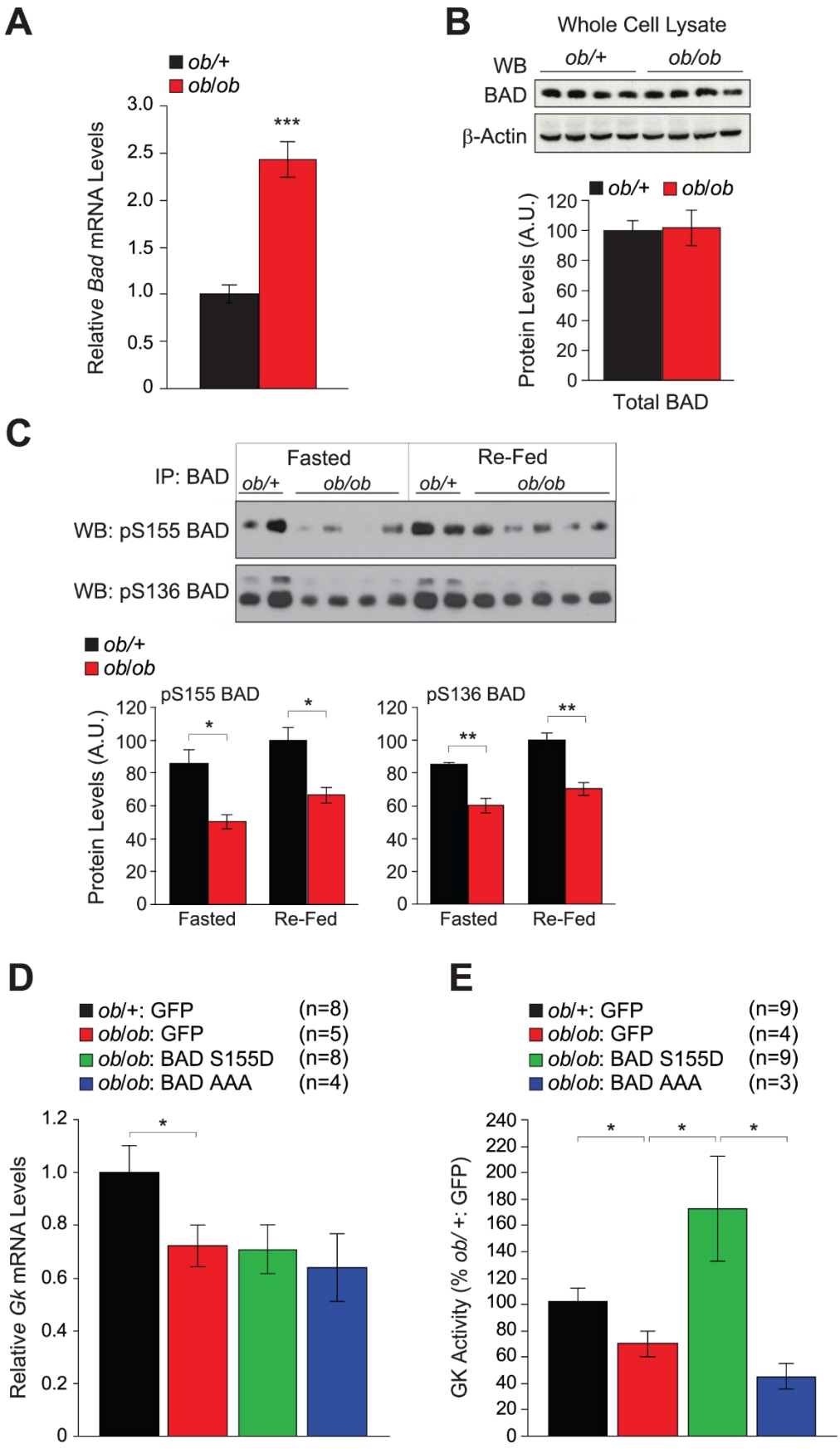


Figure 3.12. (Continued)

Figure 3.13. Metabolic effects of BAD in *ob*/*ob* and HFD-treated mice

(A-D) Fasting glucose levels (A), liver *Pck1* mRNA abundance (B), pyruvate (C) and glucose (D) tolerance tests following hepatic reconstitution of *ob/ob* mice with the indicated adenoviruses (n=10-14). Asterisks in (C-D) compare *ob/ob* mice treated with BAD S155D versus GFP adenoviruses. **(E)** GTT in C57BL/6J mice subjected to high-fat diet for 10 weeks prior to hepatic reconstitution with the indicated adenoviruses (n=9). Asterisks in (E) compare HFD mice treated with BAD S155D versus GFP adenoviruses.

Error bars, ± SEM. *p < 0.05; **p < 0.01, ***p < 0.001.

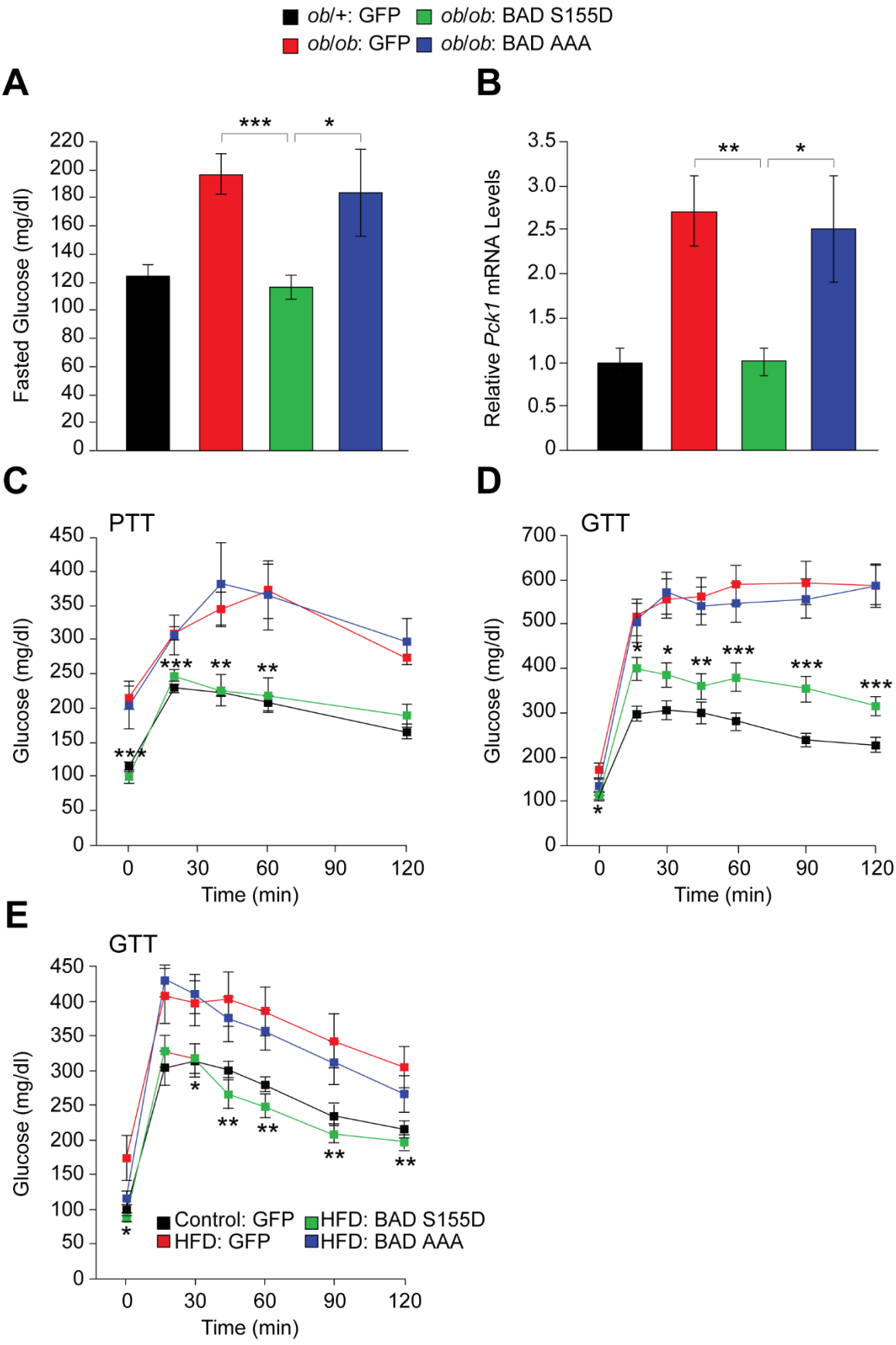


Figure 3.13. (Continued)

Thus, the differential effect of BAD phospho-mutants in hepatic reconstitution of ob/ob mice co-segregates with their effect on GK activity.

The *ob/ob* genetic model is a severe model of diabetes with a complex myriad of chronic pathophysiologic perturbations. We also tested the metabolic consequence of BAD in the high-fat diet (HFD) model. Acute hepatic delivery of BAD S155D to wild-type mice after 10 weeks of high-fat feeding effectively improved fasting hyperglycemia and glucose tolerance, while the BAD AAA variant was inert in this setting (Figure 3.13E). The GTT profiles of HFD mice treated with BAD S155D were comparable to normal chow (control)-fed mice treated with GFP viruses.

DISSCUSSION

Our combined use of multiple genetic tools, including the *Bad*-null and phosphorylation knock-in mice, liver-specific *Bad* knockdown, as well as informative BAD mutants enabled biochemical and systemic evaluation of BAD's significance in hepatic substrate metabolism. These studies show that hepatic loss of BAD or interference with its phosphorylation is linked to reduced glycolysis, enhanced FAO, and unrestrained gluconeogenesis. Moreover, BAD deficiency is associated with impaired insulin-mediated suppression of HGP and attenuated insulin signaling. Our collective observations suggest that exaggerated gluconeogenesis in the absence of BAD can be mapped to a combination of altered substrate and energy metabolism, as well as loss of hepatic insulin sensitivity.

BAD's capacity to modulate hepatic glucose utilization and production is regulated by its phosphorylation, which is in turn sensitive to the fed/fasted nutritional states and insulin. When phosphorylated, BAD activates GK, promoting glycolysis and inhibiting FAO. Upon BAD dephosphorylation, glycolysis is diminished, FAO is dis-inhibited, and pyruvate is preferentially partitioned to gluconeogenesis. These observations are consistent with the possibility that BAD phosphorylation may help mitochondria distinguish the glycolytic versus gluconeogenic source of pyruvate and its metabolic fate. The idea that GK is an important mechanistic component of BAD modulation of hepatic metabolism is supported by two lines of investigation. *First*, the selective capacity of BAD BH3 variants to modulate hepatic metabolism in both primary hepatocytes and whole animal liver reconstitution assays co-segregates with their differential GK-activating property. *Second*, BAD's ability to coordinately regulate hepatic energy metabolism and gluconeogenesis is abolished in the absence of GK, providing evidence in favor of an "epistatic" relationship between these partner proteins where GK is a downstream mediator of BAD's metabolic effects.

The notion that the BAD:GK axis is relevant for proper regulation of glycolysis and gluconeogenesis is further consistent with several metabolic alterations that are phenocopied

when each protein is depleted in the liver, including exaggerated gluconeogenesis and impaired glucose tolerance. Hepatic GK is subject to several regulatory mechanisms, including distinct binding interactions and sub-cellular localization (Matschinsky, 2009). BAD deficiency does not lead to reduced hepatic GK expression at mRNA or protein levels, but is associated with diminished GK activity. Given the multiple mechanisms that converge on hepatic GK regulation, loss of BAD is not expected to recapitulate the full phenotypic spectrum of GK loss-of-function in the liver. Within this context, the finding that several metabolic alterations are shared between mice with hepatic knockdown of *Bad* and animals with hepatic knockdown of *Gk* is remarkable.

Changes in hepatic metabolism following depletion of BAD or GK also include altered expression of several glycolytic and gluconeogenic genes, and a robust transcriptional activation of β-oxidation. This gives rise to the question as to how BAD- or GK-dependent changes in hepatic metabolism modify gene expression. Because these changes can be acutely triggered by the knockdown of either BAD or GK, it is likely that select alterations in glucose- or fatty acid-derived metabolites may modulate the activity of glucose- and fatty acid-sensing transcription factors such as ChREBP and nuclear receptors (Agius, 2013; Jump et al., 2013). Another possible scenario is alterations in chromatin- and histone-modifying enzymes that can be modulated by defined metabolites or cellular metabolic state (Kaelin and McKnight, 2013).

Our findings indicate that deregulated gluconeogenesis in the absence of BAD also extends to diminished insulin suppression of HGP. BAD phosphorylation, which can down-regulate gluconeogenesis through GK activation (Figures 3.3C, D, 3.4B, 3.7C), is normally induced by insulin. This observation together with the finding that insulin suppression of HGP is diminished in *Bad -/-* mice suggest that BAD may serve as a downstream effector of insulin in modulation of hepatic glucose production. Moreover, hepatic insulin resistance in the absence of BAD is accompanied by changes in insulin signaling. Hepatic nutrient and energy sensing pathways and insulin signaling are tightly integrated (Newgard, 2012; Samuel and Shulman, 2012), and the shared phenotype of reduced insulin signaling upon acute hepatic depletion of

BAD or GK predicts a potential interplay between reduced glucose utilization and/or increased FAO and the components of the insulin signaling axis. Notably, precedent for a link between glucose metabolism, ROS, and NADH, and the regulation of PI3K:AKT:GSK-3 signaling exists in other tissues (Pelicano et al., 2006; Yeshao et al., 2005). The precise molecular link between BAD- and GK-dependent changes in substrate metabolism and alterations in insulin signaling awaits additional studies.

The observation that hepatic delivery of BAD S155D reinstates proper regulation of gluconeogenesis and allays fasting hyperglycemia in the *ob/ob* and HFD-treated mice provides a powerful endorsement for the physiologic relevance of BAD phospho-regulation. We have shown that the BAD S155D variant and hydrocarbon stapled BAD BH3 helices that bear the phospho-mimic S155D modification (BAD SAHB compounds) can directly trigger GK activity and stimulate insulin secretion in primary islets (Danial et al., 2008; Szlyk et al., 2014). The studies presented here suggest that, in addition to boosting β-cell function, BAD BH3 phospho-mimic strategies may improve hepatic metabolism. This is consistent with published reports that GK activation imparts benefits to both β-cells and hepatocytes. Hepatic GK activation using genetic approaches or pharmacologic tools such as small molecule allosteric GK activators (GKAs) leads to increased glucose utilization, decreased glucose production, amelioration of hyperglycemia, and resistance to HFD (Ferre et al., 1996; Grimsby et al., 2003; Torres et al., 2009). However, these benefits have to be carefully leveraged against potential risk of hypoglycemia and hyperlipidemia associated with chronic GK activation above physiologic levels (Meininger et al., 2011). With advances in the development of different classes of GKAs that may elicit distinct mechanisms of action and the possibility of combination therapy with other anti-diabetic agents, the benefits of GK activation may ultimately outweigh these drawbacks (Matschinsky, 2009). Within this context, it is important to note that the mechanism by which the phospho-BAD BH3 helix activates GK is distinct from allosteric GKAs (Szlyk et al., 2014), suggesting phospho-BAD BH3 mimetic compounds may define a separate class of GKAs. The findings reported here highlight the

potential therapeutic utility of phospho-BAD BH3 mimetic strategies in diabetes and metabolic syndrome.

METHODS

Mice

Bad -/- and S155A knock-in mice have been previously described (Danial et al., 2008). These mice have been bred into the C57BL/6J genetic background for at least 14 generations and validated by genome scanning to be 99.9% congenic with C57BL/6J. Conditional *Gk* mice ($Gk^{lox/lox}$) were a generous gift of Dr. Mark Magnuson (Vanderbilt University) (Postic et al., 1999). C57BL/6J *alb-cre* mice and *ob*/*ob* mice were purchased from Jackson Laboratory and Taconics, respectively. Mice received a standard chow or high-fat diet (55% fat energy, TD93075, Harlan Laboratories), and were housed in a barrier facility with 12 hr light and dark cycles. Unless otherwise indicated, male mice at 10-12 weeks of age were used. All animal procedures were approved by the Institutional Animal Care and Use Committee of Dana-Farber Cancer Institute and Yale University School of Medicine.

Metabolic studies

PTT, GTT, basal metabolic characterization, and euglycemic-hyperinsulinemic clamps were performed as previously described (Choi et al., 2007; Danial et al., 2008; Lin et al., 2004). Adenoviral transduction was carried out as described in Supplemental Experimental Procedures.

Adenovirus production and viral transduction

The BAD S155D, S155A, and AAA mutations were made using standard site directed mutagenesis techniques to substitute aspartic acid or alanine for S155 (amino acid enumeration based on mouse BAD protein sequence) or to generate a triple-alanine substitution for L151, S155 and D156 within the BAD BH3 domain (BAD AAA). Recombinant GFP, BAD S155D, S155A, and BAD AAA adenoviruses were generated using the pAdEasy system (Stratagene). Adenoviruses carrying *Bad* shRNA or scrambled control were constructed using the Adeno-X Expression Systems 2 with Creator Technology (Clontech). Briefly, 19 bp sequences based on the BAD coding sequence were designed using Block-it RNAi designer software (Invitrogen). Oligonucleotides were then designed according to the knockout clone and confirm PCR kit

(Clontech), and cloned into RNAi-Ready pSIREN-DNR-Ds Red-Express Donor vector. Adenoviruses carrying *Gk* shRNA were a kind gift of Dr. Christopher Newgard (Duke University) (Bain et al., 2004). All virus amplification, purification, titration and verification were done using the services of ViraQuest Inc. (North Liberty, IA). Adenoviral transduction of hepatocyte cultures was carried out 24-48 hr after plating at a viral dose of $4x10^6$ pfu/ml for 3 hr. For hepatic reconstitution or knockdown assays, mice were injected with a viral dose of $3x10^8$ pfu/g of body weight via tail vein.

Primary hepatocyte cultures and treatments

Primary hepatocyte isolation and cultures were carried out as previously described (Matsumoto et al., 2007). Cells were starved in serum-free M199 (Invitrogen) for 40 hr prior to dexamethasone/forskolin treatment. For assessment of lactate production, hepatocytes were plated at $5.5x10^5$ cells/ml and incubated in serum-free M199 supplemented with 0.2% BSA for 4 hr and then switched to serum-free M199 containing 0.2% BSA without or with 25 mM glucose for up to 24 hr. 100 µl aliquots of the medium were collected at the indicated times for lactate measurement as previously described (Ferre et al., 1996) and normalized to the protein content of hepatocytes. For glucose production assays, hepatocytes were cultured in M199 medium containing 0.5% BSA with or without 1 µM dexamethasone and 12 µM forskolin. Glucose production was assessed as previously described (Yoon et al., 2001). Values were normalized to protein content.

Hepatic GK activity assays

Whole livers were extracted from mice administered with the indicated adenoviruses and flash frozen in liquid nitrogen. Samples were homogenized in buffer containing 220 mM mannitol, 70 mM sucrose, 20 mM HEPES pH 7.4, 0.5 mM EGTA, and 0.1% defatted BSA that was supplemented with complete protease inhibitor cocktail (Roche). Samples were centrifuged at 600 x g for 10 min at 4°C to pellet large matter and separate a layer of fat from the homogenate, which was aspirated prior to measuring the protein concentration. Samples were diluted to 1

mg/mL total protein concentration, and assayed in a G6PDH-coupled reaction measuring the formation of NADH at 340 nm in a Costar 3596 plate at 37°C using a SpectraMax M5 microplate reader (Molecular Devices). Each well contained 400 µg of protein, 100 mM HEPES pH 7.4, 150 mM KCl, 6 mM $MgCl_2$, 5 mM ATP, 1 mM NAD, 1 mM DTT, 0.5% BSA, 2.5 units G6PDH, and either high (100 mM) or low (0.5 mM) glucose. Absorbance was recorded every two min and the change in absorbance per min was calculated using data between 10 and 30 min, where the change in absorbance was linear. Experiments were performed in triplicate. To determine the contribution from glucokinase alone, baseline-subtracted rates were calculated by subtracting the mean rate of reaction in low glucose from the mean rate of reaction in high glucose for each sample. To normalize the data, the baseline-subtracted rate of each sample was then divided by average of the baseline-subtracted rates of control mice injected with GFP [*Bad* +/+: GFP (Figure 3.4B) or *ob*/+: GFP (Figure 3.12E) from the same experiment.

Mitochondrial respirometry in intact hepatocytes

OCR was measured in intact hepatocytes in real time using the XF24 extracellular flux analyzer and the XF24 v1.5.0.69 software (Seahorse Biosciences) (Wu et al., 2007). Hepatocytes were counted using a trypan blue exclusion assay that was also used to ensure the integrity of the plasma membrane. Cells were seeded on collagen-coated XF24 V7 plates (Seahorse Biosciences) at $4x10^4$ cells/well, allowed to attach for at least 2 hr, rinsed once and kept in 600 µl of sodium bicarbonate-free M199 medium supplemented with 1% BSA, 1 µM dexamethasone and 12 µM forskolin. After baseline measurements, additions were delivered in the following order in 75 µl injections through the instrument's individual injection ports; substrates (lactate/pyruvate or palmitate), ADP, and the mitochondrial ATP synthase inhibitor oligomycin. L-lactate (Sigma) and sodium pyruvate (Cellgro, Mediatech) were injected at 10 and 1 mM, respectively. Sodium palmitate (Sigma) was injected at 200 µM together with 10 mM L-malate (Sigma). When palmitate was tested, 0.5 mM carnitine (Sigma) was included in the incubation and equilibration medium to ensure mitochondrial transport of palmitate. Where indicated, the FAO inhibitor etomoxir (Sigma)

was included in incubation and equilibration medium at 50 μM final concentration. After addition of the substrates, 5 mM ADP (Sigma) was injected to drive maximum respiration by mimicking a state of energy demand. Lastly, 1 μM oligomycin (Calbiochem) was injected to derive the portion of OCR used for ATP synthesis. In all experiments, parallel samples were run in the absence of any treatment to ensure stable baselines as a quality control parameter for the bioenergetic health of the cells. OCR was measured at 37°C in 6 replicates in independent wells of the same plate. The number of independent experiments for each OCR measurement is indicated in figure legends.

Of note, ADP can be taken up by intact hepatocytes consistent with reports in several other cell types (Chaudry, 1982), and pilot studies confirmed comparable induction of ADP-driven OCR in hepatocytes can be achieved in the absence or presence of digitonin permeabilization (data not shown). For these reasons, intact hepatocytes were used in all OCR measurements. In addition, we measured intracellular ADP levels in hepatocytes after addition of 5 mM ADP to the medium and found this concentration to be 4.25 ± 0.10 mM under these conditions. OCR values in Figures 3.5 and 3.7 represent the difference between the maximal rate in the presence of ADP and the rate after addition of oligomycin, thus indicating ATP production by mitochondrial oxidative phosphorylation. We also measured the oligomycin-inhibitable portion of OCR in the absence of ADP. Table 3.1 summarizes the OCR values in the absence and presence of ADP for all substrates and genotypes tested.

Analysis of mitochondria mass in primary hepatocytes

Primary *Bad* +/+ and -/- hepatocytes were seeded onto collagen-coated glass bottom culture dishes and cultured for 1 day. The cells were then incubated with 300 nM of MitoTracker Green (Invitrogen) for 30 min at 37°C, washed twice with HBSS, and visualized using a Leica DMI6000B microscope at a magnification of 63x. Fluorescence intensity was analyzed using the Leica Application Suite v3.5.0 and ImageJ v1.46r. All samples were processed in parallel and images captured in the same session using the same imaging parameters.

Microarray profiling and gene set enrichment analysis (GSEA)

1 µg of liver RNA was used for microarray analysis using the Affymetrix gene 1.0 ST mouse arrays containing transcripts of ~28,000 well-annotated genes. Affymetrix array hybridization and scanning was performed by the Microarray Core Facility of the Dana-Farber Cancer Institute. Expression values were normalized using the Robust Multichip Analysis (RMA) algorithm (Irizarry et al., 2003). Samples from *Bad* +/+ and -/- liver were compared using GSEA (Mootha et al., 2003; Subramanian et al., 2005). Curated gene sets (C2) and Gene Ontology based gene sets (C5) were used from the Molecular Signatures Database present at the GSEA website (http:// www.broad.mit.edu/gsea/). A custom gene-set corresponding to mitochondrial β-oxidation was also added to the analysis. Gene sets were permuted 1,000 times to determine false discovery rate (FDR) corrected p-values. Over-represented gene-sets were selected by applying nominal p-value cut-off of 0.05 and FDR of 0.25.

RNA preparation and quantitative real-time PCR

For real time PCR, RNA was prepared and analyzed as previously described (Danial et al., 2008). Primers for cyclophilin served as internal controls for the quality of RNA. The sequence of primers is available upon request.

Antibodies

The following antibodies were used for assessment of BAD phosphorylation and components of the insulin signaling pathway; total BAD (#9292), pS155 BAD (#9297), pS112 BAD (#5284), and pS136 BAD (#5286), total IR (#3025), pY1162 IR (#3024), total AKT (#9272), pS308 AKT (#9275), pS473 AKT (#9271), total GSK-3β (#9315), and pSer21/9 GSK-3 α/β (#9331) (Cell Signaling Technology). The polyclonal anti-BAD antibody Ab 10929 was used for BAD immunoprecipitation (Yang et al., 1995). The anti-VDAC (anti-porin 31-HL) and anti-β-actin antibodies were purchased from Calbiochem and Sigma, respectively.

In vivo insulin signaling studies

After an overnight fast, mice were injected intraperitoneally with saline or insulin (Humulin R) at 0.1 U/g of body weight and sacrificed by cervical dislocation 10 min post injection. The liver and gastrocnemius muscle were rapidly removed and frozen in liquid nitrogen. Tissue powders were generated using liquid nitrogen-cooled mortar and pestle and extracted in 0.5 ml of lysis buffer (20 mM Tris pH 7.4, 5 mM EDTA pH 8.0, 10 mM $Na_4P_2O_7$, 100 mM NaF, 2 mM Na_3Vo_4, 1% NP-40, 1 mM PMSF, 6 µg/ml Aprotinin, and 6 µg/ml Leupeptin) using Qiagen Tissue Lyser II. The samples were centrifuged at 14,000 RPM for 30 min at 4°C, and the supernatants were transferred to fresh tubes. IRS-1-associated PI3K activity was measured in IRS-1 immunoprecipitates as previously described (Lee et al., 2012). For analysis of distal insulin signaling components, 60 µg of protein was resolved on 4-12% gradient NuPAGE gels (Invitrogen) and analyzed by western blotting using the indicated antibodies.

Assessment of insulin signaling in primary hepatocytes

Primary hepatocytes were plated at $5.0x10^5$ cells/well in 6-well plates and serum starved for 14.5 hr in M199 media. They were subsequently treated with 100 nM insulin (Sigma-I6634) for 7 min, washed in PBS, and lysed in 100 µl of lysis buffer (20 mM Tris pH 7.4, 5 mM EDTA pH 8.0, 10 mM $Na_4P_2O_7$, 10 mM NaF, 2 mM Na_3Vo_4, 1% NP-40 1%, 1 mm PMSF, 6 µg/ml Aprotinin, 6 µg/ml Leupeptin), and 30 µg of protein lysate was fractionated on a 4-12% NuPAGE gel for western blot analysis using the indicated antibodies.

Assessment of BAD phosphorylation

Wild-type C57BL/6J mice were fasted overnight or refed for 6 hr after overnight fasting. Livers were excised and homogenized on ice in lysis buffer containing (10 mM Tris pH 7.0, 15 mM EDTA pH 8.0, 0.6 M sucrose, 15 mM β-mercaptoethanol, protease and phosphatase inhibitors (Roche). The homogenates were incubated on ice for 20 min and subsequently centrifuged at 14,000 rpm for 30 min at 4°C, and supernatant collected. 60 µg of protein was analyzed by western blotting using the indicated phospho-BAD or total BAD antibodies.

For assessment of BAD phosphorylation in *ob*/*ob* and *ob*/+ mice, livers were harvested from mice fasted for 24 hr or refed for 1 hr after fasting. Livers were homogenized on ice in a buffer containing 20 mM Tris-HCl pH 7.5, 137 mM NaCl, 10% glycerol, 2 mM EDTA pH 8.0, 2 mM Na_3Vo_4, protease inhibitors (Roche), and phosphatase inhibitors (PhosStop, Roche). The homogenates were incubated on ice for 20 min and then centrifuged at 14,000 rpm for 30 min at 4°C. The supernatant was collected with a gel-loading tip (to discard the top layer of fat) and transferred to a fresh tube. 60 µg of protein lysate was analyzed for total BAD protein levels by western blot and 2 mg of protein lysate was immunoprecipitated with an anti-BAD antibody. For immunoprecipitations, a final lysate volume of 500 µl per sample was incubated with 30 µl of protein A-conjugated sepharose CL-4B beads (GE Healthcare) for 30 min at 4°C with rotation. The pre-cleared lysates were transferred to a fresh tube and incubated with a polyclonal antiserum to BAD [Ab 10929, (Yang et al., 1995)] at 1:500 dilution overnight at 4°C with rotation. Subsequently, 30 µl of protein A-conjugated sepharose beads were added and incubated for another 2 hr at 4°C with rotation. The beads were then washed 3 times with lysis buffer, resuspended in NuPAGE LDS sample buffer, heated for 5 min at 95°C, and loaded on a 4-12% NuPAGE gel for western blot analysis.

Statistical Analysis

Data are presented as mean ± SEM of the indicated number of independent experiments or mice per genotype. Statistical significance among the groups was tested with unpaired or paired Student's *t*-test and analysis of variance (ANOVA) when appropriate. Differences were considered significant at $p < 0.05$.

CONTRIBUTIONS

Elizabeth Lane contributed primarily to the insulin signaling assays in both liver samples and primary hepatocytes in collaboration with Hu Huang in Young-Bum Kim's Laboratory at BIDMC. Elizabeth Lane also performed qRT assays for gene expression analyses and measurements of BAD phosphorylation along with Luisa Garcia-Haro and Alfredo Giménez-Cassina. She also contributed to the revision of the manuscript by helping with hepatocyte isolation.

The contents of this chapter first appeared in the following publication:

Giménez-Cassina, A., Garcia-Haro, L., Choi, C.S., Osundiji, M.A., **Lane, E.A**., Huang, H., Yildirim, M.A., Szlyk, B., Fisher, J.K., Polak, K., et al. (2014). Regulation of hepatic energy metabolism and gluconeogenesis by BAD. Cell metabolism 19, 272-284.

REFERENCES

Agius, L. (2008). Glucokinase and molecular aspects of liver glycogen metabolism. Biochem J 414, 1-18.

Agius, L. (2013). High-carbohydrate diets induce hepatic insulin resistance to protect the liver from substrate overload. Biochemical pharmacology 85, 306-312.

Bain, J.R., Schisler, J.C., Takeuchi, K., Newgard, C.B., and Becker, T.C. (2004). An adenovirus vector for efficient RNA interference-mediated suppression of target genes in insulinoma cells and pancreatic islets of langerhans. Diabetes 53, 2190-2194.

Barzilai, N., Hawkins, M., Angelov, I., Hu, M., and Rossetti, L. (1996). Glucosamine-induced inhibition of liver glucokinase impairs the ability of hyperglycemia to suppress endogenous glucose production. Diabetes 45, 1329-1335.

Bechmann, L.P., Gastaldelli, A., Vetter, D., Patman, G.L., Pascoe, L., Hannivoort, R.A., Lee, U.E., Fiel, I., Munoz, U., Ciociaro, D., Lee, Y.M., Buzzigoli, E., Miele, L., Hui, K.Y., Bugianesi, E., Burt, A.D., Day, C.P., Mari, A., Agius, L., Walker, M., Friedman, S.L., and Reeves, H.L. (2012). Glucokinase links Kruppel-like factor 6 to the regulation of hepatic insulin sensitivity in nonalcoholic fatty liver disease. Hepatology 55, 1083-1093.

Burgess, S.C., He, T., Yan, Z., Lindner, J., Sherry, A.D., Malloy, C.R., Browning, J.D., and Magnuson, M.A. (2007). Cytosolic phosphoenolpyruvate carboxykinase does not solely control the rate of hepatic gluconeogenesis in the intact mouse liver. Cell Metab 5, 313-320.

Chaudry, I.H. (1982). Does ATP cross the cell plasma membrane. Yale J Biol Med 55, 1-10.

Choi, C.S., Savage, D.B., Abu-Elheiga, L., Liu, Z.X., Kim, S., Kulkarni, A., Distefano, A., Hwang, Y.J., Reznick, R.M., Codella, R., Zhang, D., Cline, G.W., Wakil, S.J., and Shulman, G.I. (2007). Continuous fat oxidation in acetyl-CoA carboxylase 2 knockout mice increases total energy expenditure, reduces fat mass, and improves insulin sensitivity. Proc Natl Acad Sci U S A 104, 16480-16485.

Clement, K., Pueyo, M.E., Vaxillaire, M., Rakotoambinina, B., Thuillier, F., Passa, P., Froguel, P., Robert, J.J., and Velho, G. (1996). Assessment of insulin sensitivity in glucokinase-deficient subjects. Diabetologia 39, 82-90.

Copps, K.D., and White, M.F. (2012). Regulation of insulin sensitivity by serine/threonine phosphorylation of insulin receptor substrate proteins IRS1 and IRS2. Diabetologia 55, 2565-2582.

Cournarie, F., Azzout-Marniche, D., Foretz, M., Guichard, C., Ferre, P., and Foufelle, F. (1999). The inhibitory effect of glucose on phosphoenolpyruvate carboxykinase gene expression in cultured hepatocytes is transcriptional and requires glucose metabolism. FEBS Lett 460, 527-532.

Danial, N.N. (2008). BAD: undertaker by night, candyman by day. Oncogene 27 Suppl 1, S53-70.

Danial, N.N., Gramm, C.F., Scorrano, L., Zhang, C.Y., Krauss, S., Ranger, A.M., Datta, S.R., Greenberg, M.E., Licklider, L.J., Lowell, B.B., Gygi, S.P., and Korsmeyer, S.J. (2003). BAD and glucokinase reside in a mitochondrial complex that integrates glycolysis and apoptosis. Nature 424, 952-956.

Danial, N.N., Walensky, L.D., Zhang, C.Y., Choi, C.S., Fisher, J.K., Molina, A.J., Datta, S.R., Pitter, K.L., Bird, G.H., Wikstrom, J.D., Deeney, J.T., Robertson, K., Morash, J., Kulkarni, A., Neschen, S., Kim, S., Greenberg, M.E., Corkey, B.E., Shirihai, O.S., Shulman, G.I., Lowell, B.B., and Korsmeyer, S.J. (2008). Dual role of proapoptotic BAD in insulin secretion and beta cell survival. Nat Med 14, 144-153.

Ferre, T., Pujol, A., Riu, E., Bosch, F., and Valera, A. (1996). Correction of diabetic alterations by glucokinase. Proc Natl Acad Sci U S A 93, 7225-7230.

Grimsby, J., Sarabu, R., Corbett, W.L., Haynes, N.E., Bizzarro, F.T., Coffey, J.W., Guertin, K.R., Hilliard, D.W., Kester, R.F., Mahaney, P.E., Marcus, L., Qi, L., Spence, C.L., Tengi, J., Magnuson, M.A., Chu, C.A., Dvorozniak, M.T., Matschinsky, F.M., and Grippo, J.F. (2003). Allosteric activators of glucokinase: potential role in diabetes therapy. Science 301, 370-373.

Gustafson, L.A., Neeft, M., Reijngoud, D.J., Kuipers, F., Sauerwein, H.P., Romijn, J.A., Herling, A.W., Burger, H.J., and Meijer, A.J. (2001). Fatty acid and amino acid modulation of glucose cycling in isolated rat hepatocytes. Biochem J 358, 665-671.

Hakimi, P., Johnson, M.T., Yang, J., Lepage, D.F., Conlon, R.A., Kalhan, S.C., Reshef, L., Tilghman, S.M., and Hanson, R.W. (2005). Phosphoenolpyruvate carboxykinase and the critical role of cataplerosis in the control of hepatic metabolism. Nutr Metab (Lond) 2, 33.

Irizarry, R.A., Hobbs, B., Collin, F., Beazer-Barclay, Y.D., Antonellis, K.J., Scherf, U., and Speed, T.P. (2003). Exploration, normalization, and summaries of high density oligonucleotide array probe level data. Biostatistics 4, 249-264.

Jump, D.B., Tripathy, S., and Depner, C.M. (2013). Fatty acid-regulated transcription factors in the liver. Annu Rev Nutr 33, 249-269.

Kaelin, W.G., Jr., and McKnight, S.L. (2013). Influence of metabolism on epigenetics and disease. Cell 153, 56-69.

Kim, T.H., Kim, H., Park, J.M., Im, S.S., Bae, J.S., Kim, M.Y., Yoon, H.G., Cha, J.Y., Kim, K.S., and Ahn, Y.H. (2009). Interrelationship between liver X receptor alpha, sterol regulatory element-binding protein-1c, peroxisome proliferator-activated receptor gamma, and small heterodimer partner in the transcriptional regulation of glucokinase gene expression in liver. J Biol Chem 284, 15071-15083.

Lee, D.H., Huang, H., Choi, K., Mantzoros, C., and Kim, Y.B. (2012). Selective PPARgamma modulator INT131 normalizes insulin signaling defects and improves bone mass in diet-induced obese mice. Am J Physiol Endocrinol Metab 302, E552-560.

Lin, H.V., and Accili, D. (2011). Hormonal regulation of hepatic glucose production in health and disease. Cell Metab 14, 9-19.

Lin, J., Wu, P.H., Tarr, P.T., Lindenberg, K.S., St-Pierre, J., Zhang, C.Y., Mootha, V.K., Jager, S., Vianna, C.R., Reznick, R.M., Cui, L., Manieri, M., Donovan, M.X., Wu, Z., Cooper, M.P., Fan, M.C., Rohas, L.M., Zavacki, A.M., Cinti, S., Shulman, G.I., Lowell, B.B., Krainc, D., and Spiegelman, B.M. (2004). Defects in adaptive energy metabolism with CNS-linked hyperactivity in PGC-1alpha null mice. Cell 119, 121-135.

Magnuson, M.A., She, P., and Shiota, M. (2003). Gene-altered mice and metabolic flux control. J Biol Chem 278, 32485-32488.

Matschinsky, F.M. (2009). Assessing the potential of glucokinase activators in diabetes therapy. Nat Rev Drug Discov 8, 399-416.

Matsumoto, M., Pocai, A., Rossetti, L., Depinho, R.A., and Accili, D. (2007). Impaired regulation of hepatic glucose production in mice lacking the forkhead transcription factor Foxo1 in liver. Cell Metab 6, 208-216.

Meininger, G.E., Scott, R., Alba, M., Shentu, Y., Luo, E., Amin, H., Davies, M.J., Kaufman, K.D., and Goldstein, B.J. (2011). Effects of MK-0941, a novel glucokinase activator, on glycemic control in insulin-treated patients with type 2 diabetes. Diabetes Care 34, 2560-2566.

Mootha, V.K., Lindgren, C.M., Eriksson, K.F., Subramanian, A., Sihag, S., Lehar, J., Puigserver, P., Carlsson, E., Ridderstrale, M., Laurila, E., Houstis, N., Daly, M.J., Patterson, N., Mesirov, J.P., Golub, T.R., Tamayo, P., Spiegelman, B., Lander, E.S., Hirschhorn, J.N., Altshuler, D., and Groop, L.C. (2003). PGC-1alpha-responsive genes involved in oxidative phosphorylation are coordinately downregulated in human diabetes. Nat Genet 34, 267-273.

Newgard, C.B. (2012). Interplay between lipids and branched-chain amino acids in development of insulin resistance. Cell Metab 15, 606-614.

Oosterveer, M.H., Mataki, C., Yamamoto, H., Harach, T., Moullan, N., van Dijk, T.H., Ayuso, E., Bosch, F., Postic, C., Groen, A.K., Auwerx, J., and Schoonjans, K. (2012). LRH-1-dependent glucose sensing determines intermediary metabolism in liver. J Clin Invest 122, 2817-2826.

Payne, V.A., Arden, C., Wu, C., Lange, A.J., and Agius, L. (2005). Dual role of phosphofructokinase-2/fructose bisphosphatase-2 in regulating the compartmentation and expression of glucokinase in hepatocytes. Diabetes 54, 1949-1957.

Pelicano, H., Xu, R.H., Du, M., Feng, L., Sasaki, R., Carew, J.S., Hu, Y., Ramdas, L., Hu, L., Keating, M.J., Zhang, W., Plunkett, W., and Huang, P. (2006). Mitochondrial respiration defects in cancer cells cause activation of Akt survival pathway through a redox-mediated mechanism. J Cell Biol 175, 913-923.

Postic, C., Shiota, M., Niswender, K.D., Jetton, T.L., Chen, Y., Moates, J.M., Shelton, K.D., Lindner, J., Cherrington, A.D., and Magnuson, M.A. (1999). Dual roles for glucokinase in glucose homeostasis as determined by liver and pancreatic beta cell-specific gene knock-outs using Cre recombinase. J Biol Chem 274, 305-315.

Pryor, H.J., Smyth, J.E., Quinlan, P.T., and Halestrap, A.P. (1987). Evidence that the flux control coefficient of the respiratory chain is high during gluconeogenesis from lactate in hepatocytes from starved rats. Implications for the hormonal control of gluconeogenesis and action of hypoglycaemic agents. Biochem J 247, 449-457.

Rizza, R.A. (2010). Pathogenesis of fasting and postprandial hyperglycemia in type 2 diabetes: implications for therapy. Diabetes 59, 2697-2707.

Rossetti, L., Chen, W., Hu, M., Hawkins, M., Barzilai, N., and Efrat, S. (1997). Abnormal regulation of HGP by hyperglycemia in mice with a disrupted glucokinase allele. Am J Physiol 273, E743-750.

Rothman, D.L., Magnusson, I., Katz, L.D., Shulman, R.G., and Shulman, G.I. (1991). Quantitation of hepatic glycogenolysis and gluconeogenesis in fasting humans with 13C NMR. Science 254, 573-576.

Saltiel, A.R., and Kahn, C.R. (2001). Insulin signalling and the regulation of glucose and lipid metabolism. Nature 414, 799-806.

Samuel, V.T., and Shulman, G.I. (2012). Mechanisms for insulin resistance: common threads and missing links. Cell 148, 852-871.

Satapati, S., Sunny, N.E., Kucejova, B., Fu, X., He, T.T., Mendez-Lucas, A., Shelton, J.M., Perales, J.C., Browning, J.D., and Burgess, S.C. (2012). Elevated TCA cycle function in the pathology of diet-induced hepatic insulin resistance and fatty liver. J Lipid Res 53, 1080-1092.

Scott, D.K., O'Doherty, R.M., Stafford, J.M., Newgard, C.B., and Granner, D.K. (1998). The repression of hormone-activated PEPCK gene expression by glucose is insulin-independent but requires glucose metabolism. J Biol Chem 273, 24145-24151.

Subramanian, A., Tamayo, P., Mootha, V.K., Mukherjee, S., Ebert, B.L., Gillette, M.A., Paulovich, A., Pomeroy, S.L., Golub, T.R., Lander, E.S., and Mesirov, J.P. (2005). Gene set enrichment analysis: a knowledge-based approach for interpreting genome-wide expression profiles. Proc Natl Acad Sci U S A 102, 15545-15550.

Szlyk, B., Braun, C.R., Ljubicic, S., Patton, E., Bird, G.H., Osundiji, M.A., Matschinsky, F.M., Walensky, L.D., and Danial, N.N. (2014). A phospho-BAD BH3 helix activates glucokinase by a mechanism distinct from that of allosteric activators. Nature structural & molecular biology *21*, 36-42.

Torres, T.P., Catlin, R.L., Chan, R., Fujimoto, Y., Sasaki, N., Printz, R.L., Newgard, C.B., and Shiota, M. (2009). Restoration of hepatic glucokinase expression corrects hepatic glucose flux and normalizes plasma glucose in zucker diabetic fatty rats. Diabetes 58, 78-86.

Velho, G., Petersen, K.F., Perseghin, G., Hwang, J.H., Rothman, D.L., Pueyo, M.E., Cline, G.W., Froguel, P., and Shulman, G.I. (1996). Impaired hepatic glycogen synthesis in glucokinase-deficient (MODY-2) subjects. J Clin Invest 98, 1755-1761.

Wu, C., Okar, D.A., Stoeckman, A.K., Peng, L.J., Herrera, A.H., Herrera, J.E., Towle, H.C., and Lange, A.J. (2004). A potential role for fructose-2,6-bisphosphate in the stimulation of hepatic glucokinase gene expression. Endocrinology 145, 650-658.

Wu, M., Neilson, A., Swift, A.L., Moran, R., Tamagnine, J., Parslow, D., Armistead, S., Lemire, K., Orrell, J., Teich, J., Chomicz, S., and Ferrick, D.A. (2007). Multiparameter metabolic analysis reveals a close link between attenuated mitochondrial bioenergetic function and enhanced glycolysis dependency in human tumor cells. Am J Physiol Cell Physiol 292, C125-136.

Yamada, K., and Noguchi, T. (1999). Nutrient and hormonal regulation of pyruvate kinase gene expression. Biochem J 337 (Pt 1), 1-11.

Yang, E., Zha, J., Jockel, J., Boise, L.H., Thompson, C.B., and Korsmeyer, S.J. (1995). Bad, a heterodimeric partner for Bcl-XL and Bcl-2, displaces Bax and promotes cell death. Cell 80, 285-291.

Yeshao, W., Gu, J., Peng, X., Nairn, A.C., and Nadler, J.L. (2005). Elevated glucose activates protein synthesis in cultured cardiac myocytes. Metabolism 54, 1453-1460.

Yoon, J.C., Puigserver, P., Chen, G., Donovan, J., Wu, Z., Rhee, J., Adelmant, G., Stafford, J., Kahn, C.R., Granner, D.K., Newgard, C.B., and Spiegelman, B.M. (2001). Control of hepatic gluconeogenesis through the transcriptional coactivator PGC-1. Nature 413, 131-138.

CHAPTER 4
Discussion and Future Directions

The integrative biochemical and genetic analyses described in Chapters 2 and 3 enabled mechanistic dissection and systemic evaluation of BAD's significance in hepatic substrate metabolism. Our studies show that hepatic loss of BAD or interference with its phosphorylation is linked to reduced glycolysis and *de novo* lipogenesis, enhanced FAO, and unrestrained gluconeogenesis even in the presence of insulin. Moreover, using *Bad* -/- hepatocytes as a system where glucose-dependent hepatic gene expression is impaired, we discovered HCF-1 as a novel biochemical player in glucose-regulation of *de novo* lipogenesis. Our findings have also given rise to additional hypotheses and research opportunities that will lay the foundation for future investigations, two of which are highlighted in the following sections; the physiological relevance of the HCF-1:ChREBP axis in hepatic metabolism and insulin sensitivity, and the therapeutic potential of phospho-BAD mimicry.

4.1 The physiological relevance of the HCF-1:ChREBP axis in hepatic metabolism and insulin sensitivity

Increased hepatic lipid accumulation has been implicated as a cause of insulin resistance (Samuel and Shulman, 2018). In line with this model, hepatic steatosis is strongly linked to insulin resistance (Lallukka and Yki-Jarvinen, 2016; Samuel and Shulman, 2018). Furthermore, inhibiting hepatic *de novo* lipogenesis in mouse models of diabetes and insulin resistance, including hepatic knock down of ChREBP, results in improved glycemia and insulin sensitivity (Dentin et al., 2006; Iizuka et al., 2006; Samuel and Shulman, 2018; Savage et al., 2006). However, given the spectrum of transcriptional programs regulated by ChREBP, including both glucose and lipid metabolism genes, the physiologic consequences of ChREBP *in vivo* are complex with ChREBP deficiency having beneficial or adverse effects depending on the context [reviewed in (Abdul-Wahed et al., 2017; Agius, 2016)]. Specifically, the beneficial effects of ChREBP deletion/depletion in lowering hepatic steatosis and blood glucose levels seem to predominantly manifest in the context of lipid overload as in long-term high carbohydrate treatment or in certain genetic models of diabetes and obesity. Overexpression of ChREBP has also been shown to

decrease hyperglycemia and improve hepatic insulin sensitivity despite increased hepatic steatosis (Benhamed et al., 2012). These seemingly conflicting outcomes of ChREBP depletion and overexpression both improving blood glucose levels and insulin sensitivity may be potentially reconciled by the possibility that different lipid species have distinct cellular effects. ChREBP depletion may inhibit the production of lipids, preventing accumulation of potentially harmful lipid species. Overexpression of ChREBP may also reduce harmful lipid species by stimulating their conversion to neutral or more beneficial lipid species. For example, accumulation of diacylglycerols (DAGs) and ceramides may result in insulin resistance, while accumulation of triacylglycerols (TAGs) and monounsaturated fatty acids (MUFAs) may be neutral or even beneficial in hepatocytes (Benhamed et al., 2012; Birkenfeld and Shulman, 2014; Meikle and Christopher, 2011).

In vivo relevance of HCF-1 in hepatic metabolism and insulin sensitivity. Identification of HCF-1 as a novel modulator of ChREBP activity and lipogenic gene transcription in response to glucose warrants investigation of its *in vivo* relevance in hepatic metabolism as well as its specific contribution to ChREBP function in the liver. *HCF-1* knockdown was shown to improve glycemia in the leptin resistant *db*/*db* model, and this was attributed to decreased gluconeogenesis (Ruan et al., 2012). However the possibility that these benefits could also be partly mediated by changes in ChREBP was not tested. Additional studies are needed to examine the full spectrum of metabolic changes associated with hepatic HCF-1 manipulation *in vivo*, including potential effects on insulin sensitivity. Within this context, hyperinsulinemic clamp studies will be particularly informative. Furthermore, a ChREBP variant that cannot bind HCF-1 will be an informative reagent in similar studies, and will help determine the contribution of HCF-1 to the *in vivo* functions of ChREBP.

Given the finding that the HGF-1:OGT:ChREBP complex is induced by high carbohydrate diet (HCD) in the liver, interrogation of HCF-1's role in the hepatic response to HCD (70% sucrose) treatment is warranted. Short-term HCD treatment (18 hrs) augments ChREBP activity and

lipogenic gene expression, but actual increases in hepatic triglycerides (TGs) and impairment in glucose tolerance are apparent only upon long-term (8-12 wks) HCD treatment. For this reason, examination of the consequences of altered HCF-1 in both short- and long-term HCD feeding is warranted. In light of the findings described in Chapter 3, hepatic depletion of HCF-1 is predicted to diminish HCD-dependent recruitment of ChREBP to promoters of lipogenic genes, and to phenocopy ChREBP depletion by lowering hepatic steatosis and improving glucose tolerance in the HCD model.

The contribution of HCF-1 to transcriptional activation of lipogenic genes. HCF-1 is best known for its function as a transcriptional co-regulator and its capacity to bridge interactions between transcription factors and chromatin modifiers (Cai et al., 2010; Tyagi and Herr, 2009; Wysocka et al., 2003; Yokoyama et al., 2004). This warrants examination of whether glucose-dependent recruitment of HCF-1 to lipogenic gene promoters is commensurate with HCF-1-dependent epigenetic modulation of lipogenic gene activation in conjunction with and beyond HCF-1-dependent ChREBP activation. Among epigenetic modifiers that are found in active promoter complexes with HCF-1 and OGT are H3K4 trimethyltransferases such as Mixed-Lineage Leukemia 5 (MLL5) and Set Domain Containing 1A (SETD1A) (Lee and Skalnik, 2008; Nin et al., 2015; Yokoyama et al., 2004). H3K4me3 is a histone mark associated with transcription start site of actively transcribed genes. Interestingly, evidence suggests that MLL5 and SETD1A are regulated by O-GlcNAcylation, which is proposed to enhance their enzymatic activity and/or facilitate their assembly into higher order promoter complexes (Hahne et al., 2013; Nin et al., 2015). In light of these observations, it is possible that glucose stimulation promotes an active chromatin state through recruitment of epigenetic modifiers to lipogenic gene promoters (Figure 4.1).

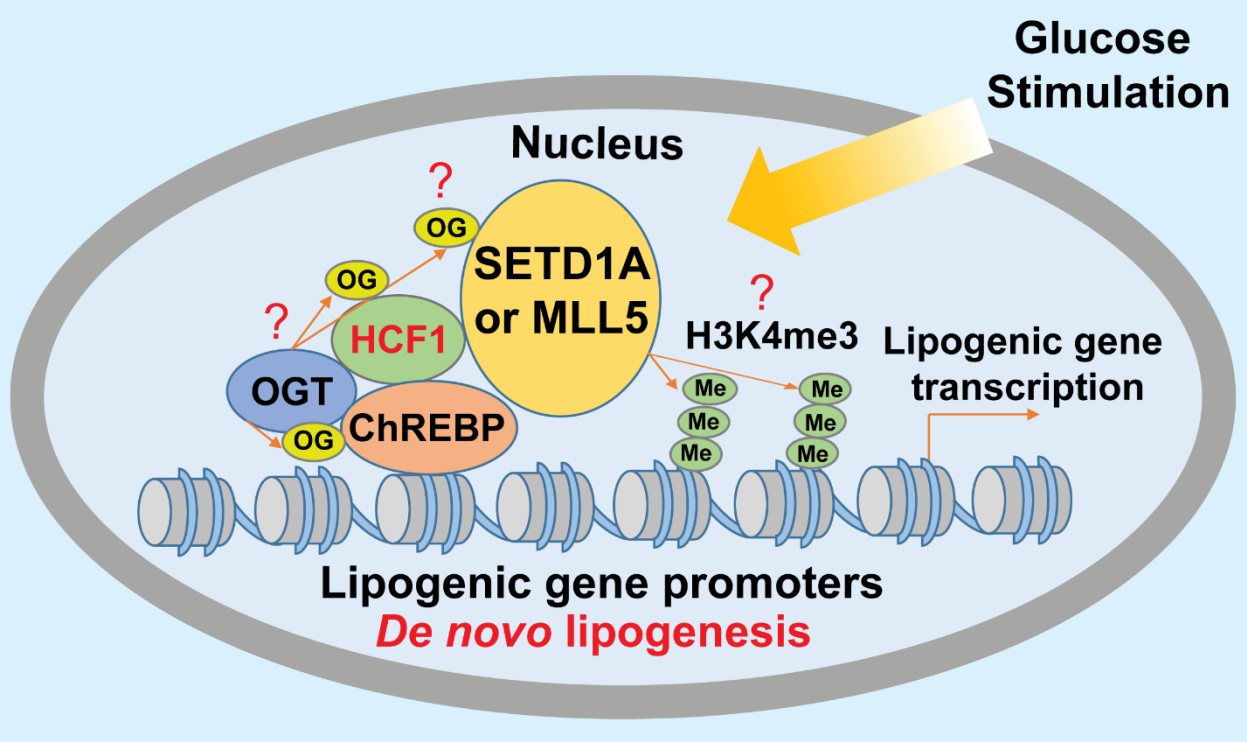


Figure 4.1. Potential mechanism for epigenetic regulation of lipogenic genes by HCF-1

Schematic of a potential mechanism whereby HCF-1 recruits H3K4 trimethyltransferases to the promoters of lipogenic genes in response to glucose stimulation, thereby promoting an active chromatin state and lipogenic gene transcription.

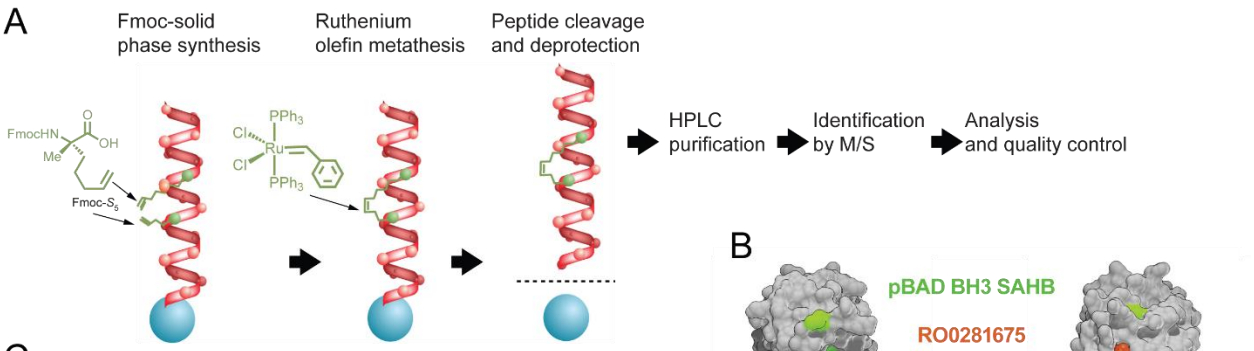
4.2 Therapeutic potential of phospho-BAD mimicry

Given its tissue restricted expression and function, GK remains an attractive therapeutic target in diabetes. To date, drug discovery efforts for GK activator (GKA) compounds have identified small molecules that bind an allosteric site in GK and markedly increase its affinity for glucose with K_m changes from 7–8 mM to ~1–2 mM (Bonadonna et al., 2010; Efanov et al., 2005; Futamura et al., 2006; Grimsby et al., 2003; Kamata et al., 2004; Kesavan et al., 1997; Meininger et al., 2011; Pfefferkorn et al., 2012; Szlyk et al., 2014).The effect of these "allosteric GKAs" is similar to the kinetic properties of naturally-occurring human GK gain-of-function mutations, which predominantly occur at the allosteric site. Clinical trials of several allosteric GKAs have shown promising short-term effects (Bonadonna et al., 2010; Ericsson et al., 2012). However, the therapeutic benefits of these compounds are curtailed by the risk of hypoglycemia due to drastic lowering of glucose threshold for GK activation as well as unexplained loss of efficacy and toxicity over time (Agius, 2014; Kiyosue et al., 2013; Meininger et al., 2011; Wilding et al., 2013). In addition, allosteric GK activation can lead to excess lipogenesis and fatty liver (De Ceuninck et al., 2013; Meininger et al., 2011). The successes and shortcomings of allosteric GKAs warrant exploration of alternative pharmacologic modalities for GK activation, particularly of those with a more tempered effect on glucose affinity.

The BAD BH3 domain is both necessary and sufficient to activate GK. This is evident from the capacity of hydrocarbon-stapled peptides modeled after the phospho-BAD BH3 helix to activate GK (Danial et al., 2008; Giménez-Cassina and Danial, 2015). Unlike non-stapled peptides, these chemically modified peptides- referred to as Stabilized Alpha-Helices of BCL-2 domains (SAHBs)- preserve the natural structure of bioactive helices (Braun et al., 2010; Danial et al., 2008). BAD SAHBs modeled after the BAD BH3 phospho-variants are cell permeable and phenocopy the full length BAD protein and its phospho-variants in terms of their capacity to stimulate GK activity, glucose metabolism and ChREBP activity (Danial et al., 2008; Ljubicic et al., 2015) (data not shown). Importantly, the metabolic effects of BAD SAHB compounds modeled

after the phospho-BAD BH3 helix (BAD SAHB SD) is target (GK)-dependent as evident from the following two lines of evidence. *First*, BAD SAHB SD is ineffective in GK-depleted cells. *Second*, BAD SAHB compounds modeled after the BAD BH3 variant that cannot activate GK (BAD SAHB AAA) do not produce the metabolic effects seen with BAD SAHB SD. This has built confidence that the BAD BH3 stapled peptides are bona fide pharmacologic mimetics of BAD by all parameters we have investigated to date and that their metabolic effect is mediated by GK.

Molecular and structural mapping of the BAD BH3 helix on GK using BAD SAHBs revealed that this helix directly engages GK near its active site at a novel region wholly distinct from the enzyme's allosteric site (Figure 4.2A and B). The mechanism of GK activation by phospho-BAD BH3 mimicry is also distinct from allosteric GKAs in that Vmax is increased without drastic changes in glucose affinity (Figure 4.2C). Preliminary studies to test the efficacy of BAD SAHB compounds *in vivo* have been promising. Specifically, intraperitoneal injection of BAD SAHB SD was sufficient to lower fasting hyperglycemia and improve GTT in leptin resistant *ob*/*ob* mice analogous to hepatic expression of the full length BAD SD variant (data not shown). Additional studies are required to confirm and extend these findings to other pre-clinical models of diabetes, and to characterize the long-term effects of these compounds vis-à-vis allosteric GKAs. Furthermore, full characterization of pharmacokinetic properties of BAD SAHBs awaits future studies. Given GK as their target, we expect BAD SAHBs to have dual benefits in liver and insulin producing β-cells. Recent studies in human islets comparing the outcome of pharmacologic GK activation by phospho-BAD mimicry versus allosteric GKAs have revealed distinct long-term effects on β-cell survival and functional β-cell mass (Fu, *in revision*). Specifically, BAD SAHB SD but not allosteric GKAs is β-cell protective under diabetes-related stress stimuli. Overall, a novel GK binding site, together with distinct mechanism of action and potential differences in long-term effects, warrant the pursuit of phospho-BAD BH3 mimicry as a



C

Treatment	V_{max}(% Veh)	$S_{0.5}$(mM)	^{n}H
Vehicle (DMSO)	100	7.49 ± 0.18	1.61 ± 0.03
BAD SAHB SD	144 ± 4.64***	6.54 ± 0.15**	1.71 ± 0.03
BAD SAHB AAA	110 ± 3.77	7.56 ± 0.87	1.59 ± 0.05
GKA (RO0281675)	138 ± 6.15***	1.62 ± 0.13***	1.71 ± 0.06

Figure 4.2. Comparison of phospho-BAD SAHB and the allosteric GKA RO0281675

(**A**) Schematic of olefin metathesis and hydrocarbon stapling of peptides modeled after the BAD BH3 domain (BAD SAHBs). (**B**) The location of the pSAHB binding site with respect to glucose binding (light blue) and the allosteric (orange) sites of GK (PDB:4DCH) is shown. (**C**) Summary of GK kinetic parameters in the presence of vehicle or 5 μM of the indicated BAD $SAHB_A$ (n=6). BAD SAHB SD (green) is modeled after the Serine to Aspartic acid phospho-mimic BAD BH3 variant, while BAD AAA (blue) is modeled after a phospho-deficient BAD BH3 variant that cannot activate GK. V_{max}, maximal rate of reaction; $S_{0.5}$, the glucose concentration that allows half maximal activity; Hill coefficient (n_H).

therapeutic approach to targeting GK in diabetes.

While there is precedence for a stapled peptide in clinical trials for hematologic and solid tumors [p53 stapled peptide (ALRN-6924), https://clinicaltrials.gov/ct2/show/NCT02909972], it is possible that even with a fair amount of efforts to improve pharmacokinetics, BAD stapled peptides may have limited clinical utility for metabolic disease. However, this does not diminish the utility of the information gained using these reagents as tool compounds, including the opportunity to delve deeply into the structural characteristics of the BAD BH3 helix and GK interaction. In addition, BAD SAHBs can be leveraged as “pharmacologic guides” for discovering small molecules that target the novel GK activation site as in a chemical displacement screen. Such efforts will also help expand our chemical tool box to learn about the biophysical and structural characteristics of GK that contribute to its unique metabolic biology.

References

Abdul-Wahed, A., Guilmeau, S., and Postic, C. (2017). Sweet Sixteenth for ChREBP: Established Roles and Future Goals. Cell Metab *26*, 324-341.

Agius, L. (2014). Lessons from glucokinase activators: the problem of declining efficacy. Expert opinion on therapeutic patents *24*, 1155-1159.

Agius, L. (2016). Dietary carbohydrate and control of hepatic gene expression: mechanistic links from ATP and phosphate ester homeostasis to the carbohydrate-response element-binding protein. Proc Nutr Soc *75*, 10-18.

Benhamed, F., Denechaud, P.-D.D., Lemoine, M., Robichon, C., Moldes, M., Bertrand-Michel, J., Ratziu, V., Serfaty, L., Housset, C., Capeau, J., et al. (2012). The lipogenic transcription factor ChREBP dissociates hepatic steatosis from insulin resistance in mice and humans. The Journal of clinical investigation *122*, 2176-2194.

Birkenfeld, A.L., and Shulman, G.I. (2014). Nonalcoholic fatty liver disease, hepatic insulin resistance, and type 2 Diabetes. Hepatology (Baltimore, Md.) *59*, 713-723.

Bonadonna, R.C., Heise, T., Arbet-Engels, C., Kapitza, C., Avogaro, A., Grimsby, J., Zhi, J., Grippo, J.F., and Balena, R. (2010). Piragliatin (RO4389620), a novel glucokinase activator, lowers plasma glucose both in the postabsorptive state and after a glucose challenge in patients with type 2 diabetes mellitus: a mechanistic study. The Journal of clinical endocrinology and metabolism *95*, 5028-5036.

Braun, C.R., Mintseris, J., Gavathiotis, E., Bird, G.H., Gygi, S.P., and Walensky, L.D. (2010). Photoreactive stapled BH3 peptides to dissect the BCL-2 family interactome. Chemistry & biology *17*, 1325-1333.

Cai, Y., Jin, J., Swanson, S.K., Cole, M.D., Choi, S.H., Florens, L., Washburn, M.P., Conaway, J.W., and Conaway, R.C. (2010). Subunit composition and substrate specificity of a MOF-containing histone acetyltransferase distinct from the male-specific lethal (MSL) complex. The Journal of biological chemistry *285*, 4268-4272.

Danial, N.N., Walensky, L.D., Zhang, C.Y., Choi, C.S., Fisher, J.K., Molina, A.J., Datta, S.R., Pitter, K.L., Bird, G.H., Wikstrom, J.D., et al. (2008). Dual role of proapoptotic BAD in insulin secretion and beta cell survival. Nature medicine *14*, 144-153.

De Ceuninck, F., Kargar, C., Ilic, C., Caliez, A., Rolin, J.O., Umbdenstock, T., Vinson, C., Combettes, M., de Fanti, B., Harley, E., et al. (2013). Small molecule glucokinase activators disturb lipid homeostasis and induce fatty liver in rodents: a warning for therapeutic applications in humans. British journal of pharmacology *168*, 339-353.

Dentin, R., Benhamed, F., Hainault, I., Fauveau, V., Foufelle, F., Dyck, J.R., Girard, J., and Postic, C. (2006). Liver-specific inhibition of ChREBP improves hepatic steatosis and insulin resistance in ob/ob mice. Diabetes *55*, 2159-2170.

Efanov, A.M., Barrett, D.G., Brenner, M.B., Briggs, S.L., Delaunois, A., Durbin, J.D., Giese, U., Guo, H., Radloff, M., Gil, G.S., et al. (2005). A novel glucokinase activator modulates pancreatic islet and hepatocyte function. Endocrinology *146*, 3696-3701.

Ericsson, H., Roshammar, D., Wollbratt, M., Heijer, M., Persson, M., Ueda, S., Leonsson-Zachrisson, M., and Norjavaara, E. (2012). Tolerability, pharmacokinetics, and pharmacodynamics of the glucokinase activator AZD1656, after single ascending doses in healthy subjects during euglycemic clamp. International journal of clinical pharmacology and therapeutics *50*, 765-777.

Fu, A., Alverez-Perez, J.C., Avizonis, D., Kin, T., Bridon, G., Evans, L., Rosselot, C., Bird, G.H., Shapiro, A.M.J., Walensky, L.D., et al. Glucose-dependent partitioning of arginine to urea cycle spares beta cells from inflammation. *In revision*.

Futamura, M., Hosaka, H., Kadotani, A., Shimazaki, H., Sasaki, K., Ohyama, S., Nishimura, T., Eiki, J., and Nagata, Y. (2006). An allosteric activator of glucokinase impairs the interaction of glucokinase and glucokinase regulatory protein and regulates glucose metabolism. J Biol Chem *281*, 37668-37674.

Giménez-Cassina, A., and Danial, N.N. (2015). Regulation of mitochondrial nutrient and energy metabolism by BCL-2 family proteins. Trends in endocrinology and metabolism: TEM *26*, 165-175.

Grimsby, J., Sarabu, R., Corbett, W.L., Haynes, N.E., Bizzarro, F.T., Coffey, J.W., Guertin, K.R., Hilliard, D.W., Kester, R.F., Mahaney, P.E., et al. (2003). Allosteric activators of glucokinase: potential role in diabetes therapy. Science (New York, N.Y.) *301*, 370-373.

Hahne, H., Sobotzki, N., Nyberg, T., Helm, D., Borodkin, V.S., van Aalten, D.M., Agnew, B., and Kuster, B. (2013). Proteome wide purification and identification of O-GlcNAc-modified proteins using click chemistry and mass spectrometry. Journal of proteome research *12*, 927-936.

Iizuka, K., Miller, B., and Uyeda, K. (2006). Deficiency of carbohydrate-activated transcription factor ChREBP prevents obesity and improves plasma glucose control in leptin-deficient (ob/ob) mice. American journal of physiology. Endocrinology and metabolism *291*, E358-364.

Kamata, K., Mitsuya, M., Nishimura, T., Eiki, J., and Nagata, Y. (2004). Structural basis for allosteric regulation of the monomeric allosteric enzyme human glucokinase. Structure (London, England : 1993) *12*, 429-438.

Kesavan, P., Wang, L., Davis, E., Cuesta, A., Sweet, I., Niswender, K., Magnuson, M.A., and Matschinsky, F.M. (1997). Structural instability of mutant beta-cell glucokinase: implications for the molecular pathogenesis of maturity-onset diabetes of the young (type-2). Biochem J *322 (Pt 1)*, 57-63.

Kiyosue, A., Hayashi, N., Komori, H., Leonsson-Zachrisson, M., and Johnsson, E. (2013). Dose-ranging study with the glucokinase activator AZD1656 as monotherapy in Japanese patients with type 2 diabetes mellitus. Diabetes, obesity & metabolism *15*, 923-930.

Lallukka, S., and Yki-Jarvinen, H. (2016). Non-alcoholic fatty liver disease and risk of type 2 diabetes. Best practice & research. Clinical endocrinology & metabolism *30*, 385-395.

Lee, J.H., and Skalnik, D.G. (2008). Wdr82 is a C-terminal domain-binding protein that recruits the Setd1A Histone H3-Lys4 methyltransferase complex to transcription start sites of transcribed human genes. Molecular and cellular biology *28*, 609-618.

Ljubicic, S., Polak, K., Fu, A., Wiwczar, J., Szlyk, B., Chang, Y., Alvarez-Perez, J.C., Bird, G.H., Walensky, L.D., Garcia-Ocaña, A., et al. (2015). Phospho-BAD BH3 mimicry protects β cells and restores functional β cell mass in diabetes. Cell reports *10*, 497-504.

Meikle, P.J., and Christopher, M.J. (2011). Lipidomics is providing new insight into the metabolic syndrome and its sequelae. Current opinion in lipidology *22*, 210-215.

Meininger, G.E., Scott, R., Alba, M., Shentu, Y., Luo, E., Amin, H., Davies, M.J., Kaufman, K.D., and Goldstein, B.J. (2011). Effects of MK-0941, a novel glucokinase activator, on glycemic control in insulin-treated patients with type 2 diabetes. Diabetes care *34*, 2560-2566.

Nin, D.S., Huang, W., Ali, M., Yew, C.W., Kutateladze, T.G., and Deng, L.W. (2015). O-GlcNAcylation of MLL5beta is essential for MLL5beta-AP-1 transcription complex assembly at the HPV16/18-long control region. Journal of molecular cell biology *7*, 180-183.

Pfefferkorn, J.A., Guzman-Perez, A., Litchfield, J., Aiello, R., Treadway, J.L., Pettersen, J., Minich, M.L., Filipski, K.J., Jones, C.S., Tu, M., et al. (2012). Discovery of (S)-6-(3-cyclopentyl-2-(4-(trifluoromethyl)-1H-imidazol-1-yl)propanamido)nicotini c acid as a hepatoselective glucokinase activator clinical candidate for treating type 2 diabetes mellitus. Journal of medicinal chemistry *55*, 1318-1333.

Ruan, H.B., Han, X., Li, M.D., Singh, J.P., Qian, K., Azarhoush, S., Zhao, L., Bennett, A.M., Samuel, V.T., Wu, J., et al. (2012). O-GlcNAc transferase/host cell factor C1 complex regulates gluconeogenesis by modulating PGC-1alpha stability. Cell Metab *16*, 226-237.

Samuel, V.T., and Shulman, G.I. (2018). Nonalcoholic Fatty Liver Disease as a Nexus of Metabolic and Hepatic Diseases. Cell metabolism *27*, 22-41.

Savage, D.B., Choi, C.S., Samuel, V.T., Liu, Z.X., Zhang, D., Wang, A., Zhang, X.M., Cline, G.W., Yu, X.X., Geisler, J.G., et al. (2006). Reversal of diet-induced hepatic steatosis and hepatic insulin resistance by antisense oligonucleotide inhibitors of acetyl-CoA carboxylases 1 and 2. The Journal of clinical investigation *116*, 817-824.

Szlyk, B., Braun, C.R., Ljubicic, S., Patton, E., Bird, G.H., Osundiji, M.A., Matschinsky, F.M., Walensky, L.D., and Danial, N.N. (2014). A phospho-BAD BH3 helix activates glucokinase by a mechanism distinct from that of allosteric activators. Nature structural & molecular biology *21*, 36-42.

Tyagi, S., and Herr, W. (2009). E2F1 mediates DNA damage and apoptosis through HCF-1 and the MLL family of histone methyltransferases. The EMBO journal.

Wilding, J.P., Leonsson-Zachrisson, M., Wessman, C., and Johnsson, E. (2013). Dose-ranging study with the glucokinase activator AZD1656 in patients with type 2 diabetes mellitus on metformin. Diabetes, obesity & metabolism *15*, 750-759.

Wysocka, J., Myers, M.P., Laherty, C.D., Eisenman, R.N., and Herr, W. (2003). Human Sin3 deacetylase and trithorax-related Set1/Ash2 histone H3-K4 methyltransferase are tethered together selectively by the cell-proliferation factor HCF-1. Genes & development *17*, 896-911.

Yokoyama, A., Wang, Z., Wysocka, J., Sanyal, M., Aufiero, D.J., Kitabayashi, I., Herr, W., and Cleary, M.L. (2004). Leukemia proto-oncoprotein MLL forms a SET1-like histone methyltransferase complex with menin to regulate Hox gene expression. Molecular and cellular biology *24*, 5639-5649.